Automated treatment planning and non-coplanar beam angles in radiotherapy

Linda Rossi

Automated treatment planning and non-coplanar beam angles in radiotherapy

This thesis has been prepared at the Department of Radiation Oncology, Erasmus Medical Center - Cancer Institute, Rotterdam, The Netherlands.

Email for correspondence: l.rossi@erasmusmc.nl

Cover design: Gabriele Valenti and Valeria Fiorenzola (valeria.fiorenzola@gmail.com)
Layout: Gabriele Valenti and Linda Rossi

ISBN: 978-94-91462-50-4

Automated Treatment Planning and Non-coplanar Beam Angles in Radiotherapy

Geautomatiseerde planning en niet-coplanaire bundelhoeken in de radiotherapie

Thesis

to obtain the degree of Doctor from the
Erasmus University Rotterdam
by command of the
rector magnificus

Prof. dr. R.C.M.E. Engels

and in accordance with the decision of the Doctorate Board.
The public defence shall be held on

Tuesday 10 November 2020 at 15.30 hrs
by

Linda Rossi

born in Rimini, Italy

Erasmus University Rotterdam

Doctoral Committee:

Promotor:	Prof. dr. B.J.M. Heijmen
Other members:	Prof. dr. M.S. Hoogeman Prof. dr. Y. Lievens Senior lecturer M. Aznar
Copromotor:	Dr. ir. S. Breedveld

Your preparation for the real world
is not in the answers you've learned,
but in the questions
you've learned to ask yourself

Bill Watterson

Contents

List of Abbreviations

BAO	Beam Angle Optimization
SBRT	Stereotactic Body Radiation Therapy
CP	CoPlanar
NCP	Non-CoPlanar
F-NCP	Fully Non-CoPlanar
CS	Class Solution
iBAS	individualized Beam Angle Selection
CK	CyberKnife
VMAT	Volumetric Modulated Arc Therapy
B-VMAT	Butterfly-VMAT
IMRT	Intensity Modulated Radiation Therapy
EBRT	External Beam Radiation Therapy
LINAC	LINear ACcelerator
MLC	Multi Leaf Collimator
TPS	Treatment Planning System
HDR	High Dose Rate
QA	Quality Assurance
QoL	Quality of Life
CT	Computed Tomography
MRI	Magnetic Resonance Imaging
GTV	Gross Tumor Volume
CTV	Clinical Tumor Volume
PTV	Planning Tumor Volume
OAR	Organ At Risk
PZ	Peripheral Zone
DVH	Dose Volume Histogram
LTCP	Logarithmic Tumor Control Probability
CI	Conformity Index
VS	Vestibular Schwannoma
ML	Mediastinal Lymphoma

Chapter 1

Introduction

Each year, cancer is diagnosed in 17 million people worldwide. Radiation therapy (radiotherapy) is one of the main treatment modalities, together with surgery and chemotherapy. It can be used for curative tumor eradication, tumor size reduction, tumor bed cleansing or palliative purposes.

Radiotherapy uses ionizing radiation to inflict damage on tumor cells for eradication of the disease. The main technique is the use of external X-ray beams that interact with tissue, resulting in delivered radiation dose in the patient. This is called external beam radiation therapy (EBRT), which was used for the studies in this thesis.

The ionizing beams are generated by a LINear ACcelerator (linac) and routed toward the patient. While the beam passes through the patient, it interacts and delivers dose to all tissues, not only the malignant ones. Healthy cells can therefore also be affected by the treatment. It is physically impossible to fully spare them while also delivering a dose to eradicate the tumor. Thus, an important goal of a treatment is to maximally limit the possible negative impact of the irradiation on the patient's Quality of Life (QoL) by limiting dose delivery to healthy tissues.

In order to minimize dose to healthy tissues, multiple beams are targeted at the tumor, essentially creating a cross-fire. As a result, the surrounding dose is relatively low, which contributes to reducing the damage to healthy tissues. An important challenge lies in selecting a beam geometry (number of beams and directions) which is 1) able to deliver the desired minimum dose to the tumor, and 2) maximally reduce the dose to the surrounding healthy tissues.

Since some healthy tissues are more radiosensitive than others, different trade-offs

are generally required, e.g. it may be desirable to not let a radiation beam pass through some tissues at all. This type of knowledge on the healthy tissues surrounding the tumor has to be taken into consideration when beam geometry and beam contributions (intensity profiles) are defined.

Background of the performed investigation

In the common intensity-modulated radiotherapy (IMRT), treatment planning is the process of defining the beam geometry and intensity profiles for delivery of the prescribed tumor dose, while minimizing the dose to radiosensitive healthy tissues (organs-at-risk, OAR) surrounding the tumor.

In current clinical practice, the beam geometry is usually defined by a template (the same beam configuration for all patients with a certain tumor type) which may be adapted by the planner for an individual patient. Alternatively, the planner can select angles from experience. Generally, it is not known whether the selected beam setup can be significantly improved or not.

A linac can rotate the beam over 360° around the patient, with beam directions perpendicular to the patient's axis. These are called coplanar beams. In addition, the patient couch can also rotate, resulting in non-coplanar beams. Allowing non-coplanar setups highly increases the degrees of freedom in beam selection, which can result in significant increases in plan quality. However, allowing non-coplanar plans can imply i) an increased complexity in choosing beams, especially due to the current lack of clinically available beam angle optimization (BAO) algorithms, ii) an increased treatment time, especially for linacs that only have manual couch rotation, and iii) an reduced delivery accuracy in case the patient moves as a reaction to the moving couch. In clinical routine, there is often the tendency to upfront exclude non-coplanar setups.

Treatment plans are generated with the aid of a commercial software application, called Treatment Planning System (TPS). In the worldwide mostly applied conventional planning, this is done in an interactive trial-and-error procedure (manual planning). Based on the initially selected beam geometry, the planner defines a mathematical optimization problem (i.e. cost functions, objectives, weights and/or additional parameters) that is subsequently used by the computer to generate beam intensities profiles. If the result is a not high-quality plan, the planner can e.g. modify the optimization problem or change beam geometry for another run of optimization. This interactive and iterative process stops if the plan is considered adequate, or if there are no more ideas or time, or if significant improvements with further optimization are considered unlikely.

Automation of treatment planning has the potential to avoid inter- and intra-planner variability in plan quality and to minimize planning time, depending on the applied au-

toplanning algorithm. In our institute, Erasmus-iCycle was developed for automated planning [22]. It is a system for a priori multi-criterial plan optimization [73]. For each patient, a single plan is generated that is both Pareto-optimal and clinically favourable [23]. Erasmus-iCycle is in use since 2010, both for research and for clinical planning [25, 38, 67, 69, 144, 145, 155, 159, 185, 186]. The system features integrated optimization of beam profiles and (non-coplanar) beam geometries. This unique feature was intensively employed for the investigations in this thesis.

The performed investigations

Erasmus-iCycle was used to systematically investigate the impact of beam configurations on plan quality, and to investigate plan quality improvements relative to conventional manual planning. The automated planning allowed generation of large numbers of plans for statistically firm conclusions, and for investigating multiple alternative beam configuration approaches.

In Chapter 2, Erasmus-iCycle was used to investigate plan quality variations related to different beam geometries, with a focus on non-coplanar vs. coplanar setups, and on the number of applied beams. Hereto, 1500 plans were generated for 10 patients.

In Chapter 3, non-coplanar beam angle class solutions for prostate SBRT were developed and compared with individualized BAO with Eramus-iCycle. Aim of the investigations was to explore avoidance of time consuming, individualized BAO. Moreover, a beam angle class solution could potentially be used in other centers that do not have access to algorithms featuring BAO. Different recipes for class solution generation were explored. Erasmus-iCycle was used to generate 1060 plans for 30 patients.

In Chapter 4, non-coplanar robotic treatment with a CyberKnife was compared to coplanar Volumetric Modulated Arc Therapy (VMAT) on a regular C-arm linac. The CyberKnife can easily deliver non-coplanar beams with high geometric precision due to tumor tracking, but at cost of increased treatment time. VMAT can offer fast coplanar treatments, but target margins have to be increased due to the lack of tracking. Erasmus-iCycle was coupled to both the CyberKnife and the VMAT clinical TPS to automatically generate clinically deliverable prostate SBRT plans for the treatment technique comparisons.

The use of automated non-coplanar planning to increase plan quality for vestibular schwannoma radiosurgery compared to manual planning was explored in Chapter 5. The focus was on investigating whether autoplanning could reduce the dose bath in these young patients with benign tumors, without losses in plan quality for the tumor or the OARs, or increases in treatment time.

In Chapter 6, Erasmus-iCycle was used to compare 24 beam configuration approaches for a challenging and anatomically highly heterogeneous group of mediastinal lym-

phoma patients. The investigations included coplanar and non-coplanar approaches, both using individualized beam configuration optimization and beam angle class solutions. 600 plans were automatically generated for 25 patients.

Chapter 7 focused on investigating a new treatment approach, designated VMAT+, which merges the benefits of fast VMAT treatments with those of non-coplanar beam arrangements. This approach was used to develop the VMAT+CS treatment approach, combining VMAT with a beam angle class solution (CS) consisting of two IMRT beams with fixed directions. VMAT+CS plans were compared with VMAT and 30-beam non-coplanar IMRT. A total of 740 plans was generated for 20 patients.

In Chapter 8, challenges and opportunities of automated planning with and without BAO, and of the use of non-coplanar beam configurations are discussed. The chapter finishes with an outlook on potential future research.

On the beam direction search space in computerized non-coplanar beam angle optimization for IMRT - prostate SBRT

2

Linda Rossi[1,2], Sebastiaan Breedveld[1], Ben Heijmen[1],
Peter Voet[1], Nico Lanconelli[2], Shafak Aluwini[1]

[1]Department of Radiation Oncology,
Erasmus MC, Rotterdam
[2]Alma Mater Studiorum, Department of Physics,
Bologna University, Italy

Published:
Phys. Med. Biol.
57 (2012) 5441–5458

Abstract

In a recent paper we have published a new algorithm, designated 'iCycle', for fully-automated multi-criterial optimization of beam angles and intensity profiles. In this study, we have used this algorithm to investigate the relationship between plan quality and the extent of the beam direction search space, i.e. the set of candidate beam directions that may be selected for generating an optimal plan.

For a group of 10 prostate cancer patients, optimal IMRT plans were made for Stereotactic Body Radiation Therapy (SBRT), mimicking High Dose Rate (HDR) brachytherapy dosimetry. Plans were generated for 5 different beam direction input sets, a coplanar set and four non-coplanar sets. For coplanar (CP) treatments, the search space consisted of 72 orientations (5° separations). The non-coplanar CK-space contained all directions available in the robotic CyberKnife treatment unit. The fully non-coplanar (F-NCP) set facilitated the highest possible degree of freedom in selecting optimal directions. CK^{+} and CK^{++} were subsets of F-NCP to investigate some aspects of the CK-space. For each input set, plans were generated with up to 30 selected beam directions.

Generated plans were clinically acceptable, according to an assessment of our clinicians. Convergence in plan quality occurred only after around 20 included beams. For individual patients, variations in PTV dose delivery between the 5 generated plans were minimal, as aimed for (average spread in V_{95}: 0.4%). This allowed plan comparisons based on organ at risk (OAR) doses, with the rectum considered most important. Plans generated with the non-coplanar search spaces had improved OAR sparing compared to the CP search space, especially for the rectum. OAR sparing was best with the F-NCP, with reductions in rectum D_{Mean}, V_{40Gy}, V_{60Gy} and $D_{2\%}$ compared to CP of 25%, 35%, 37%, and 8%, respectively. Reduced rectum sparing with the CK search space compared to F-NCP could be largely compensated by expanding CK with beams with relatively large direction components along the superior-inferior axis (CK^{++}). Addition of posterior beams ($CK^{++} \rightarrow$ F-NCP) did not lead to further improvements in OAR sparing. Plans with 25 beams performed clearly better than 11-beam plans. For coplanar plans, an increase from 11 to 25 involved beams resulted in reductions in rectum D_{Mean}, V_{40Gy}, V_{60Gy} and $D_{2\%}$ of 39%, 57%, 64%, and 13%, respectively.

2.1 Introduction

SBRT involves hypofractionated delivery of high radiation doses and requires highly conformal treatment plans and optimal geometrical precision in daily dose delivery [17]. Hypofractionation may result in a treatment benefit for prostate cancer, as the α/β ratio could be as low as 1.5 [24, 54, 88, 119]. Several randomized studies have demonstrated advantages of moderate hypofractionation in prostate cancer [7, 129, 134, 198].

Based on promising results with the strongly hypofractionated prostate HDR brachytherapy [39, 62], interest has grown in developing non-invasive external beam radiotherapy (EBRT) techniques with as little as four fractions. Several of these studies were based on the robotic CyberKnife treatment unit (Accuray, Inc) with its image-guided tumour tracking technology and easy use of non-coplanar beams [5, 56, 56–58, 74, 80, 85, 87, 90, 172].

The impact of beam angle optimization on the quality of treatment plans has been investigated in many studies [3, 135, 136, 184, 189, 196]. To our knowledge, very little is known on the importance of the extent of the beam angle search space in computer optimization of beam orientations, especially for non-coplanar techniques.

Computer optimization of beam angles has been investigated for many years in our institution [135, 184, 189, 196]. Most papers relate to 3D conformal techniques [135, 184, 196], or to CyberKnife treatments with circular cones, [189]. Recently, we developed a new algorithm, designated 'iCycle', [22], for multi-criterial optimization of beam angles and IMRT fluence profiles. In this study we have used iCycle to investigate the importance of the beam angle search space in computer optimization of prostate SBRT plans that mimic HDR brachytherapy dose distributions. Plan comparisons were made for 5 different search spaces, including one with only coplanar directions, and one with the orientations available at the CyberKnife.

2.2 Material and Methods

2.2.1 Patients

Planning CT-scans of ten prostate cancer patients, previously treated in our institution with the CyberKnife, were included in this study. Patients were treated with a dose of 38 Gy, delivered in 4 fractions with a dose distribution that resembled prostate HDR brachytherapy. The CT-scan slice distances were 1.5 mm, the average scan length was

47.4 ± 6.7 cm (range: 35.7-55.7 cm). PTVs included the entire delineated GTV plus a 3 mm margin. The average volume was 90.8 ± 23.1 cc (range: 69.5-145.4 cc). Within the GTV, the peripheral zone (PZ) was defined with the help of MR-images. Patients had 4 implanted markers for image guidance and were treated supine with their feet towards the robotic manipulator.

2.2.2 iCycle

All treatment plans were generated with iCycle, our novel in-house developed algorithm for automated, multi-criterial optimization of beam angles and IMRT fluence profiles. The algorithm is described in detail in [22]. Here a brief summary of its features is provided.

Fully-automated plan generation with iCycle is based on a 'wish-list', defining hard constraints that are strictly met and prioritised objectives [23]. The higher the priority of an objective, the higher the chance that the goal will be approached closely, reached or even exceeded. Furthermore, a list of candidate beam orientations for inclusion in the plan is needed. The beam direction search spaces and wish-list used in this study are described in detail below in the sections 2.2.3 and 2.2.4, respectively. A plan generation starts with zero beams. Optimal directions are sequentially added to the plan in an iterative procedure, up to a user-defined maximum number of beams. After each beam addition, iCycle generates a Pareto optimal IMRT plan including the beam directions selected so far. Consequently, plan generation for a patient always results in a series of Pareto optimal plans with increasing numbers of beams. For example, in this study the selected maximum number of beams is 30, resulting for each case in Pareto optimal IMRT plans with 30, 29, 28, 27, . . . beams. By design, addition of a beam improves plan quality regarding the highest prioritized objective that can still be improved on [22].

2.2.3 Investigated beam direction input sets (search spaces)

In this study, the isocentre was placed in the centre of the tumour. Beam directions were defined by straight lines (beam axes) connecting the isocentre with focal spot positions situated on a sphere centred around the isocentre. The five investigated beam direction search spaces were defined as follows:

1. **CP** (coplanar): 72 equi-angular orientations in the axial plane through the isocentre, covering 360° around the patients (angular separation 5°).
2. **CK** (used by the CyberKnife robotic treatment unit): graphical presentation shown in figure 2.1. The set consists of 117 directions. Interesting features are the absence

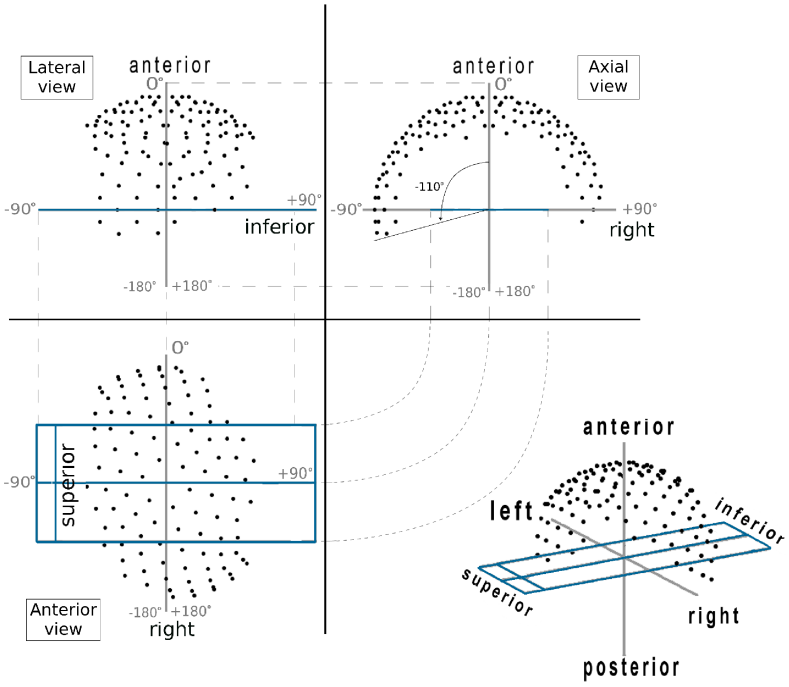

Figure 2.1: CyberKnife (CK) search space. Dots represent focal spot positions.

of beams with a large posterior component (right upper panel in figure 2.1: available directions in the axial plane are limited to [-110°,110°]), and the asymmetry in the beam direction set (left lower panel in figure 2.1) related to the asymmetric position of the robotic manipulator relative to the treatment couch.

3. **F-NCP** (fully non-coplanar): largest set of all 5, theoretical, i.e. not related to a particular treatment device. Ideally, it should represent the search space as defined by all focal spots on a complete sphere around the isocentre. In the axial plane, through the isocentre, the angular distance between directions is 5° (F-NCP includes CP). Non-coplanar directions are separated by 10°. However, iCycle removes the non-coplanar treatment beams that enter (partially) through the end of the CT dataset, which limits the available number of beam directions due to the finite lengths of the CT data sets (sect. 2.2.1). Because of this limitation, the maximum deviation from the AP-axis in the sagittal plane is around 55°. F-NCP includes around 500 beam orientations, depending on the patient.

4. **CK^{++}**: as F-NCP, however excluding (*only*) directions with a posterior component

outside the borders of the CK search space. In the axial plane this results in exclusion of beams outside the [-110°,110°] range (figure 2.1, upper right panel). Depending on the patient, CK^{++} has around 300 beam directions.

5. **CK^{+}**: as F-NCP, however excluding *all* directions outside the borders of the CK search space (figure 2.1). Because of the higher focal spot density, the number of available directions in CK^{+} is higher than for CK, i.e. 186 vs. 117.

2.2.4 iCycle generation of prostate SBRT plans

iCycle was used to optimize beam angles and intensity profiles for high quality SBRT plans, mimicking HDR brachytherapy dose distributions. Table 2.1 shows the applied wish-list with planning constraints and objectives in the upper and lower parts, respectively. The wish-list was established in a trial-and-error procedure to ensure for this patient population, generation of high quality plans with the desired balance between the clinical objectives (see also [22, 184]). Most important clinical goals were adequate PTV coverage and a maximally reduced rectum dose.

The two highest priority objectives, defined with Logarithmic Tumour Control Probability (LTCP) functions [1] aimed at adequate PTV dose delivery. The first focused on control of PTV doses around 34-38 Gy, while the second mainly steered PTV doses around 55-60.8 Gy. For each patient, the goal was to generate, for all 5 beam angle search spaces (sect. 2.2.3), plans with highly similar PTV dose delivery, all close to the dose delivered in the clinical plan, allowing comparison of search spaces based on OAR plan parameters. To this purpose, prior to the final plan generations for a patient, trial plans were generated to fine-tune the LTCP sufficient and α parameters [21] for a PTV maximum dose constraint (table 2.1) equal to the maximum dose in the clinical plan. For each patient, a fixed set of sufficient, α, and PTV maximum dose values was used for the final plan generation for all five search spaces.

As in clinical practice, reduction of rectum dose delivery was the most important OAR objective (priority 3 in table 2.1), aiming at a mean dose of 0 Gy. With this choice, the optimizer would only reduce doses to other OARs to the extent that this would not compromise reaching the lowest possible mean rectum dose. Other OAR considered with lower priorities were urethra, bladder, penis, scrotum and femoral heads. Other structures, *Rings*, were defined to control and reduce the dose to healthy tissues: 'Ring 1' includes all tissue between 2 and 3 cm from the PTV, 'Ring 2' was all tissue between the body contour and the body contour-2cm and 'Ring 3' referred to all tissue in between Ring 1 and Ring 2. Hard constraints on Ring 1 and Ring 2 had to enforce a steep dose fall-off outside the target and to limit the entrance dose, respectively. The priority 7 objective on Ring 3 aimed at dose reduction to healthy tissues, also if not part of an

OAR.

For all beam direction search spaces considered in this study, the simulations assumed that beam collimation was performed with a dynamic multi-leaf collimator (MLC) with a 5 mm leaf width. Maximum field size was 10×12 cm^2 and leaves had full interdigitation and overtravel. For dose calculations, percentual depth dose curves and profiles of an Elekta Synergy 6MV beam, collimated with an MLCi2, were used. Pencil beam kernels for optimization were derived as described in [164]. Equivalent path length correction was used for inhomogeneity correction.

Constraints

Structure	Type	Limit
PTV	maximum	59-69 Gy
Rectum	maximum	38 Gy
Urethra	maximum	40 Gy
Bladder	maximum	41.8 Gy
Penis Scrotum	maximum	4 Gy
Penis Scrotum	mean	2 Gy
Ring 2	maximum	15 Gy
Ring 1	maximum	20 Gy

Objectives

Priority	Structure	Type	Goal	Parameters (D_p, α, sufficient)
1	PTV	LTCP	1	(34-38 Gy, 0.7, 0.003-0.20)
2	PTV	LTCP	4	(55-60.8 Gy, 0.1-0.2, 4-26)
3	Rectum	mean	0 Gy	
4	PZ	LTCP	1	(45 Gy, 0.9)
5	Urethra	mean	0 Gy	
6	Bladder	mean	0 Gy	
7	Ring 3	maximum	15 Gy	
8	Rectum	maximum	30 Gy	
9	Bladder	maximum	35 Gy	
10	Penis Scrotum	maximum	0	
11	L and R Femur head	maximum	24	

Table 2.1: Applied wish-list for all study patients. For definition of Ring 1, 2 and 3 see sect. 2.2.4.

2.2.5 Details on plan evaluation and comparison

The plans in this study were evaluated by a clinician (SA) to check clinical acceptability. In accordance with the ICRU-83 report [105], $D_{2\%}$ and $D_{98\%}$ were reported instead of maximum and minimum doses, respectively. In line with QUANTEC findings [117], rectum dose delivery reporting included V_{40Gy} and V_{60Gy}, calculated by first converting delivered doses to a 2 Gy/fraction regime using an alpha/beta parameter of 3 Gy. Apart from doses

delivered to the PTV, PZ and OARs, we also analyzed V_{10Gy}, V_{20Gy}, and V_{30Gy}, the patient volumes receiving more than 10, 20, and 30 Gy, respectively. Evaluations also included the conformity index (CI) calculated as the ratio of the total tissue volume receiving 38 Gy or more and the PTV (almost 100% of the PTV received 38 Gy, see Results section). Hard constraints on dose delivery to the penis and the scrotum guaranteed negligible doses to these structures in all plans (table 2.1), which are not reported in the Results section.

As described in section 2.4, for each patient we aimed at highly similar PTV doses for all five search spaces. In the Results section it is demonstrated that differences were indeed very small. For this reason comparison of plans and search spaces could be based on doses delivered to healthy tissues with the rectum being the most important one. The two-sided Wilcoxon signed-rank test was used to compare plan parameters in the various search spaces. A p-value of <0.05 was defined as statistically significant.

2.2.6 Treatment time calculation for the CK search space

We calculated treatment times for the hypothetical situation that the CyberKnife would be equipped with an MLC. Treatment times consist of beam-on time, linac travel time, and imaging time. For calculation of beam-on times, we used a leaf sequencing algorithm described in [148], assuming a linac output of 1000 MU/min (as available for the current CyberKnife), a maximum leaf speed of 2.5 cm/s and full leaf interdigitation and overtravel (see also section 2.2.4). Leaf synchronization was not applied. The linac travel time is the time to travel through all selected focal spot positions. However, CyberKnife movements are not totally free, i.e. it can not freely travel from each spot position to any other, but it sometimes has to pass unselected (but allowed, figure 2.1) positions to reach a next selected position. The applied travel time calculation algorithm selects the shortest path, considering all possible movements between spot positions [189]. For the treatment time calculations, we assumed that prior to dose delivery from a focal spot position, images were acquired to verify, and if needed, correct alignment of the beam to be delivered with the current tumour position. Imaging time takes only 2 seconds. However, CK has some node positions from which it is not possible to take an image. To handle this, the machine has to travel to the nearest node position from which imaging is allowed and come back to the delivery position. This aspect was also considered in the calculation of the treatment times.

2.3 Results

2.3.1 Generated plans

In this section, plans and analyses performed for the first study patient are described in some detail to provide examples of the investigations performed for all 10 patients.

Figure 2.2 shows an axial dose distribution for the 25-beam plan generated with the CK search space. Clearly visible are the high degree of rectum sparing, the reduced dose in the urethra, and the increased dose in the peripheral zone (PZ), as enforced by the applied wish-list (table 2.1).

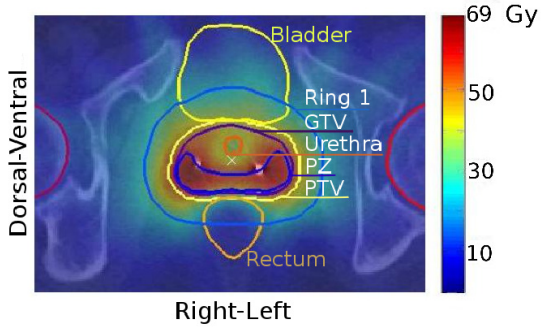

Figure 2.2: Axial dose distribution for the 25-beam plan generated with the CK search space for the first study patient. For definition of Ring 1 see sect. 2.2.4.

Figure 2.3 shows DVHs for the 25-beam plans generated with each of the 5 search spaces in this study. As aimed for (sect. 2.2.4), PTV coverages for the 5 plans were highly similar (upper left zoom). Rectum sparing was best for F-NCP and CK^{++}, while for the coplanar (CP) plan, rectum dose was clearly highest (lower left zoom). F-NCP was best for bladder and CK^{++} for urethra, with F-NCP second. Obviously, plans for the the non-coplanar search spaces with the largest extents (F-NCP and CK^{++}) were most favorable for this patient.

Figure 2.4 shows plan parameters as a function of the number of beams in the plan. For all beam numbers, PTV coverage was very similar for the 5 search spaces. The second row shows that for all search spaces, rectum dose parameters improved with increasing numbers of beams, with some levelling off between 15-20 beams. Also bladder D_{Mean}, urethra D_{Mean}, V_{10Gy}, V_{20Gy}, and V_{30Gy} improved with increasing numbers of beams. A very similar behavior of plan quality on numbers of involved beams was seen for all 10

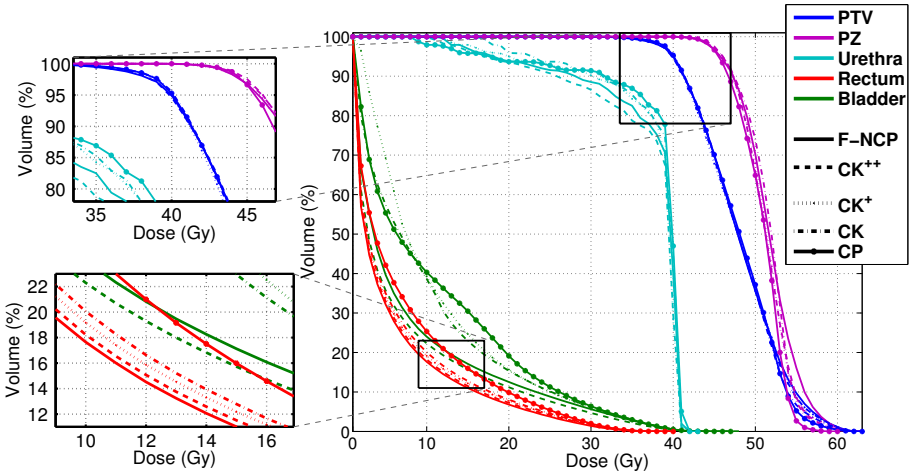

Figure 2.3: DVH comparison for patient 1 for five 25-beam plans, each generated for one of the five studied search spaces.

patients in this study. In the next section, population data will be provided for PTV and rectum.

2.3.2 Plan quality vs number of beams in plans, PTV and rectum

The left panel in figure 2.5 shows the average PTV V_{95} and PTV D_{98} for the 10 study patients, as a function of the number of beams in the plans, normalized to the CP 10-beam plan. For each search space, these quantities are largely independent of the number of beams (normalized values differ up to 0.8% and 2% for average PTV V_{95} and D_{98}, respectively). The trend to slightly reduced PTV dose delivery with increasing number of beams is (partly) related to enhanced urethra sparing with more beams (no data presented). For all beam numbers, these PTV dose parameters are also highly similar for the 5 search spaces with variations up to less then 0.5%. The right panel demonstrates substantial differences between the search spaces in population averaged rectum D_{Mean} and rectum V_{60Gy}, with lowest values for F-NCP and least favorable values for CP. For 20 beams, F-NCP averaged rectum D_{Mean} and V_{60Gy} were 29% and 45% lower compared to CP. For all 5 search spaces, rectum dose improved with increasing number of beams. None of the curves in the right panel fully levels off, but reductions with beam number are clearly most prominent up to around 20 beams. In the remainder of this paper, data for 25-beam plans will be reported, unless stated otherwise.

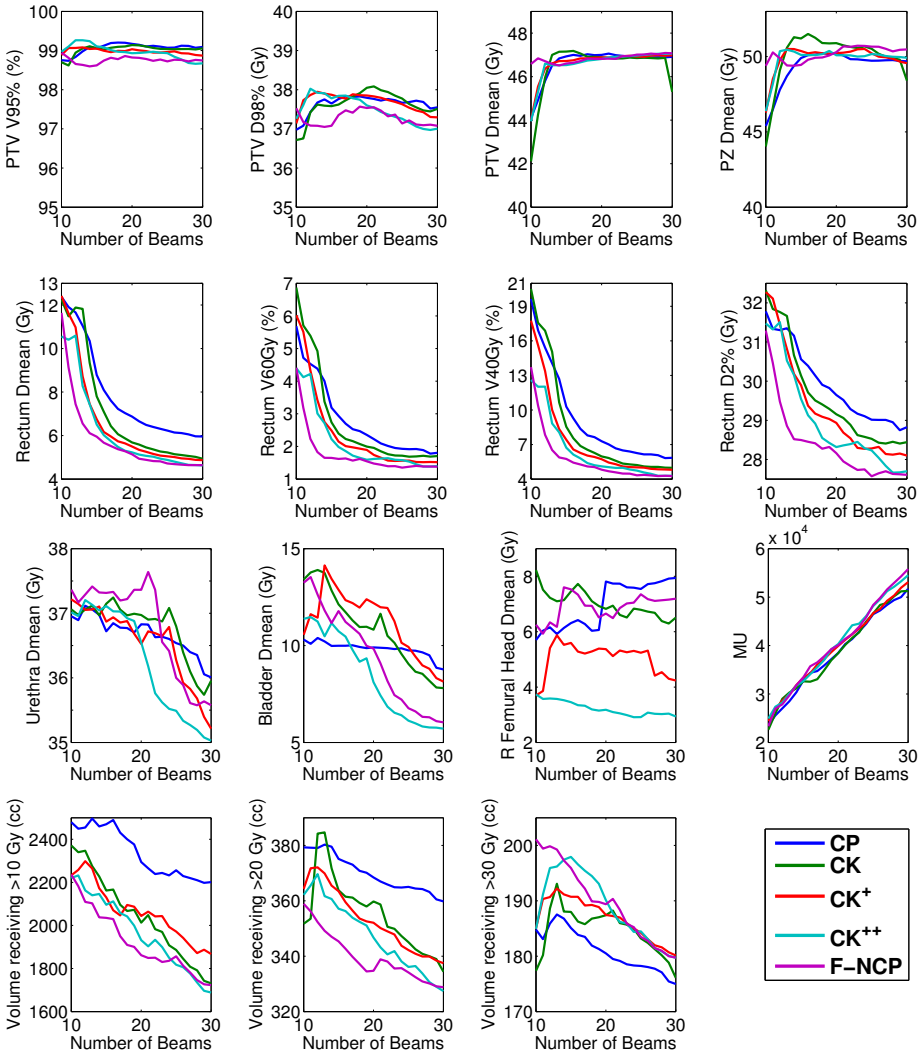

Figure 2.4: Dosimetrical results for patient 1 for plans with 10 up to 30 beams for the 5 studied input beam sets.

2.3.3 25-beam plans - Coplanar (CP) vs non-coplanar beam direction search spaces

Table 2.2 provides a comparison of the CP search space with the four non-coplanar spaces regarding plan parameters of the generated 25-beam plans.

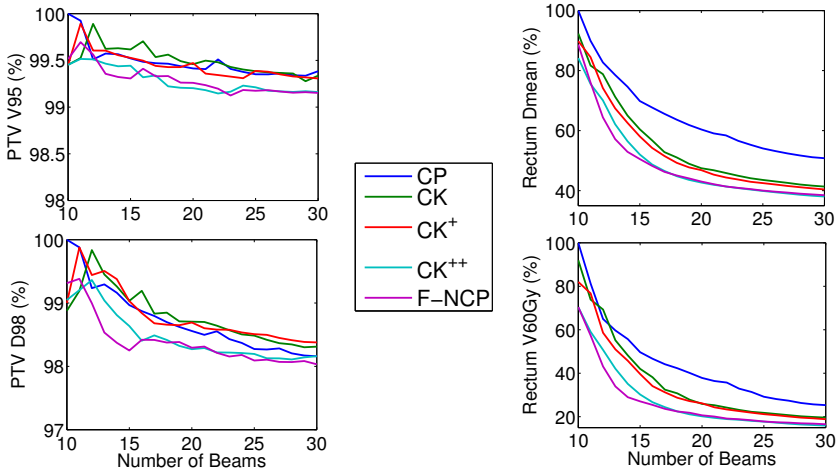

Figure 2.5: Population averaged PTV (left) and rectum (right) plan parameters as function of beam number, for 10-30 beam plans. All percentages are relative to absolute population mean values of the CP 10-beam plan, i.e. PTV V_{95}=99.5%, PTV D_{98}=37.8 Gy, Rectum D_{Mean}=11.3 Gy and Rectum V_{60Gy}=8%.

As aimed for (sect. 2.2.4), differences in PTV D_{Mean}, PTV V_{95} and PTV $D_{98\%}$ between the 5 search spaces were clinically and/or statistically insignificant. Compared to CP, only PTV $D_{2\%}$ was around 3% higher for non-coplanar set-ups ($p<0.05$), but clinically these increases were considered unimportant. No relevant differences were observed in the PZ parameters. Because of this high similarity in target dose for the 5 search spaces, in the remainder of this paper, plan comparisons are focused on organs at risk and especially on the rectum.

The rectum population mean plan parameters were clearly lowest for the 4 non-coplanar search spaces (table 2.2). For the largest search space, F-NCP, population mean reductions relative to CP in rectum D_{Mean}, V_{40Gy}, V_{60Gy}, and $D_{2\%}$ were as large as 25.0%, 34.9%, 36.5%, and 7.5%, respectively. For CK, these reductions were smallest but still highly relevant (18.5%, 23.2%, 21.4% and 3.9%, respectively). Figure 2.6 demonstrates that the superiority of the non-coplanar search spaces holds for all individual patients. Patient 7 had the highest CP rectum dose parameters, while percentual reductions with the non-coplanar set-ups were also highest (figure 2.6). Regression analyses showed, for all 4 non-coplanar search spaces, increasing percentual reductions in rectum dose parameters for increasing CP parameters ($p=0.001$-0.03), i.e. patients with less favorable CP rectum parameters had largest reductions when switching to a non-coplanar plan.

Population mean urethra doses were equal for all 5 search spaces (table 2.2). Differences between non-coplanar spaces and CP in mean bladder dose were highly patient specific. F-NCP and CK^{++} had on average ≈9% lower mean bladder doses, while for CK^{+}

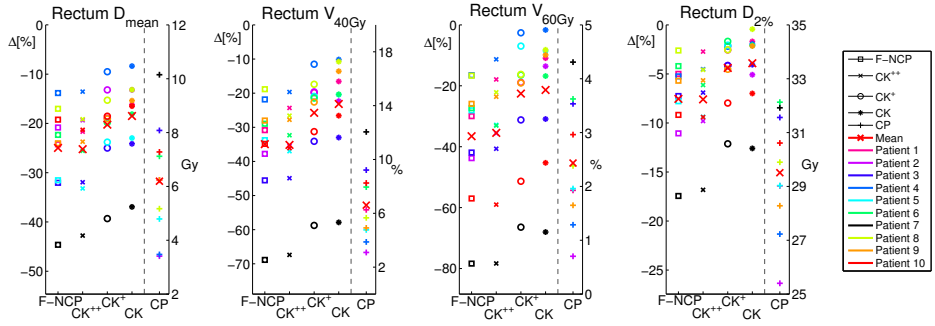

Figure 2.6: Comparison of the CP search space with the four non-coplanar spaces for four rectum plan parameters. On the right of each panel, the CP absolute values for each patient are reported. The four columns on the left report the percentage differences for non-coplanar search spaces with the CP plan. For all patients and all parameters, differences $\Delta[\%]$ are below zero, showing the improved rectum sparing with non-coplanar beam search spaces. All plans are with 25 beams.

and CK, mean bladder doses were around ≈11% higher compared to CP. None of these differences were statistically significant. With CP, doses in the femoral heads were already low, but substantial percentual reductions were seen for the non-coplanar beam sets. Also V_{10Gy} and V_{20Gy} were lowest for the non-coplanar sets.

V_{30Gy}, the total delivered number of MU and the conformity index (CI) were the only parameters for which CP plans did on average (slightly) better than non-coplanar setups. V_{30Gy} and MU were 3-5% and 8% lower in the CP plans. The mean CI in the CP plans for the 10 study patients was 1.2, which increased to 1.27-1.31 for the non-coplanar sets.

2.3.4 25-beam plans - Comparison of non-coplanar search spaces

As described in detail in section 2.2.3, non-coplanar search spaces increased in extent when going from CK to CK^+ to CK^{++} and finally to F-NCP. Briefly, CK^+ had the same boundaries as CK but a higher spot density, CK^{++} was an expansion of CK^+ with beams with relatively large direction components along the superior-inferior axis and F-NCP was an extension of CK^{++}, making it the only non-coplanar search space with posterior beams. In this section, changes in plan parameters related to these increases in degree of freedom for selecting optimal non-coplanar beam angles are discussed.

CK → CK^+ As also visible in table 2.2, CK has the highest mean rectum dose parameters of the 4 non-coplanar beam direction search spaces. Increasing the focal spot density did only marginally improve rectum dose delivery, although reductions in D_{Mean} of 2.2% and in V_{40Gy} of 3.2% were statistically significant. For urethra and bladder, differences in delivered dose were negligible (table 2.2). Significant differences were found for femoral

head doses. With CK^{+}, D_{Mean} and $D_{2\%}$ for right and left head decreased by 15%, 9%, 11% and 10%, respectively (p-values: 0.02, 0.04, 0.04, 0.03). Small, but statistically significant, differences were found for V_{20Gy} (CK^{+} 1% lower, p=0.01), V_{30Gy} (CK^{+} 1.1% higher, p=0.02), and for CI (CK^{+} 1.5% higher, p=0.01).

$CK^{+} \rightarrow CK^{++}$ With this increase in search space, population mean rectum D_{Mean}, V_{40Gy}, V_{60Gy} and $D_{2\%}$ were reduced by as much as 6.8%, 12.0%, 16.9%, and 3.5%, respectively (p=0.002). Large improvement was also found for the bladder with a reduction in D_{Mean} of 26.9% (p=0.01). V_{20Gy} was also improved with CK^{++} (1.7%, p=0.002). CI was slightly better for CK^{+} (2.3%, p=0.001).

$CK^{++} \rightarrow$ F-NCP Adding posterior beams by going from CK^{++} to F-NCP did not result in relevant further reductions in rectum dose (table 2.2). Very small improvements were seen for V_{20Gy} (1.5%, p=0.006), V_{30Gy} (1.6%, p=0.001), and CI (2.0%, p=0.004).

2.3.5 25-beam plans - Distribution of selected beam orientations

Figure 2.7 shows selected beam directions for the 25-beam F-NCP plan of each individual study patient. Clearly, there is a preference for beams with a large lateral component. Comparison of the right panels of figures 2.7 and 2.8 shows that most high-weight beams in the F-NCP plans are within the CK^{++} search space. Apparently, beams with a large posterior component are not frequently selected or have low weights.

2.3.6 25-beam plans - Treatment times for the CK search space

Treatment times for the 25-beam CK plans were on average 18.1±0.5 minutes, including dose delivery, robot motion and imaging and set-up correction prior to delivery of each beam (section 2.2.6).

2.3.7 11 vs 25-beam coplanar plans

As visible in figure 2.4 for patient 1 and in the right panel of figure 2.5 for the patient population, OAR plan parameters may substantially improve with increasing numbers of beams in the plans. On regular treatment units, IMRT plans are generally delivered with coplanar beam set-ups with ≤11 beams. Table 2.3 compares coplanar plans with 11 and 25 beams. Although differences in PTV parameters are statistically significant, they are small, and clinically the obtained PTV doses are considered highly comparable. An important consideration here is that the difference in PTV V_{95}, our most important

parameter for PTV dose evaluation, is very small. The most striking differences were found for the rectum with improvements in D_{Mean}, V_{40Gy}, V_{60Gy} and $D_{2\%}$ of 39.2%, 57%, 63.7%, and 12.6% (p=0.002), when increasing the number of beams from 11 to 25. Bladder D_{Mean} and $D_{2\%}$ reduced by 14.4% (p=0.002) and 5.3% (p=0.004), respectively, and V_{10Gy} improved by 11.1% (p=0.002). When switching to 25-beam plans, the MU increased on average by 75.7% (p=0.002).

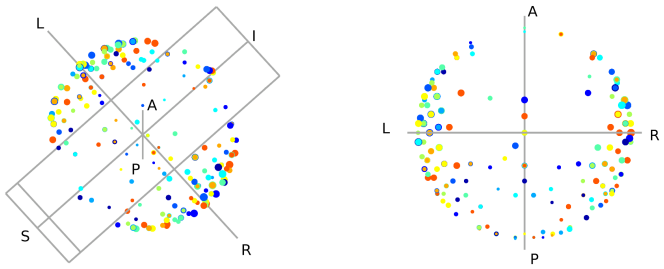

Figure 2.7: Selected focal spots/beams by iCycle for 25-beam F-NCP plans for all 10 patients in a 3D (left) and an axial view (right). Colours refer to different patients, beam weights are proportional to the dot diameters.

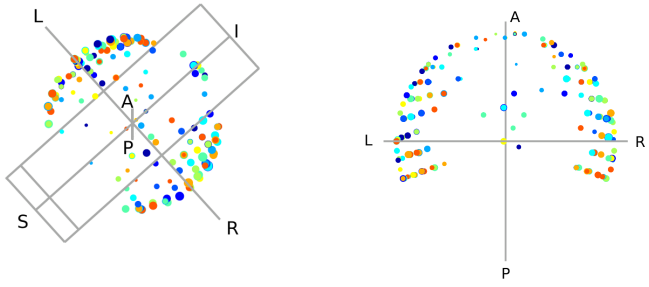

Figure 2.8: Selected focal spots/beams by iCycle for 25-beam CK^{++} plans for all 10 patients in a 3D (left) and an axial view (right). Colours refer to different patients, beam weights are proportional to the dot diameters.

2.3.8 Calculation times

iCycle simulations were done in Matlab 7.12, R2011a, The Mathworks Inc., on a 4 socket 10-core Intel Xeon E7. Plan optimization required ≈35 hours to generate for one patient F-NCP plans with up to 25 beams, i.e. 25 complete plans have been generated and all data are individually available, and around ≈45 hours for up to 30 beams. These times reduced to ≈15 and ≈25 hours to generate coplanar treatment plans.

	CP		F-NCP - CP (%)			CK^{++} - CP (%)			CK^{+} - CP (%)			CK - CP (%)		
	Mean±1SD	[Range]	ΔMean±1SD	[Range]	p	ΔMean±1SD	[Range]	p	ΔMean±1SD	[Range]	p	ΔMean±1SD	[Range]	p
Target														
PTV D_{Mean}	**46.7** ± 2.2 (Gy)	[44.1,50.9]	**0.4** ± 1.2	[-0.4,3.4]	NS	**0.6** ± 1.3	[-0.7,4.1]	NS	**0.3** ± 1.0	[-0.3,3.0]	.01	**0.3** ± 0.8	[-0.4,2.4]	NS
PTV V_{95}	**99.0** ± 0.6 (%)	[97.4,99.7]	**-0.3** ± 0.5	[-1.5,0.1]	NS	**-0.3** ± 0.4	[-1.5,0.1]	.006	**-0.1** ± 0.3	[-0.8,0.2]	NS	**-0.1** ± 0.3	[-0.8,0.2]	NS
PTV $D_{98\%}$	**37.2** ± 0.7 (Gy)	[35.7,38.1]	**-0.3** ± 1.2	[-2.4,1.3]	NS	**-0.2** ± 1.2	[-2.5,1.3]	NS	**0.1** ± 1.1	[-1.8,1.2]	NS	**0.1** ± 0.9	[-1.7,1.0]	NS
PTV $D_{2\%}$	**56.5** ± 3.8 (Gy)	[51.0,63.5]	**2.7** ± 4.0	[-1.1,12.2]	.02	**3.2** ± 4.8	[-3.5,14.3]	NS	**3.1** ± 4.1	[-0.0,13.5]	.01	**3.3** ± 4.0	[0.1,13.1]	.01
PZ D_{Mean}	**50.4** ± 2.3 (Gy)	[47.0,54.6]	**0.9** ± 2.0	[-1.5,4.3]	NS	**1.3** ± 2.1	[-2.2,5.6]	NS	**0.5** ± 1.9	[-2.0,3.1]	NS	**0.3** ± 1.7	[-1.7,2.3]	NS
PZ $D_{98\%}$	**37.2** ± 0.7 (Gy)	[35.7,38.1]	**-0.3** ± 1.2	[-2.4,1.3]	NS	**-0.2** ± 1.2	[-2.5,1.3]	NS	**0.1** ± 1.1	[-1.8,1.2]	NS	**0.1** ± 0.9	[-1.7,1.0]	NS
Rectum														
D_{Mean}	**6.2** ± 2.1 (Gy)	[3.4,10.2]	**-25.0** ± 9.0	[-44.6,-13.8]	.002	**-25.2** ± 8.5	[-42.8,-13.5]	.002	**-20.2** ± 8.1	[-39.3,-9.5]	.002	**-18.5** ± 8.0	[-36.9,-8.4]	.002
V_{40Gy}	**6.6** ± 2.7 (%)	[3.1,12.1]	**-34.9** ± 14.2	[-68.9,-18.8]	.002	**-35.2** ± 13.5	[-67.4,-19.7]	.002	**-25.8** ± 13.3	[-58.7,-11.5]	.002	**-23.2** ± 14.1	[-57.8,-10.1]	.002
V_{60Gy}	**2.4** ± 1.1 (%)	[0.7,4.3]	**-36.5** ± 19.3	[-78.4,-16.5]	.002	**-35.4** ± 20.1	[-78.3,-11.3]	.002	**-22.6** ± 21.8	[-66.4,3.7]	.004	**-21.4** ± 20.8	[-68.0,-1.7]	.002
$D_{2\%}$	**29.5** ± 2.2 (Gy)	[25.4,32.1]	**-7.5** ± 4.3	[-17.4,-2.6]	.002	**-7.6** ± 4.0	[-16.8,-2.7]	.002	**-4.4** ± 3.3	[-12.1,-1.7]	.002	**-3.9** ± 3.6	[-12.6,-0.4]	.002
Urethra														
D_{Mean}	**32.2** ± 3.5 (Gy)	[26.4,36.5]	**-0.4** ± 1.3	[-2.2,2.1]	NS	**-0.3** ± 2.0	[-2.9,3.7]	NS	**-0.3** ± 1.6	[-2.5,3.0]	NS	**-0.4** ± 1.2	[-2.5,1.8]	NS
$D_{2\%}$	**40.0** ± 0.2 (Gy)	[39.8,40.3]	**-0.4** ± 0.6	[-1.4,0.5]	NS	**-0.4** ± 0.6	[-1.2,0.3]	NS	**-0.4** ± 0.6	[-1.5,0.3]	NS	**-0.3** ± 0.5	[-1.3,0.5]	NS
Bladder														
D_{Mean}	**8.8** ± 2.4 (Gy)	[3.7,12.6]	**-9.0** ± 18.4	[-43.6,20.0]	NS	**-8.5** ± 23.3	[-46.5,22.6]	NS	**11.2** ± 17.3	[-13.5,44.3]	NS	**10.6** ± 18.7	[-17.1,48.0]	NS
$D_{2\%}$	**34.4** ± 3.4 (Gy)	[25.4,37.9]	**0.9** ± 1.6	[-2.6,2.5]	NS	**0.1** ± 3.6	[-7.8,4.2]	NS	**2.4** ± 2.1	[-1.0,5.0]	.01	**2.5** ± 1.7	[0.1,5.2]	.002
Femorals														
R D_{Mean}	**9.1** ± 2.7 (Gy)	[5.4,14.5]	**-35.1** ± 21.5	[-67.8,-8.6]	.002	**-34.2** ± 19.8	[-72.1,-14.1]	.002	**-34.3** ± 15.5	[-62.9,-12.0]	.002	**-20.8** ± 16.3	[-50.8,-2.4]	.002
R $D_{2\%}$	**15.6** ± 0.7 (Gy)	[14.8,17.1]	**-24.2** ± 13.9	[-46.2,-7.2]	.002	**-23.9** ± 10.2	[-50.3,-14.8]	.002	**-18.7** ± 4.5	[-29.2,-14.2]	.002	**-9.7** ± 7.1	[-25.4,-1.5]	.002
L D_{Mean}	**9.0** ± 2.5 (Gy)	[5.7,13.2]	**-32.6** ± 26.9	[-76.1,2.3]	.004	**-42.4** ± 25.7	[-76.5,3.5]	.004	**-31.3** ± 19.6	[-62.9,4.8]	.004	**-23.3** ± 14.7	[-50.8,-7.1]	.002
L $D_{2\%}$	**15.4** ± 0.8 (Gy)	[14.2,16.8]	**-19.9** ± 15.0	[-56.6,-2.6]	.002	**-22.2** ± 15.6	[-52.0,-6.5]	.002	**-18.9** ± 13.8	[-47.4,1.5]	.004	**-9.8** ± 6.6	[-22.0,-0.6]	.002
Other														
V_{10Gy} *	**2020** ± 331 (cc)	[1624,2758]	**-17.0** ± 5.8	[-28.6,-9.4]	.002	**-15.9** ± 7.2	[-28.0,-8.7]	.002	**-13.4** ± 4.7	[-19.0,-3.7]	.002	**-14.7** ± 3.6	[-21.1,-9.3]	.002
V_{20Gy} *	**352** ± 63 (cc)	[285,500]	**-8.3** ± 2.2	[-13.4,-6.1]	.002	**-6.9** ± 2.0	[-10.0,-3.3]	.002	**-5.3** ± 1.8	[-7.9,-2.2]	.002	**-4.3** ± 1.7	[-7.0,-2.4]	.002
V_{30Gy} *	**169** ± 31 (cc)	[137,242]	**3.4** ± 2.5	[-2.1,6.6]	.006	**5.0** ± 2.7	[-0.1,8.8]	.004	**4.5** ± 2.3	[-0.2,7.3]	.004	**3.4** ± 2.0	[-0.4,5.8]	.004
CI	**1.2** ± 0.1	[1.1,1.3]	**7.0** ± 2.9	[1.8,11.4]	.002	**9.2** ± 3.1	[4.4,13.7]	.002	**7.1** ± 2.2	[3.5,10.6]	.002	**5.5** ± 2.3	[2.7,9.2]	.002
MU	**43533** ± 2694	[39264,46572]	**8.4** ± 4.8	[4.1,19.3]	.002	**8.2** ± 6.6	[3.1,23.1]	.002	**7.4** ± 6.0	[0.5,19.5]	.002	**6.9** ± 6.8	[-2.0,22.0]	.01

Table 2.2: Comparison of dosimetric plan parameters of the generated 25-beam plans, for the five investigated beam angle search spaces. Mean values, standard deviations (SD) and ranges refer to the 10 patients in the study. The first data column reports the results obtained with the coplanar (CP) search space. In the next columns, percentage differences of the other spaces with CP are shown, i.e. 100∗(other_search_space - CP)/CP. (*) refers to all tissues receiving >10, >20 or >30 Gy. Statistically non-significant (NS) for p>0.05.

	11 beams, CP		**25 vs 11 beams**, CP (%)		
	Mean ± 1SD	[Range]	ΔMean ± 1SD	[Range]	p-value
Target					
PTV D_{Mean}	**45.1** ± 1.0 (Gy)	[43.4,46.7]	**3.4** ± 3.1	[0.2,9.1]	.002
PTV V_{95}	**99.4** ± 0.4 (%)	[98.7,99.9]	**-0.5** ± 0.5	[-1.8,0.3]	.01
PTV $D_{98\%}$	**37.8** ± 0.5 (Gy)	[37.1,38.6]	**-1.5** ± 1.4	[-3.9,1.6]	.02
PTV $D_{2\%}$	**52.8** ± 1.8(Gy)	[49.5,56.1]	**7.0** ± 4.2	[1.6,13.2]	.002
PZ D_{Mean}	**48.1** ± 0.9 (Gy)	[46.5,48.9]	**4.6** ± 4.5	[-0.8,11.5]	.006
PZ $D_{98\%}$	**42.5** ± 1.0 (Gy)	[39.8,43.3]	**-12.4** ± 2.8	[-16.4,-5.4]	.002
Rectum					
D_{Mean}	**10.2** ± 2.9 (Gy)	[5.5,13.7]	**-39.2** ± 9.0	[-48.0,-18.6]	.002
V_{40Gy}	**15.2** ± 4.9 (%)	[7.8,22.2]	**-57.0** ± 9.2	[-63.3,-34.3]	.002
V_{60Gy}	**6.5** ± 2.4 (%)	[3.2,10.9]	**-63.7** ± 9.3	[-78.1,-46.9]	.002
$D_{2\%}$	**33.7** ± 1.5 (Gy)	[31.3,35.4]	**-12.6** ± 4.2	[-19.0,-7.4]	.002
Urethra					
D_{Mean}	**33.1** ± 3.3 (Gy)	[27.5,36.9]	**-2.6** ± 1.2	[-4.7,-0.9]	.002
$D_{2\%}$	**40.0** ± 0.2 (Gy)	[39.7,40.5]	**-0.2** ± 0.5	[-1.2,0.7]	NS
Bladder					
D_{Mean}	**10.2** ± 2.3 (Gy)	[5.1,13.7]	**-14.4** ± 9.1	[-28.1,-2.5]	.002
$D_{2\%}$	**36.3** ± 3.0 (Gy)	[27.9,37.9]	**-5.3** ± 3.7	[-9.8,0.6]	.004
Femural Heads					
R D_{Mean}	**7.8** ± 2.5 (Gy)	[4.7,12.3]	**19.9** ± 30.1	[-14.0,92.1]	NS
R $D_{2\%}$	**15.3** ± 2.0 (Gy)	[12.9,18.4]	**3.5** ± 13.0	[-11.0,27.4]	NS
L D_{Mean}	**8.0** ± 1.7 (Gy)	[6.0,10.8]	**12.7** ± 17.3	[-19.5,44.5]	.03
L $D_{2\%}$	**15.2** ± 1.3 (Gy)	[13.8,17.3]	**2.0** ± 8.7	[-12.2,12.5]	NS
Other					
V_{10Gy} *	**2274** ± 382 (cc)	[1824,3163]	**-11.1** ± 2.6	[-15.2,-6.9]	.002
V_{20Gy} *	**365** ± 67 (cc)	[295,520]	**-3.4** ± 2.7	[-7.4,2.2]	.006
V_{30Gy} *	**178** ± 33 (cc)	[143,257]	**-4.8** ± 3.0	[-9.4,0.2]	.004
CI	**1.2** ± 0.1	[1.1,1.3]	**-2.5** ± 4.5	[-10.0,3.1]	NS
MU	**24791** ± 1302	[22624,26844]	**75.7** ± 9.2	[56.8,91.7]	.002

Table 2.3: Results for 10 patients for 11 and 25 coplanar beam plans. The first column reports the results obtained with the 11 beam coplanar configuration. In the next columns, the percentage decrease from the 11 beams CP results are shown. (*) refers to all tissues receiving >10, >20 or >30 Gy.

2.4 Discussion

Recently, we have presented iCycle, our in-house developed algorithm for integrated, multicriterial optimization of beam angles and profiles [22]. For plan generation, iCycle uses a *priori* defined plan criteria (wish-list, section 2.2.4 and table 2.1) and a beam direction search space. The wish-list is used to fully automatically generate high quality plans without interactive tweaking of parameters such as weighting factors in the cost function. For a plan with *N* selected orientations, the solution is Pareto optimal regarding the generated beam profiles [21, 22]. To ensure generation of clinically acceptable

plans with favourable balances in the outcomes for the various plan objectives, wish-lists are developed in close collaboration with treating clinicians. This study is based on 1500 treatment plans generated with iCycle (10 patients, 5 beam sets, 30 beams). Due to the automation, the plan generation workload was minimal and plan quality was independent of the experience and skills of human planners. To our knowledge, this is the first paper investigating in details the impact of the extent of the beam angle search space in computer optimization of IMRT dose distributions.

For each individual patient, PTV doses in the iCycle generated plans for the five investigated search spaces were highly similar (figures 2.3, 2.4, 2.5 and table 2.2), and tuned to be in close agreement with the clinically delivered dose. This allowed focusing plan comparisons on OARs, and specifically on the highest priority OAR, the rectum. Rectum doses for all four non-coplanar beam direction search spaces were clearly superior when compared to doses obtained with the coplanar search space (figures 2.3, 2.4, 2.5, 2.6 and table 2.2). Also for the femoral heads, V_{10Gy} and V_{30Gy}, non-coplanar plans performed better (table 2.2). Coplanar plans had (slightly) improved V_{30Gy}, CI and MU.

The CK^{+} and CK^{++} search spaces were used to study dosimetrical consequences of limitations in the extent of the CK space (figure 2.1, sections 2.2.3, 2.3.4 and 2.3.5). The data presented in section 2.3.4 do clearly demonstrate that extension of the CK space to include beams with larger direction components along the superior-inferior axis could substantially enhance plan quality ($CK^{+} \longrightarrow CK^{++}$). On the other hand, further addition of beams with larger posterior components did not improve plans ($CK^{++} \longrightarrow$ F-NCP). Comparison of the right panels in figures 2.7 and 2.8 shows that also in case of availability of the posterior beams (F-NCP), most selected high-weight beams are within the borders of the CK^{++} space that lacks posterior beams. As plan quality for F-NCP and CK^{++} is highly similar, it may be concluded that omission of posterior beams does not limit the quality of generated plans.

As demonstrated in figures 2.4 and 2.5, for all search spaces, plan quality continued to improve with increasing numbers of involved beams, with some levelling off for >20 beams. Table 2.3 details the very significant improvements that can be obtained with 25 coplanar beam configurations compared to 11 coplanar beams. This observation might seem in striking contrast with the broadly applied ≤9 beams for prostate in clinical practices. However, it has to be considered here that HDR like dose distributions were investigated in this paper, aiming at highly inhomogeneous PTV doses with some sparing of the urethra and enhanced dose delivery in the peripheral zone. In an on-going study we are investigating the use of large numbers of beams for more regular prostate IMRT dose distributions.

Also for very large beam numbers, non-coplanar configurations performed clearly better than coplanar set-ups (figures 2.5, 2.6, table 2.2). On conventional treatment units

with L-shaped gantries, delivery of non-coplanar plans with many beams would result in impractically long treatment times and a high workload because of the involved couch rotations. The latter would also limit treatment accuracy. The performed treatment time calculations for a robotic CyberKnife equipped with an MLC (sections 2.2.6 and 2.3.6) demonstrated that treatment times of around 18 minutes could be obtained with such a system, including intra-fraction imaging and position correction prior to delivery of each of the 25 beams.

As mentioned in section 2.2.4, for each patient, PTV doses in iCycle plans were highly similar to the dose in the plan generated with the clinical treatment planning system for actual treatment with the CyberKnife. On the other hand, it was observed that rectum doses in iCycle plans were highly superior to corresponding doses in the clinical plans (not described in detail in this paper). This may seem unexpected for the CK search space that contains the feasible beam directions of the CyberKnife treatment unit. A possible explanation may be that clinical plans were generated with 3 circular cones per patient, while for the iCycle simulations it was assumed that beam collimation was performed with an MLC. These observations are now being investigated in great detail, to be reported in a separate paper.

In this study, minimization of the mean rectum dose was used as the highest priority objective, aiming at rectum sparing (table 2.1). Many studies have been performed to establish plan parameters that correlate most with rectum toxicity, see [117] for an overview. The QUANTEC group suggests V_{60}, but using this objective directly in the optimization leads to less desirable results because of the focus on a single dose-point. Instead we used rectum D_{Mean} as an objective in the optimizations, while V_{60} was included in plan evaluations.

In iCycle, the wish-list is used to generate plans with favourable balances between the various treatment goals. In our investigations we imposed a very strong drive for minimization of the mean rectum dose (table 2.1: priority 3, Goal: 0 Gy). Such a focus on rectum dose minimization has a danger that slightly higher rectum doses could potentially result in (unobserved) much improved doses to other OAR. In the trial plan generations for creating the applied wish-list (section 2.2.4), no evidence was found that this would actually occur. In the near future, we will however study the value of navigation tools [33, 120, 167] for exploring the solution space around iCycle generated plans. Anyway, as in this study the same wish-list was used for all search spaces, numbers of involved beams and patients, it is believed that the impact of not performing navigation on main conclusions of the work will be minimal.

In this paper we compared plan quality of treatments with up to 30 optimized coplanar beam directions with optimized non-coplanar techniques. There is no existing machine that can deliver treatments for all investigated beam search spaces. The CyberKnife

search space does not include 72 equi-angular coplanar beams, neither does it contain all directions defined for CK^{+} and CK^{++}. The fully non-coplanar (F-NCP) space cannot be realized with any of the commercially available systems, e.g. because of linac-bunker floor collisions, gantry-couch collisions, or beams going through heavy couch elements. However, the F-NCP dose distributions give an upper limit of what could theoretically be obtained with optimized non-coplanar set-ups. To make conclusions on the impact of the beam search space on plan quality independent of the applied optimizer, the type of beam shaping, and the beam characteristics, all optimizations were performed with the iCycle optimizer, using the same dose calculation engine for the same MLC (section 2.2.4).

Optimization results may depend on dose calculation accuracy [77]. It is well known that dose calculations using pencil beams and equivalent path length correction have limited accuracy, especially in low density tissues. In this study on prostate cancer, these tissues were largely absent in the treatment fields. Moreover, the same dose calculation algorithm was used for all beam direction search spaces. Therefore, we believe that limitations in the applied dose calculation engine do not jeopardize our main conclusions on ranking of the beam search spaces.

As described in section 2.3.8, optimization times were long, especially for the largest non-coplanar search spaces. There are many possibilities for substantial reductions and this is an area of active research in our group. On the other hand, based on an *a priori* defined, fixed wish-list per patient group, iCycle optimized plans are generally of very high quality, and do not require further iterations with new iCycle runs [22] (as explained in section 2.2.4, in this study, PTV constraints and objectives were tuned per patient to reproduce different clinical PTV dose distributions). In a recent prospective clinical study for evaluation of iCycle in head and neck IMRT, for each patient the treating physician was presented a plan based on iCycle and a plan made by dosimetrists with the clinical treatment planning system. In 32 out of 33 plan selections, the treating physician selected the iCycle based plan. Also objectively, the latter plans were clearly of higher quality [186].

This study focused on generation of prostate SBRT plans that mimicked HDR brachytherapy dose distributions. Conclusions on the importance of non-coplanar beams, on the favorable use of large numbers of beams (>20), and on the limited importance of posterior beams may not be valid in other circumstances. Recently, we demonstrated for a group of head and neck cancer patients that inclusion of non-coplanar beams in the search space did only marginally improve IMRT plans [184]. Studies for other treatment sites are on-going.

2.5 Conclusion

For prostate SBRT, IMRT plans generated with all four investigated non-coplanar search spaces had clearly improved organ at risk (OAR) sparing compared to the coplanar (CP) search space, especially for the rectum which was the most important OAR in this study. OAR sparing was best with the fully non-coplanar search space (F-NCP), with improvements in rectum D_{Mean}, V_{40Gy}, V_{60Gy} and $D_{2\%}$ compared to CP of 25%, 35%, 37%, and 8%, respectively. Reduced rectum sparing with the CyberKnife (CK) search space compared to F-NCP could be largely compensated by extending the CK space with beams with relatively large direction components along the superior-inferior axis (CK^{++}). Further addition of posterior beams to define the F-NCP search space, did not result in plans with clinically relevant further reductions in OAR sparing. Plans with 25 beams performed clearly better than plans with only 11 beams. For coplanar set-ups, an increase in involved number of beams from 11 to 25 resulted in reductions in rectum D_{Mean}, V_{40Gy}, V_{60Gy} and $D_{2\%}$ of 39%, 57%, 64%, and 13%, respectively.

Noncoplanar Beam Angle Class Solutions to Replace Time-Consuming Patient-Specific Beam Angle Optimization in Robotic Prostate Stereotactic Body Radiation Therapy

3

Linda Rossi, Sebastiaan Breedveld,
Shafak Aluwini, Ben Heijmen

Department of Radiation Oncology,
Erasmus MC, Rotterdam

Published:
Int. J. Radiat. Oncol. Biol. Phys.
92 (2015), 762-770

Abstract

Purpose: To investigate development of a recipe for the creation of a beam angle class solution (CS) for noncoplanar prostate stereotactic body radiation therapy to replace time-consuming individualized beam angle selection (iBAS) without significant loss in plan quality, using the in-house "Erasmus-iCycle" optimizer for fully automated beam profile optimization and iBAS.

Methods and Materials: For 30 patients, Erasmus-iCycle was first used to generate 15-, 20-, and 25-beam iBAS plans for a CyberKnife equipped with a multileaf collimator. With these plans, 6 recipes for creation of beam angle CSs were investigated. Plans of 10 patients were used to create CSs based on the recipes, and the other 20 to independently test them. For these tests, Erasmus-iCycle was also used to generate intensity modulated radiation therapy plans for the fixed CS beam setups.

Results: Of the tested recipes for CS creation, only 1 resulted in 15-, 20-, and 25-beam noncoplanar CSs without plan deterioration compared with iBAS. For the patient group, mean differences in rectum D1cc, V60GyEq, V40GyEq, and Dmean between 25-beam CS plans and 25-beam plans generated with iBAS were 0.2 ± 0.4 Gy, 0.1% ± 0.2%, 0.2% ± 0.3%, and 0.1 ± 0.2 Gy, respectively. Differences between 15- and 20-beam CS and iBAS plans were also negligible. Plan quality for CS plans relative to iBAS plans was also preserved when narrower planning target volume margins were arranged and when planning target volume dose inhomogeneity was decreased. Using a CS instead of iBAS reduced the computation time by a factor of 14 to 25, mainly depending on beam number, without loss in plan quality.

Conclusions: A recipe for creation of robust beam angle CSs for robotic prostate stereotactic body radiation therapy has been developed. Compared with iBAS, computation times decreased by a factor 14 to 25. The use of a CS may avoid long planning times without losses in plan quality.

3.1 Introduction

Several reports have suggested a benefit for stereotactic body radiation therapy (SBRT) for patients with prostate cancer [7, 24, 87, 134, 198]. The robotic CyberKnife (Accuray Inc, Sunnyvale, CA) may be used for easy delivery of noncoplanar beams and for image-guided tumor tracking based on implanted fiducials [6, 14, 55, 57, 74, 80, 81, 89, 90].

In clinical practice, development of a high-quality noncoplanar plan may be a lengthy procedure. Moreover, the common trial-and-error tweaking of treatment planning system (TPS) parameters by dosimetrists to steer the TPS toward an acceptable solution results in a plan quality that may heavily depend on the skills and experience of the dosimetrist.

Several studies have shown potential benefit of automatic treatment planning [19, 22, 68, 98, 100, 101, 185, 186, 197, 199]. In our institution, the Erasmus-iCycle TPS has been developed for fully automated multicriteria optimization of beam profiles (intensity modulated radiation therapy, IMRT) and individualized beam angle selection (iBAS) [22]. Each Erasmus-iCycle plan generation for an individual patient is based on a treatment site–specific "wishlist" with hard constraints and prioritized objectives, established a priori in collaboration with treating physicians to ensure generation of clinically desired, Pareto optimal IMRT plans [68, 98, 135, 143, 184–186].

In a prospective clinical study on head and neck cancer, we demonstrated that IMRT plans generated using Erasmus-iCycle were superior to "manually" generated plans in the clinical routine; in 97% of cases the treating physician selected the Erasmus-iCycle–based plan for patient treatment [186]. For prostate cancer, automatically generated volumetric modulated arc therapy plans were as good as plans generated by an expert planner spending up to 4 hours' hands-on time on tweaking of TPS parameters [185]. Our clinical head and neck cancer, cervix cancer, and prostate cancer plans are currently generated fully automatically using Erasmus-iCycle [68].

The proven high plan quality together with the avoidance of both workload and operator dependency make the Erasmus-iCycle an interesting tool for objective comparisons of treatment strategies based on planning studies with a large number of plans. Recently, the Erasmus-iCycle was used in various studies: (1) to systematically investigate the impact of beam number and noncoplanar beam setups in head-and-neck cancer IMRT [184]; (2) to compare treatment strategies for prostate cancer patients with hip prostheses [186]; and (3) to investigate the beam direction search space in prostate SBRT, mimicking high-dose rate brachytherapy dosimetry, as used in our clinical practice [143]. In the latter study, coplanar and noncoplanar IMRT treatments with up to 30 beams were investigated. For both, improvements in plan quality obtained by adding

(computer-selected) beam directions only started to level off after 20 beams. Noncoplanar (CyberKnife) setups were clearly superior to coplanar beam arrangements, especially for rectum sparing. Patient-specific beam angle optimization may be time consuming, and most TPSs do not have advanced algorithms for it. In this study, we used Erasmus-iCycle to search for a fixed set of beam directions for all patients (i.e. a beam-angle class solution [CS]), which could replace iBAS without loss in plan quality.

3.2 Methods and Materials

3.2.1 Patients

Computed tomography scans of 30 previously treated CyberKnife prostate SBRT patients with 1.5-mm slice thickness were used in this project. The planning target volume (PTV) was defined as prostate plus 3-mm margin. The peripheral zone was contoured using magnetic resonance images. Average PTV size was 95.6 ± 20.3 cm^3 (range, 55.9-147.2 cm^3). Other contoured organs at risk (OARs) were rectum, bladder, urethra, femoral heads, scrotum, and penis. A total dose of 38 Gy was delivered in 4 fractions with a heterogeneous distribution mimicking high–dose rate brachytherapy dosimetry. In this study an arbitrarily selected subgroup of 10 "training" patients was used to create beam-angle CSs. The same patients plus the remaining 20 "test" patients were used for CS validation.

3.2.2 Erasmus-iCycle plan generation

As described in detail below, Erasmus-iCycle was first used to automatically generate 15-, 20-, and 25-beam iBAS plans for a CyberKnife equipped with a multileaf collimator (MLC). With these plans, 6 recipes for creation of beam-angle CSs were investigated. To validate these CSs, Erasmus-iCycle was also used to generate IMRT plans using them instead of iBAS.

Automated treatment planning with Erasmus-iCycle has been described in detail elsewhere [22, 68, 135, 143, 184–186], and a brief summary is provided in the Introduction. The wishlist used in this study, containing the hard constraints and planning objectives with ascribed priorities for generation of clinically desired prostate SBRT dose distributions, is presented in Tables 3.1 (constraints and objectives). Constraints (that will always be respected in Erasmus-iCycle plans) are mainly used to control Dmax in the target and OARs, the entrance dose, and the dose fall-off close to the PTV. Planning target volume coverage and an inhomogeneous dose distribution mimicking high-dose rate brachy-

therapy dosimetry are the objectives with the highest priorities (i.e. 1 and 2), optimized through LTCP (logarithmic tumor control probability) functions, defined as follows:

$$LTCP = \frac{1}{m}\sum_{j=1}^{m} e^{-\alpha(d_j - D^p)} \tag{3.1}$$

where m is the number of voxels in the target structure, D^p the prescribed dose, d_j the dose in voxel j, and α a parameter, called cell sensitivity (see reference [143] for details). The OAR objective with the highest priority (3) is reduction of the rectum mean dose as close as possible to 0 Gy.

We used the 102 beam directions of a CyberKnife M6 system as input for iBAS and CS development. Currently only circular beam shapes, realized with fixed cones or a variable aperture collimator, are available for clinical CyberKnife treatment. However, an MLC is being developed by Accuray Inc, and in the near future the systems at our facility will be equipped with one. The reported investigations have been performed for a system with an MLC (characteristics provided by Accuray Inc and summarized in reference [143]).

3.2.3 Workflow for generation of acceptable N-beam CSs

In a recent study [143] we demonstrated that average CyberKnife plan quality for our clinical prostate SBRT dose prescription only began to level off after inclusion of at least 20 beams. Therefore, the initial investigations focused on creation of a 25-beam CS. For a subgroup of 10 patients, Erasmus-iCycle was first used to generate 25- beam plans with individualized beam angles. For each of the 6 investigated recipes for CS creation (described below), the 25-beam CS was then generated and validated as follows: (1) Based on the 10 generated iBAS plans, select 25 (fixed) beam directions according to the recipe; (2) Use Erasmus-iCycle to generate IMRT plans with fixed beam directions determined in step 1 for the chosen subset of 10 patients; and (3) Normalize for each patient the CS and iBAS plans to have exactly equal V95% in the PTV dose-volume histograms, and compare plan parameters.

This first step of the investigations allowed selection of a subset of recipes that resulted in 25-beam CSs with clinically acceptable differences in plan quality compared with iBAS, as evaluated by the clinician participating in the study (S.A.).

With a CyberKnife treatment unit, treatment time generally increases with the number of treatment beams, and not all patients benefit equally from 25 beams [143]. Therefore, in a second step, we investigated whether the recipes also worked for generation of 20-

Constraints

Volume	Type	Limit
PTV	max	65 Gy
PZ	max	69 Gy
Rectum	max	38 Gy
Urethra	max	40 Gy
Bladder	max	41.8 Gy
Penis Scrotum	max	4 Gy
Penis Scrotum	mean	2 Gy
Ring 1*	max	20 Gy
Ring 2†	max	15 Gy

Objectives

Priority	Volume	Type	Goal	Parameters (D_p, α, sufficient)
1	PTV	↓LTCP	0.03	(35 Gy, 0.7, 0.03)
2	PTV	↓LTCP	3.1(4.1‡)	(58 Gy, 0.1, 3.1(4.1))
3	Rectum	↓mean	0 Gy	
4	PZ	↓LTCP	1	(45.6 Gy, 0.9)
5	Urethra	↓mean	0 Gy	
6	Bladder	↓mean	0 Gy	
7	From Ring 1 to Ring 2	↓max	15 Gy	
8	Rectum	↓max	30 Gy	
9	Bladder	↓max	35 Gy	
10	Penis Scrotum	↓max	0	
11	Left and right Femur head	↓max	24	

Table 3.1: Wishlist applied for all iBAS and CS plan generations for all 30 study patients. Abbreviations: CS = class solution; iBAS = individualized beam angle selection; PTV = planning target volume; PZ = peripheral zone. LTCP = logarithmic tumor control probability.

*All tissues between 2 and 3 cm from the PTV. †All tissues between the body contour and the body contour-2cm. ‡Depending on PTV homogeneity.

and 15-beam CSs. The latter was only performed for the subset of the 6 recipes, stated below, that resulted in clinically acceptable 25-beam CSs, as selected in the previous step. For these recipes, the 15- and 20-beam CSs were again created using the 10 training patients (step 1 above). However, validation was now performed for all 30 patients (steps 2 and 3 above with 30 instead of 10 patients), with the 20 extra patients serving as an independent test group, not involved in CS generation.

3.2.4 Investigated recipes for beam angle CS creation

The following 6 intuitively promising recipes for CS creation were investigated. For the initial studies on 25-beam CSs (above), these recipes were evaluated in chronological order, each one selected after a failure of the previous one in generating a CS that could

replace iBAS without loss in plan quality. For all but 1 of these 6 recipes the beam selection criteria were based on plan parameters (eg beam weights) of Erasmus-iCycle iBAS plans. For each recipe the methodology for choosing N (equal to 25, 20, or 15) directions for a resulting N-beam CS is described.

- Recipe 1: Choose the N directions that were most frequently found in the iBAS plans of the 10 training patients.
- Recipe 2: Choose N directions that ensure a uniform spread of beams over the entire CyberKnife beam angle space.
- Recipe 3: Choose the N directions with the highest average contributions to PTV D95% in the iBAS plans of the 10 training patients.
- Recipe 4: Choose the N directions with the highest average contributions to PTV Dmean in the iBAS plans of the 10 training patients.
- Recipe 5: Choose the N directions with the highest average contributions to the ratio PTV Dmean/rectum Dmean in the iBAS plans of the 10 training patients.
- Recipe 6: As in recipe 4, choice of directions was based on contribution to PTV Dmean; however, after a priori removal of directions from the CyberKnife beam angle space. In the initial iBAS plans for the 10 training patients, all directions with a large lateral component had high average contributions to PTV Dmean. To favor inclusion of also other directions in CS6, 25 of these lateral directions were first removed from the full 102 direction CyberKnife beam set, and new iBAS-plans were then generated for the 10 training patients using the remaining 77 available angles as input. Recipe 4 was then applied again using the new iBAS-plans. In the remainder of the article, CSi refers to a CS generated with recipe i.

3.2.5 Evaluation and comparison of iBAS and CS plans

Generated plans were evaluated by a physician (S.A.) to verify clinical acceptability. Planning target volume dose delivery was evaluated by V95% and the near-minimum dose, D98%. Organ at risk parameters compared in corresponding iBAS and CS plans were rectum D1cc, V60GyEq, V40GyEq, and Dmean (in accordance with QUANTEC, Quantitative Analysis of Normal Tissue Effects in the Clinic [117]); urethra D1%, D10%, D50%; and bladder D1cc and Dmean. As in our clinical practice, rectum sparing was considered most important in plan generation (see above) and plan comparison. Strong hard constraints on femoral heads, penis, and scrotum (Table 3.1) guaranteed very low doses in all plans, which are not reported in the Results. All CS-iBAS plan comparisons were done after normalizing the higher PTV V95% plan to the lower, to make a comparison

based on OAR sparing with equal PTV coverage, without violating the constraints. Two-sided Wilcoxon signed-rank tests were used to compare plan parameters in iBAS and CS plans. Differences with a P value <.05 were considered statistically significant. To decide on acceptability of a CS, differences with iBAS in mean plan parameter values were considered relevant if both clinically and statistically significant.

3.2.6 Robustness of the final 25-beam CS for changes in PTV margin and PTV dose inhomogeneity

The final 25-beam CS was developed to generate plans for our clinical conditions (e.g. a 3-mm PTV margin and a desired highly inhomogeneous PTV dose distribution). In case of patient treatment without CyberKnife intrafraction prostate tracking, we would use a PTV margin of 5 mm. Other groups apply less inhomogeneous PTV doses as compared with our institution. Therefore, in a separate study we investigated whether the 25-beam CS developed for our clinical situation could still replace iBAS in case of a PTV margin of 5 mm, or a change in the goal value of the second LTCP cost function in the wishlist from 3.1 to 4.1 to generate plans with reduced PTV dose inhomogeneity.

3.3 Results

The upper 3 rows of Table 3.2 show PTV plan parameters for 15-, 20-, and 25-beam iBAS plans, and differences with CS plans generated with recipe 6. As mentioned above, compared iBAS and CS plans were first normalized to have equal PTV V95%. Clearly, near-minimum PTV doses and dose homogeneities also were very similar. Therefore, in the remainder of this article only OAR doses are reported. As visible in Figure 3.1a, CyberKnife M6 node positions are not symmetrically distributed around the patient, especially in the inferior-superior direction. Therefore, in an introductory study we established the preferable patient setup on the treatment couch, to be used in CS and iBAS plan comparisons.

To this purpose, 25-beam iBAS plans, generated with the patient's head directed toward the CyberKnife robot, were compared with plans with the feet pointing toward the robot. This study showed consistently better rectum sparing for the latter plans (on average 2.1 Gy, 0.4%, -1.3%, and 1.0 Gy for D1cc, V60GyEq, V40GyEq, and Dmean, respectively), although bladder D1cc and Dmean were on average increased by 3.8 Gy and 1.0 Gy, respectively (Fig. 3.A1; available at the end of the chapter or online at www.redjournal.org).

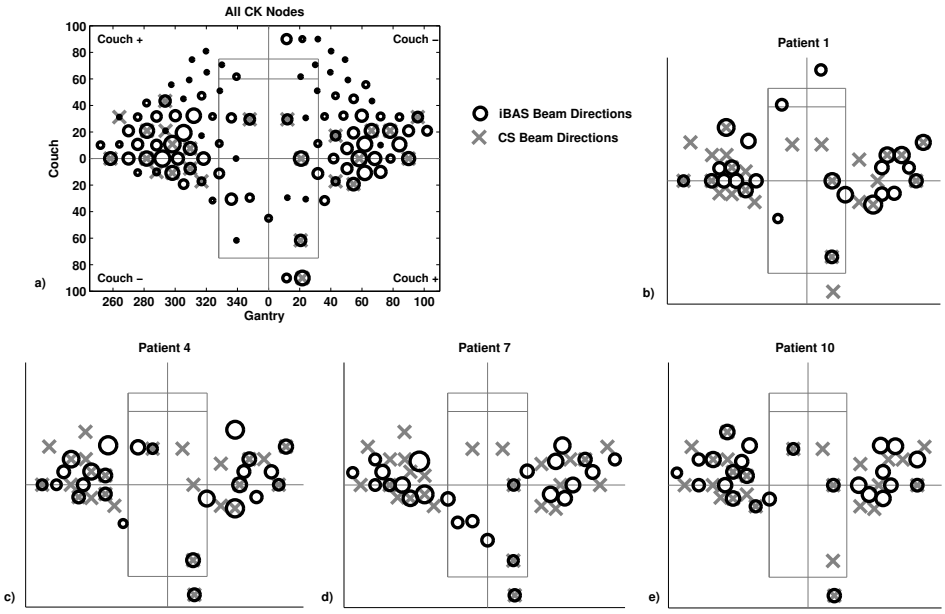

Figure 3.1: (a) The full CyberKnife beam angle space (102 directions, indicated by dots and circles), and the 25 directions in the 25-beam class solution (CS)6 (grey crosses). (b-e) For 4 training patients, beam directions selected with individualized beam angle selection (iBAS) in 25-beam plans (circles) and the 25 CS6 directions (grey crosses). The dots in (a) represent beam directions that were not selected during 25-beam iBAS for any of the 10 training patients. In all graphs, the size of the circles is proportional to the contribution to planning target volume Dmean in iBAS plans; that is, in (a) mean contributions for the 10 training patients are depicted. The couch is schematically represented, and nodes are indicated by their gantry (x) and couch (y) angles.

	25 Beam CS*					20 Beam CS					15 Beam CS				
	iBAS		CS - iBAS			iBAS		CS - iBAS			iBAS		CS - iBAS		
	Mean	**[Range]**	**Mean**	**±SD**	**p**	**Mean**	**[Range]**	**Mean**	**±SD**	**p**	**Mean**	**[Range]**	**Mean**	**±SD**	**p**
PTV															
$V_{95\%}$ (%)	**98.4**	[97.2,99.4]	**-0.1**	±0.2	.005	**98.5**	[97.5,99.6]	**-0.4**	±0.3	<.001	**98.9**	[97.7,100.0]	**-0.3**	±0.3	<.001
$D_{98\%}$ (Gy)	**36.6**	[35.0,38.0]	**-0.2**	±0.3	.007	**36.8**	[35.4,38.3]	**-0.5**	±0.3	<.001	**37.1**	[35.7,38.8]	**-0.4**	±0.4	<.001
$D_{5\%}/D_{95\%}$ ()	**1.5**	[1.5,1.6]	**0.0**	±0.0	.164	**1.5**	[1.5,1.6]	**0.0**	±0.0	.002	**1.5**	[1.4,1.6]	**0.0**	±0.0	.023
Rectum															
D_{1cc} (Gy)	**29.2**	[22.2,34.4]	**0.1**	±0.5	.339	**30.1**	[24.2,35.6]	**-0.7**	±0.6	<.001	**32.0**	[26.6,36.8]	**-0.5**	±0.8	.002
V_{60GyEq} (%)	**1.6**	[0.1,3.5]	**0.1**	±0.2	.289	**2.0**	[0.2,5.5]	**-0.2**	±0.3	<.001	**3.2**	[0.6,10.8]	**-0.4**	±0.5	<.001
V_{40GyEq} (%)	**4.4**	[1.0,8.7]	**0.2**	±0.3	.006	**5.2**	[1.6,12.4]	**-0.3**	±0.3	<.001	**7.7**	[2.4,22.2]	**-0.5**	±0.9	.003
D_{mean} (Gy)	**4.9**	[3.0,7.7]	**0.1**	±0.2	<.001	**5.4**	[3.2,9.3]	**-0.1**	±0.2	<.001	**6.8**	[3.9,13.5]	**-0.3**	±0.5	.002
Urethra															
$D_{1\%}$ (Gy)	**40.5**	[39.7,42.1]	**-0.1**	±0.4	.133	**40.5**	[39.8,41.9]	**-0.4**	±0.5	<.001	**40.6**	[39.9,41.5]	**-0.5**	±0.5	<.001
$D_{10\%}$ (Gy)	**39.6**	[38.8,40.9]	**-0.1**	±0.5	.537	**39.7**	[38.6,41.2]	**-0.4**	±0.5	<.001	**39.8**	[39.0,40.7]	**-0.4**	±0.4	<.001
$D_{50\%}$ (Gy)	**37.9**	[36.6,39.4]	**-0.0**	±0.4	.918	**38.1**	[36.7,39.4]	**-0.3**	±0.4	.001	**38.3**	[36.5,39.5]	**-0.3**	±0.4	<.001
Bladder															
D_{1cc} (Gy)	**42.2**	[36.0,45.2]	**0.5**	±0.4	<.001	**42.1**	[35.3,44.9]	**0.7**	±0.6	<.001	**42.3**	[36.0,44.5]	**0.5**	±0.6	<.001
D_{mean} (Gy)	**10.6**	[4.3,15.8]	**1.1**	±0.7	<.001	**11.5**	[5.0,16.9]	**1.1**	±0.9	<.001	**13.1**	[6.6,18.9]	**0.9**	±1.1	<.001

Table 3.2: For 15, 20, and 25 beams, comparisons of iBAS and CS6 plans including all 30 patients. Absolute values for iBAS plans are presented and absolute differences between CS6 and iBAS.* Difference statistically significant, but smaller than .05.

25 Beams CS*	3mm PTV margin, Normal Inhomog.					5mm PTV margin, Normal Inhomog.					3mm PTV margin, Lower Inhomog.				
	iBAS**		CS - iBAS			iBAS		CS - iBAS			iBAS		CS - iBAS		
	Mean	[Range]	Mean	±SD	p	Mean	[Range]	Mean	±SD	p	Mean	[Range]	Mean	±SD	p
PTV															
$V_{95\%}$ (%)	**98.2**	[97.0,99.5]	**0.0**	±0.0	1.000	**98.4**	[97.5,98.9]	**0.0**	±0.0	1.000	**98.2**	[97.2,99.4]	**0.0**	±0.0	1.000
$D_{98\%}$ (Gy)	**36.3**	[34.9,37.8]	**0.0**	±0.1	.140	**36.5**	[35.4,37.1]	**0.0**	±0.1	.460	**36.4**	[35.0,38.0]	**0.0**	±0.1	.430
$D_{5\%}/D_{95\%}$ ()	**1.4**	[1.3,1.5]	**0.0**	±0.0	.990	**1.5**	[1.5,1.6]	**0.0**	±0.0	.030	**1.6**	[1.5,1.6]	**0.0**	±0.0	.200
Rectum															
D_{1cc} (Gy)	**29.0**	[21.8,33.7]	**0.1**	±0.4	.050	**34.1**	[26.1,37.1]	**-0.3**	±0.7	.050	**29.0**	[21.9,34.4]	**0.2**	±0.4	.010
V_{60GyEq} (%)	**1.5**	[0.1,3.3]	**0.1**	±0.1	.010	**4.2**	[0.6,8.4]	**-0.2**	±0.4	<.001	**1.5**	[0.1,3.4]	**0.1**	±0.2	<.001
V_{40GyEq} (%)	**4.1**	[0.9,8.2]	**0.2**	±0.2	<.001	**8.0**	[2.2,15.1]	**-0.6**	±0.7	<.001	**4.3**	[1.0,8.7]	**0.2**	±0.3	<.001
D_{mean} (Gy)	**4.6**	[2.8,7.0]	**0.1**	±0.1	<.001	**6.4**	[3.7,10.0]	**-0.7**	±0.7	<.001	**4.9**	[3.0,7.7]	**0.1**	±0.2	<.001
Urethra															
$D_{1\%}$ (Gy)	**40.0**	[39.0,40.9]	**0.1**	±0.5	.170	**40.4**	[38.7,41.6]	**-0.5**	±0.7	<.001	**40.2**	[39.0,41.8]	**0.1**	±0.5	.520
$D_{10\%}$ (Gy)	**39.2**	[38.0,40.1]	**0.1**	±0.4	.110	**39.5**	[37.9,40.6]	**-0.4**	±0.6	<.001	**39.3**	[38.4,40.6]	**0.1**	±0.5	.270
$D_{50\%}$ (Gy)	**37.7**	[36.3,39.0]	**0.2**	±0.4	.040	**38.0**	[36.6,39.3]	**-0.3**	±0.6	.010	**37.7**	[36.3,39.2]	**0.2**	±0.5	.040
Bladder															
D_{1cc} (Gy)	**40.5**	[33.8,44.0]	**0.6**	±0.5	<.001	**43.0**	[38.4,44.8]	**-1.2**	±1.6	<.001	**41.9**	[35.7,45.2]	**0.7**	±0.6	<.001
D_{mean} (Gy)	**9.3**	[2.9,14.7]	**1.1**	±0.6	<.001	**12.8**	[5.2,20.4]	**-1.4**	±2.0	<.001	**10.6**	[4.3,15.8]	**1.1**	±0.7	<.001

Table 3.3: For all 30 patients, comparison of 25-beam iBAS and CS6 plans for: (1) the clinical PTV margin and dose homogeneity (left columns); (2) an increased PTV margin (middle columns); and (3) a reduced PTV dose inhomogeneity (right columns).CS6 was derived using the clinical settings. Absolute values for iBAS plans are presented and absolute differences between CS6 and iBAS. *CS = Class Solution. **iBAS = individualized Beam Angle Selection.

In the remainder of the study, plans were generated for a patient set up with the feet in the direction of the robot. Figure 3.1b-e shows examples of individualized beam angle selection. Although there are clear differences between the 4 presented patients in selected orientations, all patients show a strong preference for beam angles with a large lateral component (compare with Fig. 3.1a).

3.3.1 Selection of the final recipe for generation of acceptable CSs

For each of the investigated CS recipes, Figure 2 shows the differences in rectum parameters between 25-beam CS and iBAS plans for the 10 training patients. Clearly, CS6 resulted in rectum doses that were very similar to those obtained with iBAS. With recipes 2, 3, and 5, for each patient, all rectum plan parameters were deteriorated in the CS plans. Recipes 1 and 4 resulted in CSs with some deterioration in rectum doses, which were smallest with the former. These observations led to the decision to consider recipes 1 and 6 for further validation and use them to generate also CSs for 15- and 20-beam plans, to be compared with iBAS plans with equal numbers of beams.

Figure 3.3 shows for recipes 1 and 6 differences in rectum dose delivery for all 30 patients for 15, 20, and 25 beams, clearly demonstrating that only recipe 6 resulted in acceptable CS rectum dose delivery for all beam numbers. Table 3.2 confirms the acceptability of rectum doses in the CS6 plans. Furthermore, it shows that also urethra and bladder dose parameters in the CS6 plans were very close to those in the iBAS plans. Therefore, recipe 6 is the preferred recipe for CS generation. Figure 3.1a shows graphically which beam directions were selected in the 25-beam CS6 (grey crosses). Figure 3.1b-e compares the 25-beam CS6 (grey crosses) with the 25 beams selected in the iBAS plans for 4 randomly selected training patients.

3.3.2 Robustness of the final 25-beam CS for changes in PTV margin and required PTV dose inhomogeneity

The 25-beam CS6 was created using plans with a (clinical) PTV margin of 3 mm and a clinically realized D5%/D95% of 1.54 ± 0.03. Table 3.3 shows that using CS6 to generate plans for a PTV margin of 5 mm or a D5%/D95% of 1.42 ± 0.00 resulted in very similar OAR dose parameters as in corresponding iBAS plans, for all 30 patients.

3.3.3 Optimization time reduction

Using CS6 instead of iBAS in treatment planning (i.e. avoiding computationally expensive individualized beam angle selection) resulted in a reduction in optimization time

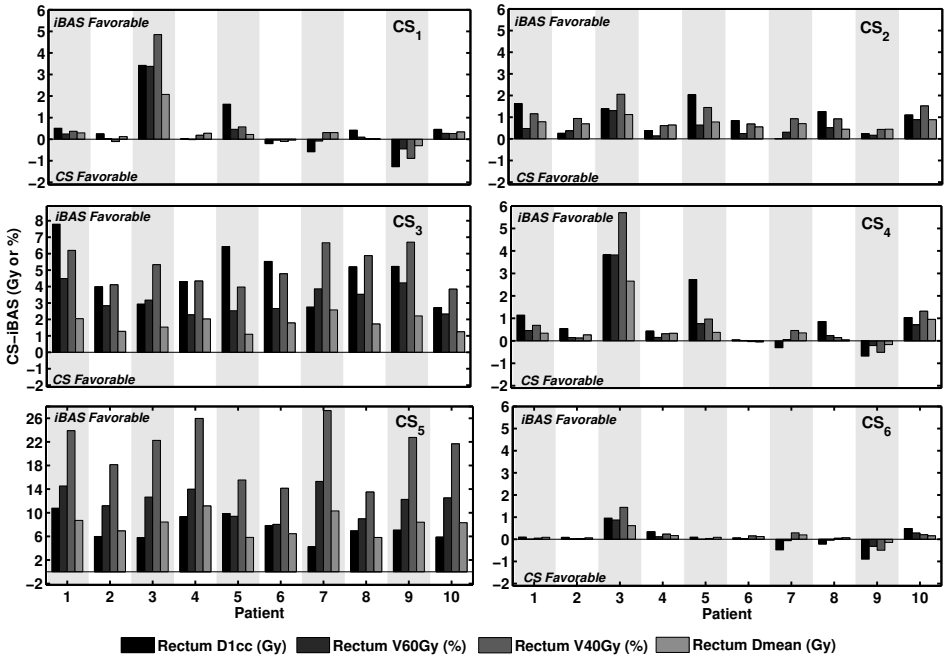

Figure 3.2: For all 6 investigated class solution (CS) recipes, comparison of rectum plan parameters for 25-beam individualized beam angle selection (iBAS) plans with corresponding 25-beam CS plans generated for the 10 training patients. Positive differences point at higher rectum doses for CS plans.

by a factor 14 to 25 without loss in plan quality. Optimization times of 4 and 13 hours for 15- and 25-beam iBAS plans decreased to 17 and 31 minutes for 15- and 25-beam CS6 plans. The calculations were performed on a dual Intel Xeon E5-2690. The code was multi-threaded and used all 16 central processing unit cores.

3.4 Discussion

In this study we investigated 6 recipes for generation of beam angle CSs for robotic prostate SBRT, to be used instead of beam angle optimization for each individual patient. A CS was considered acceptable if it resulted in clinically insignificant deteriorations in plan quality compared with iBAS. The idea of this project came from an observation in our previous work [143] of high frequency of selection of beams from the 2 lateral areas in iBAS plans for all patients.

Although all investigated recipes were intuitively considered promising, in the end only 1 resulted in acceptable CSs for 15-, 20-, and 25-beam plans. The initial studies

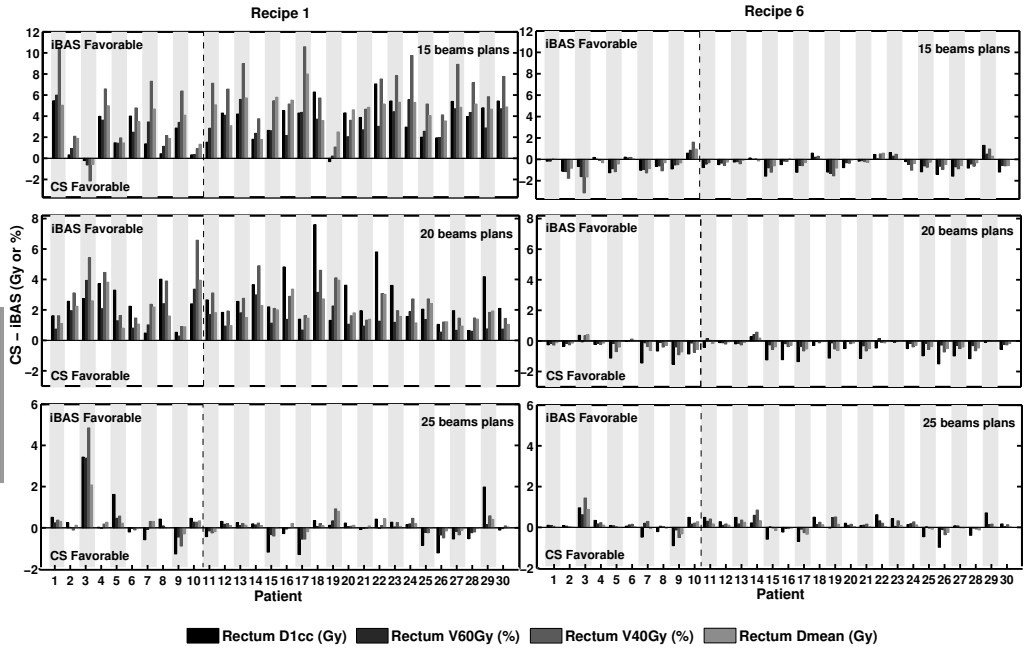

Figure 3.3: For recipes 1 (left) and 6 (right), comparison of rectum plan parameters for 15-, 20-, and 25-beam individualized beam angle selection (iBAS) plans with rectum parameters in the related 15-, 20-, and 25-beam class solution (CS) plans for all 30 patients. The first 10 patients are the training patients. Positive differences point at higher rectum doses for CS plans.

using only the 10 training patients and 25-beam plans were performed in chronological order, starting with recipe 1 and ending with recipe 6. Every time, a new recipe was introduced because the previous one was not found convincing owing to plan quality loss compared with iBAS. The first 4 recipes were rather straightforward, but these simple recipes did not result in acceptable CSs. Additionally, recipe 5 was not successful, considering both PTV Dmean and rectum Dmean together, but performing even worse than some of the simpler ones. The finally selected recipe 6 is a refinement of recipe 4. Because of the abundance of lateral beams with high PTV Dmean contributions in the 25-beam iBAS plans (Fig. 3.1a), the latter recipe resulted in a 25-beam CS with almost exclusively directions belonging to the 2 lateral areas. With the high focus on the lateral areas and the resulting lack of other directions, recipe 4 did not perform well. It was hypothesized that if some of the beams within these highly populated lateral areas (in practice 25) were removed from the input set for iBAS, equal quality iBAS plans would be generated with missing directions being substituted by remaining neighboring directions. This was indeed confirmed, and plans with no significant quality loss compared with the original iBAS plans, generated with the full CyberKnife beam angle search

space, were created. Applying then again recipe 4 (ie direction selection based on high PTV Dmean weights), the successful CS6 could be created, including also beams outside the lateral areas.

As shown in Figure 3.3 and Table 3.2, for 15-beam and 20- beam plans, CS6 performed on average even slightly better than iBAS. We do not have a definitive explanation for this. Beam angle selection is a discrete, non-convex, combinatorial problem with possibilities of finding (slightly) suboptimal solutions. Possibly, for the smaller beam numbers, some uncertainty or randomness inherent in the process used by iBAS to find the highest-quality solutions can be avoided by using CS6, which assures the use of fixed directions that, according to recipe 6, performed best on average for the population.

For this project, a large number of plans was generated: 70 plans for the pre-selection of the 2 most promising recipes, 240 more plans to select the final recipe and validate it, and another 120 plans to verify robustness of the final 25-beam CS for a change in PTV margin or prescribed PTV dose inhomogeneity. Additional plans were generated for the a a priori establishment of the wishlist for generation of high quality, clinically desirable plans. Clearly, without automated treatment planning as provided by Erasmus-iCycle, it would not have been possible to generate all these plans. Moreover, because of the automation using a unique wishlist, plan quality was not operator dependent, avoiding undesirable variations in quality (”noise”) and potential bias in the comparison of iBAS and CS plans. Another strong point of this study is that for the final recipe choice, CS and iBAS plan comparisons were not only performed for the 10 training patients used to generate the CSs but also for 20 independent patients, not considered during CS creation. What is clear is that we could identify a recipe that worked for generation of high-quality 15- to 25-beam beam-angle CSs. The 25-beam CS was also proven to be robust for changes in PTV margin and prescribed PTV dose inhomogeneity (not investigated for the 15- and 20-beam CSs). Only a few articles about coplanar CS generation are available in the literature [97, 123, 191]. This study cannot guarantee that alternative CSs do not exist that perform even better on average, nor can it guarantee that a simpler or less computationally expensive recipe cannot be generated. Clinical plans for the CyberKnife are generated with the Multiplan TPS, also provided by Accuray Inc. One of our future research topics is a study on the impact of the selected CS on plan quality and treatment planning time with Multiplan. We will also investigate whether the same recipe would work for other treatment sites.

3.5 Conclusions

Using an in-house TPS for automated IMRT treatment plan generation and individualized beam angle selection, we developed a recipe for generation of beam angle CSs for

robotic prostate SBRT, to be used instead of time-consuming beam angle optimization for each individual patient. Using the developed recipe, 15-, 20-, and 25-beam CSs could be established without loss in plan quality compared with patient-specific beam angle selection. With the CS, 25-beam plans could be generated in 31 minutes, compared with 13 hours for iBAS. Establishing a recipe for creation of high-quality beam angle CSs can be a non trivial task, because intuitively promising candidate recipes can severely fail.

Supplementary material

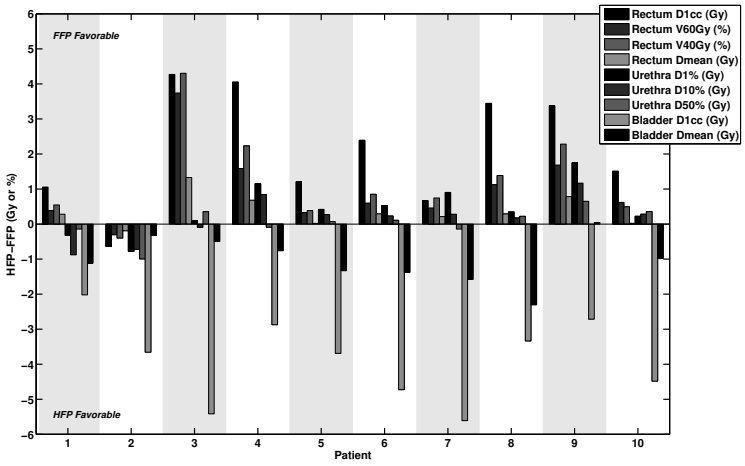

Figure 3.A1: Supplementary Figure. For all 10 training patients, comparison of rectum, urethra and bladder parameters for 25-beam iBAS plans with head first position (HFP), i.e. with head pointing towards the robot, and feet first position (FFP) patient setup. Positive differences point at higher OAR doses for HFP plans.

First fully automated planning solution for robotic radiosurgery - comparison with automatically planned volumetric arc therapy for prostate cancer

4

Linda Rossi, Abdul Wahab Sharfo, Shafak Aluwini,
Maarten Dirkx, Sebastiaan Breedveld, Ben Heijmen

Department of Radiation Oncology,
Erasmus MC, Rotterdam

Published:
Acta Oncol
57, 11 (2018), 1490–1498

Abstract

Background: For conventional radiotherapy treatment units, automated planning can significantly improve plan quality. For robotic radiosurgery, systems for automatic generation of clinically deliverable plans do not yet exist. For prostate stereotactic body radiation therapy (SBRT), few studies have systematically compared VMAT with robotic treatment.

Material and Methods: The multi-criteria autoplanning optimizer, developed at our institute, was coupled to the commercial treatment planning system of our robotic treatment unit, for fully automated generation of clinically deliverable plans (autoROBOT). The system was then validated by comparing autoROBOT plans with manually generated plans. Next, the autoROBOT system was used for systematic comparisons between autoROBOT plans and VMAT plans, that were also automatically generated (autoVMAT). CTV–PTV margins of 3 mm were used for autoROBOT (clinical routine) and autoVMAT plan generation. For autoVMAT, an extra plan was generated with 5 mm margin (often applied for VMAT). Plans were generated for a 4x9.5 Gy fractionation scheme.

Results: Compared to manual planning, autoROBOT improved rectum D_{1cm^3} (16%), V_{60GyEq} (75%) and D_{mean} (41%), and bladder D_{mean} (37%) (all $p \leq 0.002$), with equal PTV coverage. In the autoROBOT and autoVMAT comparison, both with 3 mm margin, rectum doses were lower for autoROBOT by 5% for rectum D_{1cm^3} ($p=0.002$), 33% for V_{60GyEq} ($p=0.001$), and 4% for D_{mean} ($p=0.05$), with comparable PTV coverage and other OAR sparing. With 5 mm margin for VMAT, 18/20 plans had a PTV coverage lower than requested (<95%) and all plans had higher rectum doses than autoROBOT (mean percentage differences of 13% for D_{1cm^3}, 69% for V_{60GyEq}, and 32% for D_{mean} (all $p<0.001$)).

Conclusion: The first system for fully automated generation of clinically deliverable robotic plans was built. Autoplanning did largely enhance robotic plan quality, compared to manual planning. Using autoplanning for both the robotic system and VMAT, superiority of non–coplanar robotic treatment compared to coplanar VMAT for prostate SBRT was demonstrated.

4.1 Introduction

In prostate stereotactic body radiation therapy (SBRT), patients are treated with large fraction doses, requiring high accuracy delivery and with image–guided dose delivery [6, 18, 24, 55, 57, 74, 81, 89, 108, 176]. Both C–arm linacs [43, 82, 94, 194] and robotic units [6, 55, 57, 81, 89, 176]. have been used for prostate SBRT.

Recent findings on the potential added value of non–coplanar setups for prostate SBRT instead of coplanar treatment are contradictory [43, 102, 107, 143]. Two recent studies have compared robotic treatment and VMAT for prostate SBRT [102, 107]. MacDougall et al. [107] found no discernible dosimetric differences, based on only 6 patients. Lin et al. [102] concluded that VMAT was preferable because of reduced treatment time and superior dose distribution conformality. In both studies, all plans were generated manually, and clinically delivered plans were retrospectively compared with an alternative plan. Both the manual planning and retrospective comparisons may have introduced bias and noise in the technique comparisons.

Recently, several systems have been proposed for planning automation [22, 93, 137, 138, 169, 185, 197, 199, 201], all for treatment with C–arm linacs. In this work, we have developed the first system for automatic generation of deliverable plans for non–coplanar robotic treatment (autoROBOT). Basis of the autoROBOT planning system is a multicriterial optimizer that was also the core of a recently developed system for automatic VMAT plan generation for C–arm linacs [156, 185]. The developed autoROBOT planning system was first evaluated by comparing manually generated prostate SBRT plans with autoROBOT plans. We then used the autoROBOT and autoVMAT planning systems to systematically compare robotic and VMAT treatment for prostate SBRT. The use of exactly the same plan optimization scheme for autoROBOT and autoVMAT (described below) allowed bias–free technique comparisons and allowed generation of new input for the on–going debate [43, 102, 107, 143] on potential added value of non–coplanar prostate SBRT, compared to coplanar treatment.

4.2 Materials and Methods

4.2.1 Patients

In this study, contoured CT scans of 20 prostate SBRT patients, previously treated with the robotic M6 CyberKnife (Accuray Inc, Sunnyvale, USA), were used. A planning target volume (PTV) with a 3 mm isotropic margin around the prostate (PTV3mm) was used for

clinical planning [176]. In the investigations, both autoROBOT and autoVMAT plans were generated for PTV_{3mm}. AutoVMAT plans were also generated for PTV_{5mm}, as often applied for C–arm linac prostate SBRT. Average PTV_{3mm} and PTV_{5mm} sizes were 91.2 cm^3 [57.8-142.3 cm^3] and 109.5 cm^3 [71.1-165.7 cm^3], respectively.

Contoured OARs were rectum (outer contour), rectal mucosa (3 mm wall), bladder, urethra, femoral heads, scrotum and penis. All plans simulated delivery of 38 Gy in 4 fractions, with highly heterogeneous dose distributions to emulate high dose–rate brachytherapy dosimetry [143].

Five patients were used for configuration of the autoROBOT and autoVMAT planning systems (below). The automated workflows were then applied to all 20 patients. For validation of the autoROBOT planning system, autoROBOT plans for the first 10 study patients were compared to the manually generated and clinically delivered plans. For all 20 patients, autoROBOT plans were compared with $autoVMAT_{3mm}$ plans and $autoVMAT_{5mm}$ plans.

4.2.2 Automated plan generation

4.2.2.1 The autoVMAT and autoROBOT planning systems

Basis of autoROBOT and autoVMAT plan generation was the Erasmus–iCycle multi–criterial optimizer for generating Pareto–optimal and clinically favorable plans [22]. For practical and legal reasons, Erasmus–iCycle plans cannot be directly used clinically. However, we have recently coupled Erasmus–iCycle to the Monaco treatment planning system (TPS) (Elekta AB, Stockholm, Sweden) for fully automated, multi–criterial generation of IMRT and VMAT plans for clinical delivery at a linac; based on the Erasmus–iCycle dose distribution, a patient–specific Monaco template is automatically produced, to be used for automated final plan generation. Effectively, Erasmus–iCycle first optimizes the plan, while Monaco converts it into a clinically deliverable plan, see [185] for details. The resulting plan quality is equal, or superior to the quality of manually generated plans, and the system is now in routine clinical use [38, 67, 155, 185, 186].

For this study, we have configured (see below) the system for generating dual, full–arc autoVMAT plans for prostate SBRT according to our clinical protocol, deliverable at an Elekta linac equipped with an Agility MLC. Final plans were generated with Monaco version 5.10 (Elekta AB, Stockholm, Sweden).

For automated multi–criterial generation of autoROBOT plans, a special version of Erasmus–iCycle was prepared for plan optimization for the IRIS variable aperture collimator (Accuray AB, Sunnyvale, USA), mounted on the CyberKnife. Basis was a previously

developed version for optimization with fixed cone diameters and non–coplanar beam set–ups [189]. This system was modified to handle the available non–coplanar beam directions (nodes) of our novel M6 CyberKnife systems and the IRIS collimator, i.e. 117 node positions from the full body path. For fully automated generation of final, deliverable plans, this Erasmus–iCycle version was coupled to the Multiplan TPS (version 5.1.3) that comes with the CyberKnife, similar to the system built for linacs (above). Similar to the linac solution, automatically produced individualized planning templates were used as intermediate between Erasmus–iCycle and Multiplan, aiming at generating clinically deliverable plans that dosimetrically mimicked the initial Erasmus–iCycle plans. As in clinical practice, the goal was to keep the delivery time below 45 min. Apertures from 10 to 40 mm diameter could be selected, as used clinically for manually generated plans.

4.2.2.2 Configuration of autoVMAT and autoROBOT planning

As described above, both for autoVMAT and autoROBOT planning, Erasmus–iCycle is used for plan optimization, while the respective clinical planning systems are used for mimicking the Erasmus–iCycle plan. Plan generation with Erasmus–iCycle is based on a 'wish–list', containing the hard planning constraints and planning objectives with their goal values and assigned priorities [22]. For each treatment site/treatment technique, a dedicated wish–list is configured, which is then used for automated plan generation for all involved patients, without further change.

In this study a single wish–list was generated and applied both for autoVMAT and autoROBOT planning.

Using the same wish–list for both techniques is a key aspect of this study, since it allowed to perform a fair like for like comparison of the two delivery techniques. Technical details on the developed wish–list for prostate SBRT are presented in supplementary material.

4.2.3 Plan evaluation and comparison

In this study, plan comparisons were mainly focused on our clinical aims. For the PTV, the near–minimum dose ($D_{98\%}$) and the coverage ($V_{100\%}$) were evaluated. A coverage of 95% is requested for clinical plans ($V_{100\%}$=95%), while a coverage between 93% and 95% is still acceptable if necessary to fulfil OAR constraints. Rectum is considered the most important OAR, focusing at the high doses with D_{1cm^3} <32.3 Gy. For bladder, the D_{1cm^3} requirement is <38 Gy. Urethra $D_{50\%}$ and $D_{5\%}$ constraint values are 40 and 45.5 Gy, respectively.

Apart from these clinically used plan parameters, we also evaluated and compared

D_{mean} for both rectum and bladder, V_{40Gy} and V_{60Gy} (2 Gy/fx equivalent dose) for rectum, as suggested by QUANTEC [117], as well as the dose bath, looking at patient volumes receiving >30, >20, >10, >5 and >3 Gy, as 5% of maximum dose.

When PTV coverage was achieved (>95%) for both plans, the plan with the slightly higher coverage was re–normalized to the value of the other plan. This approach minimized bias in comparison of OAR doses, related to different PTV coverages. Two–sided Wilcoxon signed–rank tests were performed to compare plan parameters, using $p<.05$ as cut–off for statistical significance.

Apart from plan quality comparisons based on DVH metrics, for each patient, autoROBOT and autoVMAT plans were also compared by the participating clinician (S.A), who scored quality differences using Visual Analogue Scales (VAS) as presented in the Results section. PTV, rectum, bladder, urethra, and overall quality were scored separately. In total 40 of these plan comparisons (20 patients; autoROBOT vs. $autoVMAT_{3mm}$ and autoROBOT vs. $autoVMAT_{5mm}$) were performed in a random order. In each comparison, the two plans were presented side–by–side to the clinician, who did not know which plan was presented on the left and which on the right of the screen (also here random ordering).

To investigate clinical deliverability of automatically generated plans, dosimetric Quality Assurance (QA) was performed , as done in our clinical routine. To this purpose, for 5 arbitrarily selected patients, independent dose calculations were performed for the autoROBOT plans, and measurements for autoVMAT plans with 3 and 5 mm margin. For the autoROBOT plans, beam directions and weights were used to recalculate the entire 3D dose distribution with the Monte–Carlo dose computation software SciMoCa (Scientific RT, Munich). For autoVMAT, plans were delivered while irradiating a 2D–array in an Octavius phantom (PTW, Freiburg). 3D (autoROBOT) and 2D (autoVMAT) gamma analyses were performed with 5% cut-off, 3% global maximum dose and 1 mm distance to agreement (3%/1mm) criteria, and 95% passing rate threshold.

4.3 Results

4.3.1 autoROBOT vs. manual robotic planning

All manually and automatically generated plans for robotic treatment fulfilled clinical requirements.

Automated planning improved plan quality compared to the manually generated plans used for patient treatments, as visible in population average DVHs in figure 4.1. Differ-

ences in PTV coverage were negligible (95.0% and 95.2% for manual and autoROBOT plans (p=0.9)), but large differences in OAR doses were observed; each patient plan improved with automated planning compared to manual planning. On average, rectum D_{1cm^3} was reduced from 31.2 to 26.3 Gy (16% reduction, p=0.002), V_{60Gy} from 2.4 to 0.6% (75% reduction, p=0.002) and rectum D_{mean} from 10.4 to 6.1 Gy (41% reduction, p=0.002). Bladder D_{mean} was improved from 14.0 (manual planning) to 6.1 Gy with automated planning (36% reduction, p=0.002).

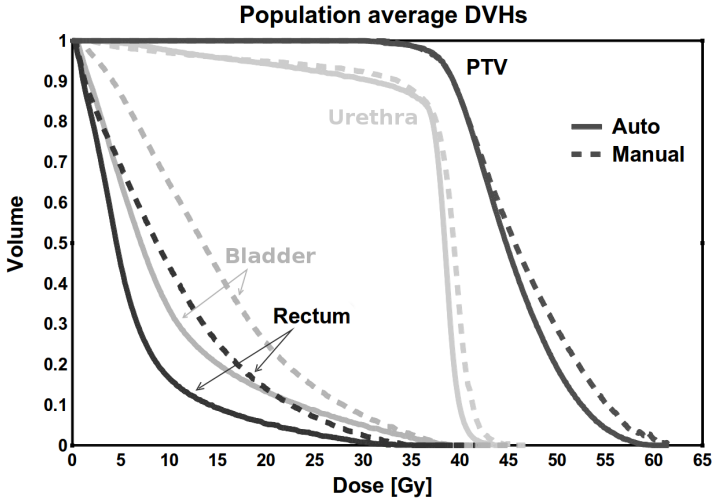

Figure 4.1: Population average DVHs for automatically generated robotic plans (autoROBOT, solid lines) and manually generated robotic plans (Manual, dashed lines), the latter used for patient treatment.

4.3.2 autoROBOT vs. autoVMAT plan quality

4.3.2.1 autoROBOT vs. autoVMAT$_{3mm}$

Both the autoROBOT and autoVMAT$_{3mm}$ plans with $V_{100\%}$ >95% could be generated for all patients, as visible in table 4.1. The near–minimum PTV dose was on average slightly higher for autoROBOT plans and the CI was lower (Table 4.1, Fig. 4.3A).

For the rectum (highest priority OAR), all parameters were on average lower for the autoROBOT with reduction of 5% for D_{1cm^3}, 32% for V_{60GyEq}, 22% for V_{40GyEq} and 4% for D_{mean}, (Table 4.1, Fig. 4.3B). Superiority in rectum dose parameters was observed in 15-17 of the 20 study patients (Table 4.1), where differences were considered to have real clinical impact for 8 patients (see clinical scoring below). For the 3-5 patients with a rectum dose advantage for autoVMAT$_{3mm}$, the differences with the robotic system were always small

	autoROBOT	autoVMAT$_{3mm}$				autoVMAT$_{5mm}$			
		VMAT - ROBOT [%]*				VMAT - ROBOT [%]			
	Mean [Range]	**Mean**	**Mean** [Range]	**p**	**#Pts****	**Mean**	**Mean** [Range]	**p**	**#Pts**
PTV									
$V_{100\%}$ [%]	**95.2** [95.0,95.5]	**95.3**	**0** [-1,0]	.3	8	**92.7**	**3** [0,7]	<.001	20
$D_{98\%}$ [Gy]	**36.1** [35.2,36.9]	**35.8**	**1** [-2,3]	.01	13	**33.7**	**7** [3,13]	<.001	20
CI***	**1.1** [1.1,1.1]	**1.2**	**6** [3,10]	<.001	20	**1.2**	**6** [2,10]	<.001	20
Rectum									
D_{1cm^3} [Gy]	**28.0** [23.0,33.5]	**29.4**	**5** [-3,18]	.002	16	**32.2**	**13** [1,23]	<.001	20
V_{60GyEq} [%]	**1.1** [0.3, 2.6]	**1.5**	**32** [-26,77]	.001	17	**3.3**	**69** [15,89]	<.001	20
V_{40GyEq} [%]	**3.8** [1.9, 6.0]	**4.9**	**22** [-13,56]	<.001	17	**9.2**	**58** [24,76]	<.001	20
D_{mean} [Gy]	**6.3** [4.2, 7.7]	**6.6**	**4** [-18,25]	.05	15	**9.3**	**32** [14,45]	<.001	20
Bladder									
D_{1cm^3} [Gy]	**37.4** [36.4,39.1]	**37.2**	**-1** [-6,2]	.3	9	**37.6**	**0** [-3,3]	.4	12
D_{mean} [Gy]	**9.7** [6.5,13.0]	**8.4**	**-18** [-45,7]	<.001	2	**9.3**	**-6** [-32,15]	.1	7
Urethra									
$D_{5\%}$ [Gy]	**40.4** [39.4,42.3]	**40.9**	**1** [-4,6]	.06	13	**41.6**	**3** [-3,8]	.001	17
$D_{50\%}$ [Gy]	**38.3** [37.5,39.2]	**38.5**	**1** [-3,3]	.2	14	**39.1**	**2** [-1,6]	<.001	17
Patient									
V_{3Gy} [cc]	**4910** [3428,7064]	**4378**	**-12** [-30,11]	.001	4	**4669**	**-5** [-22,16]	.05	6
V_{5Gy} [cc]	**3143** [2147,4779]	**3538**	**12** [-5,28]	<.001	18	**3864**	**19** [3,35]	<.001	20
V_{10Gy} [cc]	**1137** [737,1872]	**1583**	**29** [19,37]	<.001	20	**1789**	**37** [24,47]	<.001	20
V_{20Gy} [cc]	**293** [203,442]	**342**	**14** [5,20]	<.001	20	**392**	**25** [17,34]	<.001	20
V_{30Gy} [cc]	**150** [103,229]	**159**	**5** [0, 9]	<.001	20	**182**	**18** [12,24]	<.001	20

Table 4.1: For all 20 patients, comparisons of autoROBOT with autoVMAT$_{3mm}$ and autoVMAT$_{5mm}$ plans.
*Percentage differences are expressed as $\pm|100 * (\text{autoVMAT} - \text{autoROBOT})/\text{autoVMAT}|$ with positive differences representing better performance for robotic.
**Number of patients with superior plan parameter quality for robotic treatment.
***CI = Conformity index (= patient volume receiving the prescribed dose / PTV volume receiving prescribed dose)

and only for one patient considered clinically significant (see clinical scoring below).

AutoVMAT$_{3mm}$ performed significantly better for bladder Dmean, but the difference in the most important parameter, D_{1cm^3}, was small (1%) and statistically insignificant (Table 4.1). Differences in urethra dose parameters were statistically insignificant.

For all patients, the autoROBOT was superior regarding patient volumes receiving >5, >10, >20, and >30 Gy (Table 4.1 and Fig. 4.3D), with percentage mean differences of 12% for V_{5Gy}, 29% for V_{10Gy}, 14% for V_{20Gy}, and 5% for V_{30Gy}. AutoVMAT$_{3mm}$ performed better for patient volumes receiving >3 Gy, with mean percentage improvement of 12%.

Figure 4.2 shows axial dose distributions for patient 17, who demonstrated the largest advantages for autoROBOT in rectum plan parameters compared to autoVMAT (see also Fig. 4.3B), and for patient 13, with the largest rectum advantages for VMAT. Apart from a better rectum sparing, in patient 17, autoROBOT plan also showed better dose conformality, in agreement with Fig. 4.3D.

All autoROBOT and autoVMAT$_{3mm}$ plans were clinically acceptable for the participating clinician. The comparisons as presented in the upper panel of Fig. 4.4, are in line with the plan parameter evaluations above. PTV doses were found of equal quality for all patients. Apart from one patient with a small advantage for autoVMAT$_{3mm}$, rectum dose was considered equal or superior for autoROBOT. For bladder there was a balance, with only equal plan quality or small differences scored. For the urethra, the clinician had a slight preference for the autoROBOT. Overall, for 13 patients the clinician preferred autoROBOT, for 2 patients he preferred the autoVMAT$_{3mm}$ plan, and for 5 patients he scored equal quality.

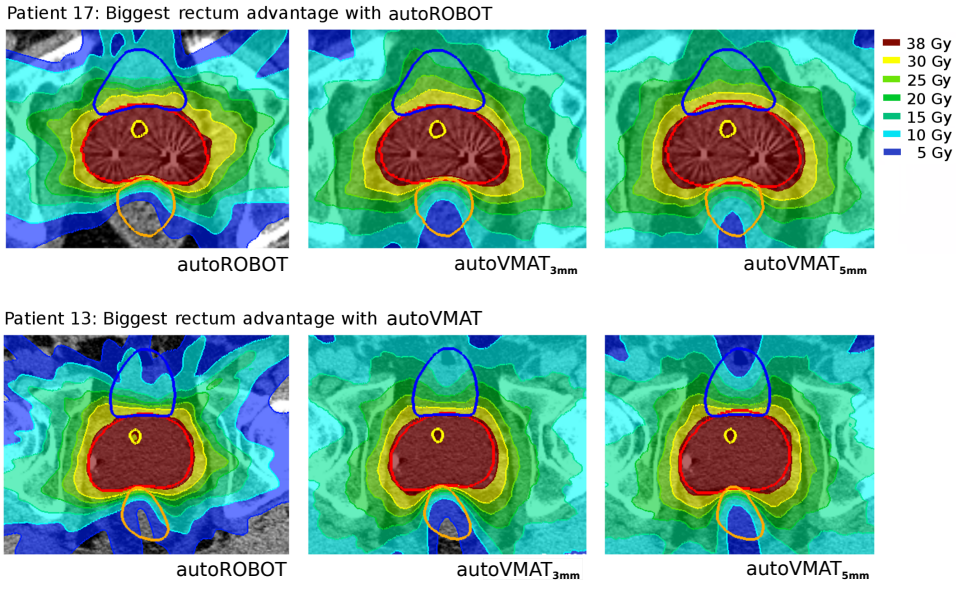

Figure 4.2: Axial dose distributions for autoROBOT, autoVMAT$_{3mm}$ and autoVMAT$_{5mm}$, for patients 17 (upper panels) and 13 (lower panels). These patients demonstrated the most pronounced advantage in rectum dose for autoROBOT instead of autoVMAT (patient 17), and the most pronounced advantage using autoVMAT compared to autoROBOT (patient 13) (see also Figure 4.3B and 4.3F). Red contour = PTV (3 mm or 5 mm), orange contour = rectum , blue contour = bladder and yellow contour = urethra.

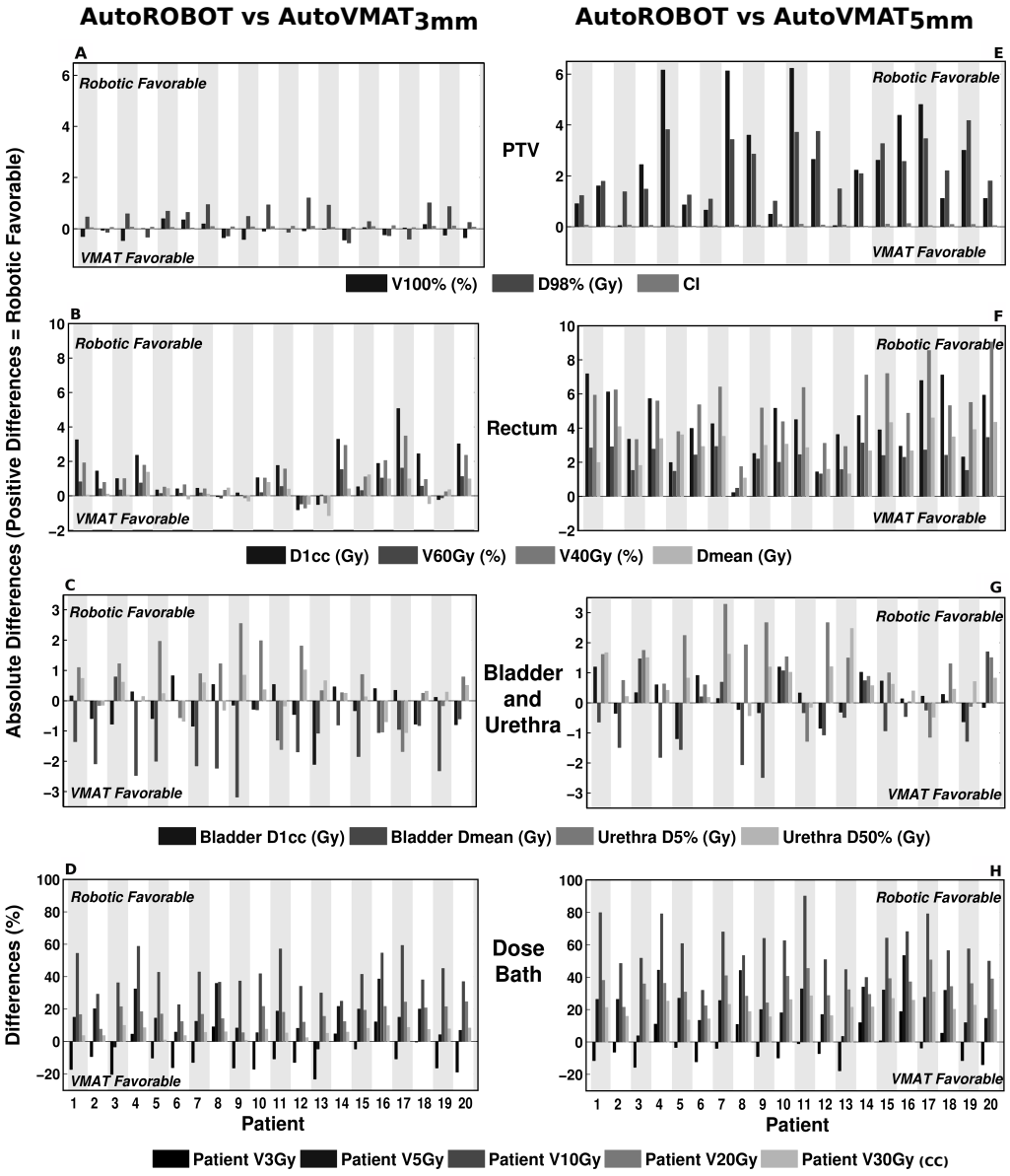

Figure 4.3: For all 20 patients, differences between autoROBOT and autoVMAT$_{3mm}$ (left panels), or autoVMAT$_{5mm}$ (right panels), expressed as $\pm|$autoVMAT $-$ autoROBOT$|$ with positive values representing better quality for autoROBOT. For dose bath percentage differences as $\pm|100 * (\text{VMAT} - \text{ROBOT})/\text{VMAT}|$ are expressed to compensate for differences in volumes [cc] range between parameters. CI=conformity index (= patient volume receiving 38 Gy/PTV receiving 38 Gy)

4.3.2.2 autoROBOT vs. autoVMAT$_{5mm}$

While for autoROBOT and autoVMAT$_{3mm}$, a PTV coverage ≥95% was obtained for all 20 patients, with autoVMAT$_{5mm}$ this was only achieved for 2 patients, due to OAR constraints. 7 other patients obtained a clinically still acceptable coverage between 95% and 93%, while for the remaining 11 patients coverage was clinically unacceptable (<93%), with a minimum of 88.8%. Also the near–minimum PTV doses were lower in the autoVMAT$_{5mm}$ plans, while the CI was higher.

Notwithstanding the lower PTV coverage for autoVMAT$_{5mm}$, rectum sparing was also unfavorable compared to autoROBOT, with mean percentage differences of 13% for rectum D_{1cm^3}, 69% for V_{60GyEq}, 58% for V_{40GyEq} and 32% for D_{mean}. Differences in bladder and urethra plan parameters were statistically insignificant. Dose bath was also favorable for autoROBOT plans, with reductions of patient irradiated volumes of 19% for V_{5Gy}, 37% for V_{10Gy}, 25% for V_{20Gy}, and 18% for V_{30Gy}. V_{3Gy} was 5% lower for autoVMAT$_{5mm}$, but this was not statistically significant. Details on the comparisons between autoROBOT and autoVMAT$_{5mm}$ are presented in the right part of Table 4.1 and Figs. 4.3E-H. Favorable plan quality for autoROBOT compared to autoVMAT$_{5mm}$ is also observed in Fig. 4.2 (right panels) and superiority of autoROBOT was also confirmed by the clinician scoring (Fig. 4.4, lower panel).

For all 20 patients, the overall quality of the autoROBOT plans was considered better than for autoVMAT$_{5mm}$. For 11 patients, the clinician expected a real clinical impact of choosing the autoROBOT plan instead of the autoVMAT$_{5mm}$ plan, for other 8 patients a possibly important impact was expected, and for 1 patient a quality gain with probably low impact was scored.

4.3.2.3 Dosimetric QA

All plans passed the QA tests, with average gamma passing rates of 98.7±0.6% for autoROBOT, 99.8±0.2% for autoVMAT$_{3mm}$ and 99.6±0.8% for autoVMAT$_{5mm}$.

4.4 Discussion

In this study, we have presented the first system for fully automated generation of clinically deliverable treatment plans for a commercial robotic treatment unit. Automated planning, including non–coplanar beam angle selection, showed to improve plan quality, compared to manual planning. With equal PTV coverage, autoROBOT plans were superior to manual plans for all patients in sparing of the rectum and bladder, with neg-

AutoROBOT vs. AutoVMAT$_{3mm}$

AutoROBOT better | Equal | AutoVMAT better

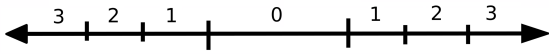

PTV				20			
Rectum	2	6	7	4	1		
Bladder			6	8	6		
Urethra		2	8	4	6		
Overall		4	9	5	2		

AutoROBOT vs. AutoVMAT$_{5mm}$

AutoROBOT better | Equal | AutoVMAT better

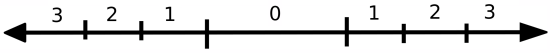

PTV	4	6	8	2			
Rectum	16	2	2				
Bladder		3	6	11			
Urethra	3	7	5	3	2		
Overall	11	8	1				

0 = no preference, similar plan quality
1 = preferred plan is better, probably low impact for patient
2 = preferred plan is better, possibly important impact for patient
3 = preferred plan is better, real impact for patient

Figure 4.4: Visual Analogue Scale (VAS) used for blind side–by–side plan comparisons by the treating clinician, and clinician scoring with the values representing numbers of plans (for each line, the sum values equal to 20).

ligible (but still superior) differences for all other clinical requirements. These findings are in line with results that we obtained on automated planning for regular linacs, using a similar approach for automatic plan generation, see M&M section and [38, 155, 185, 186]. Apparently, interactive, manual planning is so complex and dependent on the planners' skills and allotted planning time, that an optimal planning solution can often not be guaranteed. The applied wish–list approach for automated planning features for each individual patient a systematic search for finding the dosimetric parameters of a Pareto–optimal plan with clinically desirable trade–offs between all objectives. A commercial planning system is then used to realize a clinically deliverable plan, using the attained plan parameters as constraints, without any further trial–and–error planning. As described in [22] and the supplementary material, a wish–list for a treatment site is developed based on the clinical treatment protocol and a few (typically 5) plans of recently treated patients. A wish–list configuration entails repeated automatic plan generations

for the 5 patients, each time followed by an update of the wish–list that aims at a still higher plan quality in the next iteration. This iterative process is stopped if further improvements are considered not feasible. Specifically advantageous for autoROBOT planning, the upfront knowledge of feasible constraints allows the use of high resolution optimization grid in the commercial TPS for generating the deliverable plan.

Also for other systems, improvements in VMAT/IMRT plan quality by using automated planning have been reported [53, 64]. Nelms et al [124] observed large plan quality variations between 125 manual planners from various institutes, even with a very detailed and quantitative description of planning goals. Berry et al. showed large inter–planner variations in quality of plans that were manually generated within a single institution. Automated planning assisted in reducing the variations [12, 13]. Clearly, further investigations on inconsistencies in manual planning and the potential role for automated planning are warranted.

Strong points of our comparison of robotic surgery with VMAT for prostate SBRT are *i)* the use of validated automated multi–criterial planning for both techniques (validation by systematic comparison with manual planning, see [185] for autoVMAT and the Results section for autoROBOT), *ii)* the use of the same TPS and exactly the same optimization scheme for initial plan optimization for the two techniques (wish–list, see M&M section). Due to these features, a bias–free comparison between robotic treatment and VMAT could be made, based on consistent, high quality plans.

Technique comparisons were performed using dosimetric (DVH) evaluations and by blind side–by–side plan scoring by the clinician responsible for prostate SBRT in our center. The clinician scoring has important added value compared to dosimetric analyses only, as it gives integrated views, considering the full dose distribution to OARs and PTV and the global clinical quality of the plan for each individual patient. In a clinical setting, a clinician would never accept a plan comparison that is only based on DVH parameters.

AutoROBOT plans showed significant advantages compared to autoVMAT, both in the DVH analyses and the clinician's scoring. This was found for equal, 3 mm, CTV–PTV margins, and even stronger when comparing autoROBOT plans with 3 mm margin with autoVMAT plans with 5 mm margin. For 11 of the 20 patients, the autoVMAT plan with 5 mm margin was clinically unacceptable because of low PTV coverage (<93%). On top of that, rectum, bladder and urethra doses were significantly higher compared to autoROBOT. For all patients, the autoROBOT plan had a largely reduced dose bath compared to both $autoVMAT_{3mm}$ and $autoVMAT_{5mm}$. The latter may especially be important for avoidance of secondary tumors in the increasing fraction of younger prostate cancer patients, related to PSA screening.

A limitation of the study is that we did not clinically compare robotic treatment with VMAT, as needed for final conclusions, which we considered out of the scope of this paper. Another (practically unavoidable) limitation is that the autoVMAT and autoROBOT plans were calculated with different dose calculation engines as implemented in the corresponding TPS. Although both systems were thoroughly tested prior to clinical introduction, this might cause some bias in the comparisons.

Neither of the two recent studies that compared robotic treatment and VMAT for prostate SBRT [102, 107] observed the potential of a large plan quality improvement for robotic treatment, as observed in our study. Both the manual planning and retrospective plan comparisons, as used in these studies, may have introduced bias in the technique comparisons. MacDougall et. al. [107] used a 3 mm CTV–PTV margin for robotic treatment and a 5 mm margin for VMAT, and found no discernible dosimetric differences based on only 6 patients. Lin et. al. [102] used a 3 mm margin for robotic treatment and for VMAT 5 mm in all directions, except 3 mm in posterior direction. They concluded that VMAT was preferable because of reduced treatment time and superior dose distribution conformality. The study showed however large and systematic differences between robotic treatment and VMAT in PTV dose inhomogeneity and PTV coverage, which could have influenced the conclusions.

Dong et. al. compared VMAT with non–coplanar treatment at a C–arm linac [43], using with the 4π non–coplanar delivery approach involving both gantry rotations and couch displacements. For both techniques, the CTV–PTV margin was 5 mm with a reduction to 3 mm towards the rectum. As in our study, they observed clear plan quality advantages for non–coplanar treatment compared to coplanar VMAT. Automated plan generation was however only used for the non–coplanar planning, which could possibly have introduced some bias in the comparisons, favouring non–coplanar treatment. For robotic couch translations and rotations, Linthout et. al. [103] observed patient motion of up to 3 mm and 2 degrees. Nonetheless, Dong et. al. [43] used the same CTV–PTV planning margin for VMAT and non–coplanar treatment, possibly resulting in some study bias in favour of non–coplanar linac treatment. In our study, we investigated isotropic 3 mm and 5 mm CTV–PTV margins for autoVMAT. As our autoROBOT plans were already superior to VMAT with isotropic 3 mm margins, the same (and probably to a larger extent) is expected to hold for 5 mm margins with a reduction to 3 mm towards the rectum.

Delivery times of the autoROBOT plans generated in this study were around 45 min (M&M section), as used in our clinical practice for treatment with an IRIS variable aperture collimator, while VMAT treatments times were much shorter (~8-10 min). Most of the $VMAT_{5mm}$ plans were clinically unacceptable, and robotic treatment would anyway be preferable, also with the prolonged treatment time. For the other $VMAT_{5mm}$ plans, quality gains with robotic have to be weighed against the prolonged treatment dura-

tion. The same holds for $VMAT_{3mm}$ plans, that might be applicable at linacs with novel systems for intra–fraction motion correction [82, 194]. In this study, we have generated robotic plans for the variable aperture IRIS collimator. Currently, an MLC is available for the investigated robotic treatment unit [10, 59], probably resulting in reduced delivery times [75, 79, 115, 190].

As described in the M&M section, for robotic prostate SBRT plans, we try to mimic HDR brachytherapy dose distribution with intentionally inhomogeneous PTV dose delivery, with high peak doses inside the PTV. The urethra dose is minimized by dose–volume constraints. As the robot corrects for rotational tumor displacements, no PRV planning margin around the urethra is clinically used. C–arm linacs are not equipped with a system for rotation correction, implying that a PRV margin around the urethra may be needed for the inhomogeneous dose distributions studied in this paper. This could then possibly result in an enhanced percentage of patients with an unacceptably low PTV coverage. The need and implications of the use of a urethra PRV margin at a C–arm linac have not been investigated in this study.

4.5 Conclusion

The first system for fully automated generation of clinically deliverable plans for non–coplanar robotic treatment has been presented. The system features multi–criterial beam profile and beam angle optimization, resulting in plans with clinically favourable trade–offs between all treatment aims. For prostate SBRT, clinically acceptable, high quality plans could be generated that highly outperformed manually generated plans. Automatically generated robotic plans had consistently higher quality than automatically generated plans for VMAT at a linac. Further research on improvement of plan quality and plan consistency, including the role of automated planning, is warranted.

Supplementary material

Wish-list generation for prostate SBRT

For each patient, Erasmus-iCycle automatically generates a Pareto optimal plan with clinically favourable trade-offs between treatment objectives. Input for Erasmus-iCycle plan generation is a contoured CT–scan and a wish–list.

A wish-list contains the hard constraints, which always need to be fulfilled in plan generation, and treatment objectives with assigned priorities. Objectives are planning aims that need to be met as closely as possible (or superseded, if possible). Starting with the highest priority, the objectives in the wish–list are sequentially minimized, each

time followed by adding the attained objective value as a novel constraint for the next optimization problem to ensure that high priority goal values will not be deteriorated in the minimization of lower priority objective functions ([21] and [22] for more details). The wish–list is generated in an iterative procedure, starting with a first 'guess' of the wish-list by an experienced planner. This wish–list is then used for automated plan generation for a small group of (5-10) patients, followed by plan evaluation to update the wish–list for plan generation in a next iteration. This process with repeated wish–list updates stops if no further enhancement of plan quality is feasible. For groups of patients (e.g. all prostate patients treated with SBRT) this list is fixed, i.e. for all patients in the group the plan is fully automatically generated with the same wish–list.

As described in more details in the Material and Methods section, in this study, two versions of Erasmus–iCycle were used, one for non–coplanar plan generation for a robotic system equipped with a variable aperture collimator, the other for VMAT pre–optimization for an Elekta linac with MLC. Using the above described iterative procedure in parallel for the two Erasmus–iCycle versions, a single wish–list was generated for both robotic and VMAT pre–optimization.

Table 4.2 shows the wish–list used for all robotic and VMAT automated plan generations. All applied constraint and objective convex functions were used for the automated multi–criterial plan generation. These functions were selected to generate plans in line with the (not always convex) clinical planning aims (see Plan Evaluation comparison in M&M). The SE function (Sum of Exponentials) defined by Eq. 4.1 is basically a sum of exponentials of differences between attained voxel doses d_j and D_c, a user–defined critical dose.

$$SE = \frac{1}{m} \sum_{j=1}^{m} e^{\alpha (d_j - D_c)} \tag{4.1}$$

where m is the number of voxels in the structure and α is the sensitivity parameter.

For tumors, the parameter α is positive, and SE is equal to the Logarithmic Tumor Control (LTCP), as introduced by Alber & Reemtsen [1], with D_c equal to the prescribed tumor dose. The attractive characteristic of SE is that tumor underdosage is heavily penalized, while overdose has a relatively low impact on the function value. In Table 4.2, SE is used in priorities 1 and 2 to obtain clinically favourable PTV dose distributions. To limit for each patient both positive and negative deviations from the clinically requested 95% PTV coverage ($V_{100\%}$=95%), the goal value for SE in priority 1 is set automatically (Table 4.2). To this purpose, for priority 1, two plans are first generated with relatively small and large goal values, respectively. For both plans, the PTV coverage is then calculated and the final goal value for SE is determined by exponential interpolation. The aim of SE in

priority 2 is creating a large dose inhomogeneity in the PTV like in HDR brachytherapy.

For prostate SBRT, it is extremely important that especially the high doses in rectum and bladder are avoided as much as possible. To this purpose, a SE function with negative α is used in priorities 4 and 5, highly favouring avoidance of doses higher than the defined critical values D_c (Table 4.2). SE = SE (Sum of Exponentials), defined in Eq. 4.1.

Constraints

Structure	Type	Limit	Parameter
PTV_{opt}	maximum	61.5 Gy	
Rectum	maximum	36.5* Gy	
Rectum	gEUD	28	a = 20
Rectal Mucosa	maximum	27 Gy	
Overlap(Rectum,PTV+3mm)	maximum	38 Gy	
Bladder	maximum	39.5 Gy	
Bladder	gEUD	30.7	a = 20
Overlap(Bladder,PTV+3mm)	maximum	41.8 Gy	
Urethra	maximum	50 Gy	
Urethra	gEUD	39 Gy	a = 3
Penis Scrotum	maximum	1.5 Gy	
Shell 3 mm from PTV	maximum	38 Gy	
Shell 3 cm from PTV	maximum	20 Gy	
Entrance dose**	maximum	20 Gy	

Objectives

Priority	Structure	Type	Goal	Parameters (D_p, α, sufficient)
1	PTV_{opt}	SE	optimized***	(37 Gy, 0.9,as goal)
2	PTV_{opt}	SE	2.2	(57 Gy, 0.07, 2.2)
3	CTV	minimum	34 Gy	sufficient = 34 Gy
4	Rectum	SE	0 Gy	(28 Gy, -0.3)
5	Bladder	SE	0 Gy	(34 Gy, -0.1)
6	Rectum	mean	0 Gy	
7	Bladder	mean	0 Gy	
8	Urethra	mean	0 Gy	
9	Dose bath****	maximum	15 Gy	
10	Left Femur head	maximum	24 Gy	
10	Right Femur head	maximum	24 Gy	

Table 4.2: Applied wish-list for all study patients. *Maximum dose constraints were set lower than clinical requirements to account for voxel sampling for the optimizations. **Dose in 2 cm thick layer inside the body contour. ***Values are automatically set to ensure a PTV coverage of 95%, if feasible within the constraints, see text. ****Dose in patient volume in between shells at 3 cm from the PTV and 2 cm from the body contour. PTV_{opt} = PTV_{opt} is the PTV excluding overlaps with rectum, bladder and urethra. gEUD = Generalized Equivalent Uniform Dose [127]. SE = Sum of exponentials

Individualized automated planning for dose bath reduction in robotic radiosurgery for benign tumors

5

Linda Rossi, Alejandra Méndez Romero, Maaike Milder,
Erik de Klerck, Sebastiaan Breedveld, Ben Heijmen

Department of Radiation Oncology,
Erasmus MC, Rotterdam

Published:
PLoS ONE
14, 2 (2019), e0210279

Abstract

Object: To explore the use of automated planning in robotic radiosurgery of benign vestibular schwannoma (VS) tumors for dose reduction outside the planning target volume (PTV) to potentially reduce risk of secondary tumor induction.

Methods: A system for automated planning (AUTOplans) for VS patients was set up. The goal of AUTO- planning was to reduce the dose bath, including the occurrence of high dose spikes leaking from the PTV into normal tissues, without worsening PTV coverage, OAR doses, or treatment time. For 20 VS patients treated with 1x12 Gy, the AUTOplan was compared with the plan generated with conventional, manual trial-and-error planning (MANplan).

Results: With equal PTV coverage, AUTOplans showed clinically negligible differences with MANplans in OAR sparing (largest mean difference for all OARs: $\Delta D2\% = 0.2$ Gy). AUTOplan dose distributions were more compact: mean/maximum reductions of 23.6/53.8% and 9.6/28.5% in patient volumes receiving more than 1 or 6 Gy, respectively ($p<0.001$). AUTOplans also showed smaller dose spikes with mean/maximum reductions of 22.8/37.2% and 14.2/40.4% in D2% for shells at 1 and 7 cm distance from the PTV, respectively ($p<0.001$).

Conclusion: Automated planning for benign VS tumors highly outperformed manual planning with respect to the dose bath outside the PTV, without deteriorating PTV coverage or OAR sparing, or significantly increasing treatment time.

5.1 Introduction

Stereotactic radiosurgery is an increasingly used option for management of patients with benign vestibular schwannoma (VS) tumors [9, 20, 122, 147, 188]. However, an increased risk of secondary tumor formation associated with radiation exposure is well established [8, 118, 128, 140, 154]. Therefore, in radiotherapy, dose outside the planning target volume (PTV) should be avoided as much as possible, especially for patients with a long life expectancy.

High delivery accuracy can be obtained with the robotic system due to real-time image-guided tracking, allowing small PTV margins [46, 60], and non-coplanar treatment [143].

Currently, treatment plans in radiotherapy are generally generated in an interactive trial-and-error process in which the planner tries to steer the treatment planning system (TPS) towards generation of an acceptable solution ("manual planning"). This may be a time consuming process and the resulting plan quality may heavily depend on the skills and experience of the planner and on the available planning time and software. The potential of automated treatment planning for both enhancement of plan quality and drastic reduction in planning time, as alternative to manual planning, has been shown in many studies [19, 22, 92, 116, 145, 169, 170, 180, 185, 199].

However, the existing literature on automated planning is focused on reduction of high doses in OARs or enhancement of PTV dose. To the best of our knowledge, this is the first study focusing on the use of automated planning for overall reduction of dose bath. The study was inspired by observing the inability, in manual planning, to optimally reduce the dose bath, and the planning time investment in getting a possible improvement, as systematically tried.

In our institution, a system for fully automated, multi-criterial treatment plan generation has been developed, including optimization of beam directions. For this study, this system was used as a pre-optimizer for the clinical TPS, that comes with the robotic treatment unit to automatically generate deliverable plans for VS patients (AUTOplan). We investigated whether automated planning could reduce the dose bath compared to manually generated plans (MANplan), while not deteriorating dose delivery to the PTV or OARs, and keeping treatment times comparable.

5.2 Materials and methods

5.2.1 Patients and manual planning (MANplan)

Contoured CT scans of 20 vestibular schwannoma patients, previously treated at our department with the CyberKnife (CK) robotic treatment unit (Accuray Inc, Sunnyvale, USA), were included in the study. All patient-related information was fully anonymized prior conducting the research. According to the regulations of the Ethics Committee of Erasmus MC no ethical approval for this retrospective study was needed as there was no impact on treatment and the applied patient data.

The gross tumor volume (GTV) was defined as the volume of contrast enhancement on the T1-weighted MRI, after CT/MRI fusion. No margins were applied for planning (GTV = PTV). The average tumor size was 2.9 cc (1.0-7.3 cc). Delineated OARs were brainstem, trigeminal nerves, area of virtual facial nerve, optic nerves, chiasm, cochlea (when clinically relevant), pituitary gland, and eyes.

For planning, tumor coverage (>98% of the volume receiving 100% of the prescribed dose) had highest priority, while strictly fulfilling OAR Dmax constraints and high dose conformality around the target. Furthermore, the goal was to maximally reduce the dose bath, including minimizing dose spikes. Various planning strategies were clinically used to control this dose spillage, based on planners' preferences and experience. All MANplans were generated in Multiplan[151] clinical TPS (Accuray Inc, Sunnyvale, USA) that comes with the CK, with the Iris variable aperture collimator [47], avoiding diameters smaller than 10 mm and larger than 40 mm. CK full head node path was used for a total 179 non-coplanar available beam directions.

Patients were treated with a single fraction of 12 Gy, prescribed at the 80% isodose.

5.2.2 Automated planning (AUTOplan)

Clinically deliverable CK plans for VS patients were generated in a two-step process:

i For each patient, a pre-plan was automatically generated with the in-house developed Erasmus-iCycle TPS [22, 145, 155, 185]. Plan generation with Erasmus-iCycle is driven by a so-called wish-list, describing all planning constraints and objectives. The latter have ascribed priorities for steering the multi-criterial plan generation, resulting in clinically favorable trade-offs between all treatment objectives. Generated plans are Pareto-optimal. For this study, a wish-list was made for VS plan generation, minimizing dose spillage from the PTV while not deteriorating PTV

and OAR dose, or substantially increasing the treatment time. Erasmus-iCycle and wish-list building have been extensively described in the literature [22, 143].

ii The Erasmus-iCycle plan generated in step *i* was used to automatically create a patient-specific planning template for subsequent automatic plan generation by the clinical TPS Multiplan. The planning template contained the planning constraints to ensure generation in Multiplan of a clinically deliverable plan that mimicked the original Erasmus-iCycle plan.

This two-step approach was developed as for practical and regulatory reasons Erasmus-iCycle cannot be used directly for clinical plan delivery.

A similar two-step approach is currently clinically used at Erasmus MC for automated VMAT planning for prostate cancer, head and neck cancer, cervical cancer, and advanced lung cancer, using the Monaco clinical TPS (Elekta AB, Stockholm, Sweden) in the second step [185]. A distinct difference between VS autoplanning for robotic treatment and automated VMAT planning is the inclusion of non-coplanar beam-angle selection for VS.

All generated AUTOplans were based on the same planning protocol, the same choice from Iris collimators, node set, and the same dose prescription as used for clinical MANplan generation (above).

To minimize dose spillage in AUTOplans, the template for automated planning with Multiplan (step *ii* above) contained individualized Dmax constraints for shells at distances of 1, 3, and 5 cm from the PTV. For each patient, these shell constraints were obtained from the Erasmus-iCycle plan, generated in step *i*. In Erasmus-iCycle, the maximum doses at these shells were minimized, while respecting all hard planning constraints and the (higher) priorities for adequate PTV coverage and OAR sparing. AUTOplan generation in Multiplan in step *ii* was performed in high resolution with intensive treatment time reduction.

5.2.3 Automated planning with fixed shell constraints

As described above, individually optimized shell constraints, derived from the Erasmus-iCycle plan, were used in the second step of AUTOplan generation with the Multiplan TPS. In an additional analysis, we investigated whether it was possible to use for all patients the same Dmax constraints instead of patient-specific values. This study was performed to understand how patient-specific constraints impact plan quality, keeping all other parameters the same, or, opposite, to see if it was possible to use equal values for all patients without losing in plan quality.

For each shell, the population-fixed constraint was calculated as the average of the

patient-specific Dmax values found in the Erasmus-iCycle plans of the 20 study patients. Then, for each of the patients, a second AUTOplan was generated, using the fixed constraints. In the remainder of the paper, the second AUTOplans with fixed constraints are referred to as *fAUTOplans*.

5.2.4 Plan comparisons

Prior to comparisons of AUTOplans with MANplans and fAUTOplans with AUTOplans all plans were rescaled to a tumor V12Gy of 98%, when achieved (in line with the clinical planning protocol). Plans were compared using OAR near-maximum doses, D2%, conformity index (CI), and treatment time. To evaluate dose bath and spikes, patient volumes V_D with D up to 10 Gy were assessed, as well as D2%, of shells from 1 to 7 cm away from the tumor, for spillage. Two-sided Wilcoxon signed-rank tests were used to analyze plan differences, using $p<0.05$ for statistical significance.

5.3 Results

5.3.1 AUTOplan vs. MANplan

All MAN- and AUTOplans were clinically acceptable with tumor coverage >98% (98.3±0.1%) while fulfilling all OAR constraints (Table 5.1). Treatment times were comparable; 36.1±5.0 min and 38.2±4.1 ($p = 0.008$) for MAN- and AUTOplans, respectively, allowing plan comparison without unacceptable treatment time difference bias.

CIs for AUTOplans (1.16±0.06) were slightly better than for MANplans (1.18±0.09), but the difference was not significant ($p = 0.4$).

As for PTV coverage, MAN- and AUTOplans were comparable in terms of OARs sparing. For all OARs, the mean difference in near-maximum dose was below 0.2 Gy and statistically not significant. Only the brainstem Dmean was on average slightly lower for the AUTOplans, which was statistically significant, 2.2±0.7 Gy vs. 2.4±0.8 Gy, p=0.02.

Dose bath was substantially reduced in the AUTOplans (see Fig 5.1 for example). Both patient volumes receiving dose and dose spikes were reduced with autoplanning compared to manual planning. For most patients, volumes V_D receiving more than D Gy were smaller in the AUTOplans, as visible in the upper panel of Fig 5.2 and Table 5.1. Population-average percentage V_D reductions for D = 1, 2, 3, 6, 8, and 10 Gy were 23.6%, 17.5%, 15.3%, 13.5%, 9.6%, 6.1% and 2.9%, respectively (all $p<0.005$, apart from V10Gy with $p = 0.06$). AUTOplans also had reduced near-maximum doses in the shells at 1, 2, 3, 5

and 7 cm from the PTV, mostly reflecting smaller spikes and closer to the tumor. Average reductions of shell D2% with AUTOplans were 22.8%, 20.5%, 16.8%, 16.7% and 14.2%, respectively (all $p<0.001$), as visible in the lower panel of Fig 5.2 and Table 5.1.

AUTOplans used less MU (4899 vs. 5716) and nodes (56.1 vs. 66.6), but more beams (161.7 vs. 121.8), all $p<0.004$.

		AUTOplans	**MANplans**	
		Mean ± SD	**Mean ± SD**	
PTV	V12Gy	98.3 ± 0.1	98.3 ± 0.1	%
	CI*	1.2 ± 0.1	1.2 ± 0.1	
Brainstem	D2%	9.7 ± 1.5	9.8 ± 1.4	Gy
	Dmean	**2.2** ± 0.6	**2.4** ± 0.8	Gy
Trigeminal Nerve	D2%	11.7 ± 1.0	11.8 ± 0.8	Gy
Facial Nerve	D2%	14.0 ± 0.2	14.0 ± 0.3	Gy
L Optic Nerve	D2%	0.1 ± 0.0	0.2 ± 0.1	Gy
R Optic Nerve	D2%	0.1 ± 0.0	0.2 ± 0.1	Gy
Chiasm	D2%	0.3 ± 0.1	0.3 ± 0.1	Gy
Cochlea	D2%	11.6 ± 1.2	11.8 ± 1.1	Gy
Pituitary	D2%	0.3 ± 0.1	0.4 ± 0.1	Gy
L Eye	D2%	0.1 ± 0.0	0.1 ± 0.0	Gy
R Eye	D2%	0.1 ± 0.0	0.1 ± 0.0	Gy
Patient	V1Gy	**271.2** ± 142.9	**347.6** ± 162.5	cc
	V2Gy	**68.0** ± 32.2	**84.7** ± 44.8	cc
	V3Gy	**36.2** ± 16.6	**44.0** ± 22.9	cc
	V4Gy	**24.1** ± 10.9	**28.8** ± 14.9	cc
	V6Gy	**14.3** ± 6.5	**16.2** ± 8.3	cc
	V8Gy	**9.6** ± 4.6	**10.3** ± 5.3	cc
	V10Gy	6.2 ± 3.3	6.4 ± 3.4	cc
PTV Shell 1cm	D2%	**3.7** ± 0.5	**4.9** ± 0.8	Gy
PTV Shell 2cm	D2%	**2.0** ± 0.4	**2.6** ± 0.5	Gy
PTV Shell 3cm	D2%	**1.4** ± 0.3	**1.7** ± 0.3	Gy
PTV Shell 5cm	D2%	**1.0** ± 0.2	**1.2** ± 0.2	Gy
PTV Shell 7cm	D2%	**0.8** ± 0.2	**1.0** ± 0.2	Gy
Treatment Time		**38.2** ± 4.0	**36.1** ± 4.8	min
MU		**4899** ± 704	**5716** ± 996	
Nodes		**56.1** ± 10.8	**66.6** ± 21.1	
Beams		**161.8** ± 24.2	**121.8** ± 29.6	

Table 5.1: For all 20 patients, mean values for automatically generated plans (AUTOplans) and manually generated (MANplans). Bold values represent the statistically significant differences as $p<0.05$ with the Wilcoxon's signed-rank test.*CI = Conformity Index.

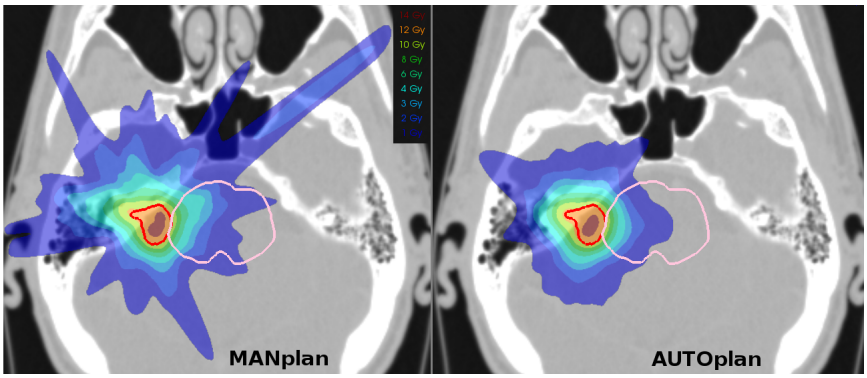

Figure 5.1: Axial dose distributions for an example patient. The AUTOplan (right) shows a reduced dose bath, with also smaller dose spikes, than the MANplan (left). Reduction in brainstem dose is also visible. (Red contour = PTV, pink contour = Brainstem.)

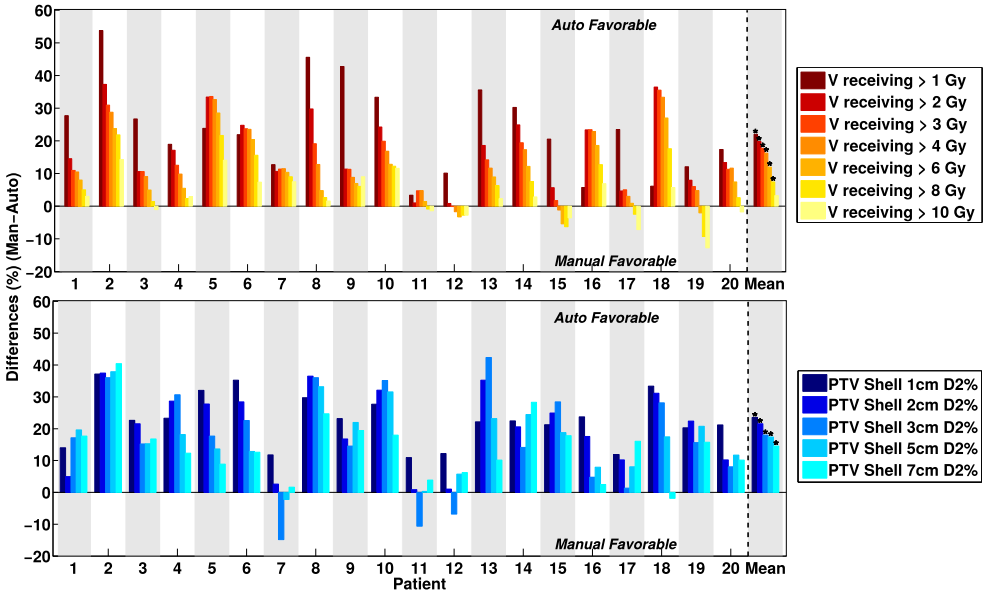

Figure 5.2: Differences between AUTOplans and MANplans in dose spillage. Positive differences reflect higher quality for the AUTOplan. Upper panel: differences in patient volumes receiving more than 1, 2, 3, ..., 10 Gy. Lower panel: differences in D2% for shells at 1, 2, ..., 7 cm away from the tumor. For the individual patients, differences were calculated as $(\text{MANplan} - \text{AUTOplan})/\text{MANplan} * 100$. The last column shows population mean differences and their statistical significance marked with * ($p<0.05$).

5.3.2 fAUTOplan vs. AUTOplan

Table 5.2 shows for each patient the Dmax for the shells at 1, 3, and 5 cm from the PTVs, as obtained from plan optimization with Erasmus-iCycle, and used as individualized shell constraints in Multiplan optimization in the second phase of the AUTOplan generation. The presented population mean values were used for all the patients to generate the fAUTOplans.

Using population average shell constraints instead of the individualized constraints (Table 2) for plan generation in Multiplan (fAUTOplan) resulted in an unacceptable PTV coverage for 5 out of 20 patients (Table 5.2, patients 14, 16, 18, 19 and 20), with a minimum of 92.3% instead of 98%, due to too tight shell constraints.

For the remainder of the patients, with equal PTV coverage, there were no statistically significant differences between fAUTOplans and AUTOplans in CI, mean and near-maximum OAR doses, patient volumes V_D receiving more than D Gy (D≤10 Gy), and D2% at shells from 1-7 cm from the PTV.

5.4 Discussion

Several studies have observed superiority of automated plan generation compared to conventional, interactive trial-and-error planning regarding enhancement of PTV dose, or reduction of OAR doses [65, 92, 155, 185, 199]. Apart from plan quality advantages, automated planning did always result in drastic reductions in planning workload.

Especially for patients with a long life expectancy, such as VS patients, dose outside the PTV should be maximally avoided to reduce the risk for secondary tumor induction. To the best of our knowledge, this is the first paper on automated planning that primarily aims at the overall reduction of low and high doses outside the PTV of a benign tumor. To this purpose, a system was set up and configured for fully automated non-coplanar plan generation for robotic stereotactic treatment of VS patients.

The project was started after observing frequent problems with controlling or improving dose bath and spikes from the PTV in manual planning (see Fig 5.1a). In this study we have demonstrated that automated planning could reduce the dose bath, without worsening PTV coverage or OAR sparing, or substantially increasing treatment time. Moreover, due to the automation, there was no workload in the plan generation.

As explained in the M&M section, final AUTOplans were generated with the commercial TPS that comes with the robotic treatment unit. Therefore, this TPS is indeed able to generate highly compact plans, with minimal dose delivery outside the PTV and avoiding

Patient-specific constraints	Shell 1 cm Dmax [cGy]	Shell 3 cm Dmax [cGy]	Shell 5 cm Dmax [cGy]
Pt 1	427	156	112
Pt 2	374	140	106
Pt 3	430	157	117
Pt 4	423	173	138
Pt 5	458	171	133
Pt 6	426	155	120
Pt 7	428	168	129
Pt 8	370	146	98
Pt 9	390	123	88
Pt 10	344	108	74
Pt 11	423	170	105
Pt 12	417	174	137
Pt 13	368	135	107
Pt 14	475	181	124
Pt 15	357	119	84
Pt 16	536	210	162
Pt 17	396	165	123
Pt 18	471	198	167
Pt 19	522	181	134
Pt 20	486	200	149
Mean±SD	**426±53**	**162±27**	**120±25**

Table 5.2: For each patient, Dmax values for shells at 1, 3 and 5 cm from the PTV as derived from the Erasmus-iCycle plan, and population mean values with standard deviations. Patient-specific Dmax values were used as constraints in AUTOplan generations, while the mean values were used for fAUTOplan generation.

dose spikes. In the autoplanning procedure, the individualized shell constraints, used in the commercial TPS to maximally avoid dose spillage, were automatically generated using a pre-optimization with our in-house developed multi-criteria optimizer (step *i*, M&M section). In conventional manual planning, shell constraints are defined for each patient in a trial-and-error procedure. Then, finding the optimal constraint values for individual patients is often impractical, because it is too time consuming to be feasible in clinical routine.

The presented workflow for AUTOplan generation of highly compact dose distributions is likely to be applicable also for other benign tumors, which will be a topic for further research.

To the best of our knowledge, this is the first study to systematically investigate a possible reduction in dose bath while mantaining treatment technique. Integral dose reduction is a reported outcome from many plan comparison studies [32, 48, 72, 131], beside the OARs evaluation, as well as different metrics have been proposed [165, 200],

reflecting the clinical relevance. However a systematic dose bath reduction can not be easily investigated without a consistent planning work flow such as the one used in this study, including the dose bath improvement without loosing quality in the PTV and OAR dose distributions.

For 5/20 patients, the applied population-based, fixed shell constraints used for generating the fAUTOplan were too tight, resulting in an unacceptably low PTV coverage. No correlation with PTV size or other features was found. For the other 15 patients, the fAUTOplan was similar in quality as the AUTOplan. This does however not necessarily imply that in clinical routine, acceptable high quality plans would have been generated for the latter patients, using the fixed constraints. fAUTOplans were generated with an automated planning workflow and it is uncertain whether using the population-based constraints with manual planning would have resulted in high quality plans for these 15 patients. This could have been dependent on the complexity of the individual cases and on the skills of the involved planners. Anyway, compared with automated planning, the workload would have increased.

On the longer term and to serve the radiotherapy community, there is a clear need for more advanced commercial treatment planning systems that are faster and/or facilitate automated plan generation.

5.5 Conclusion

Compared to conventional planning, automated plan generation for robotic treatment of patients with a benign vestibular schwannoma tumor could to a large extent reduce low to high dose outside the PTV while maintaining acceptable tumor coverage and similar OAR dose, and keeping delivery time comparable.

On the importance of individualized, non-coplanar beam configurations in mediastinal lymphoma radiotherapy

6

Linda Rossi and Patricia Cambraia Lopes
(the authors contributed equally),
Joana Leitão, Cecilie Janus, Marjon van de Pol,
Sebastiaan Breedveld, Joan Penninkhof, Ben Heijmen

Department of Radiation Oncology,
Erasmus MC, Rotterdam

Submitted

Abstract

Background and purpose: Literature is non-conclusive regarding selection of beam configurations in radiotherapy for mediastinal lymphoma (ML) radiotherapy, and published studies are based on manual planning with its inherent limitations. In this study, coplanar and non-coplanar beam configurations were systematically compared, using a large number of automatically generated plans.

Material and Methods: An autoplanning workflow, including beam configuration optimization, was configured for young female ML patients. For 25 patients, 24 plans with different beam configurations were generated with autoplanning: CP_x and NCP_x, with x=5-15 computer-optimized, patient-specific coplanar (CP) or non-coplanar beams (NCP) beams, and the coplanar VMAT and non-coplanar Butterfly VMAT (B-VMAT) beam angle class solutions (600 plans in total).

Results: Autoplans compared favorably with manually generated, clinically delivered plans, ensuring that beam configuration comparisons were performed with high quality plans. There was no beam configuration approach that was best for all patients and all plan parameters. Overall there was a clear tendency towards higher plan quality with non-coplanar configurations (NCP_x≥12 and B-VMAT). NCP_x≥12 produced highly conformal plans with on average reduced high doses in lungs and patient and also a reduced heart Dmean, while B-VMAT resulted in reduced low-dose spread in lungs and left breast.

Conclusions: Non-coplanar beam configurations were favorable for young female mediastinal lymphoma patients, with patient-specific and plan-parameter-dependent dosimetric advantages of NCP_x≥12 and B-VMAT. Individualization of beam configuration approach, considering also the faster delivery of B-VMAT vs. NCP_x≥12, can importantly improve the treatments.

6.1 Introduction

Patients treated with a combination of multi-agent chemotherapy and radiation for Hodgkin or non-Hodgkin lymphoma are mostly young at diagnosis. About 80% of these patients achieve long-term remission. Given the age at diagnosis and the favorable long-term prognosis, therapy-related late effects including secondary malignancies [37, 49, 125, 149, 166, 173, 174] and cardiovascular disease [2, 112, 177–179] have become increasingly important. In recent years, radiotherapy (RT) for lymphoma has evolved by considerably decreasing target volumes (from extended field to involved field to involved site or involved node) and radiation doses (from 40 Gy to 30 Gy or even 20 Gy in selected cases). These factors contribute to a decrease in the risk of late toxicity [28, 91, 110, 125, 149, 202].

Applied radiotherapy techniques have also evolved, with IMRT and VMAT emerging as alternatives to 3D conformal RT (3D-CRT). In this context, the typical low-dose bath of VMAT plans has been pointed at as a cause of concern, as it could increase the risk of secondary cancers relative to 3D-CRT [109]. The low-dose bath in the lungs has also been associated with increased risk of radiation pneumonitis [132]. Choice of beam arrangement may impact plan quality. This has been investigated in detail for 'butterfly' beam arrangements that can contain non-coplanar beams. In particular, the (non-coplanar) B-VMAT approach described by Fiandra et al. [50] has shown to reduce breast Dmean and V4Gy compared to VMAT, leading to similar calculated lower risks of secondary breast cancer as 3D-CRT (but risk of lung cancer relatively higher), as well as a lower risk of cardiac toxicity, in a group of patients with largely non-bulky disease, without axillary involvement [52]. Voong et al. [187] observed a reduction in heart dose (but not in breast dose) by using 5-7 IMRT beams (butterfly) with eventually 1 non-coplanar beam, relative to 3D-CRT in patients without bilateral axillary involvement. Proton therapy has also been proposed for further reductions of late toxicity in selected lymphoma patients [36, 109, 139, 171, 175].

Current literature is non-conclusive regarding the optimal choice of RT treatment technique. The International Lymphoma Radiation Oncology Group [111] has benchmarked the best practice of 10 centres in 2013, showing that (i) the applied (photon) RT technique varied largely between institutions leading to large differences in the low-dose volumes, and (ii) in practice, difficult cases were often not planned according to the standard. The authors could not provide universal/consensus recommendations. Moreover, different authors pointed at the necessity for individualized selection of planning technique [50, 113, 187]. This was in part attributed to the high heterogeneity in tumor location, shape, and size, as well as patient characteristics.

To the best of our knowledge, in all published studies comparing beam configurations for treatment of lymphoma patients, treatment plans were generated with manual trial-and-error planning, including selection of beam angles. It is well-known that manually generated plans may suffer from inter-and intra-planner quality variations. Moreover, finding optimal beam configurations with trial-and-error planning is extremely complex and time-consuming. The latter put heavy constraints on the number of beam configurations that were compared in published studies, and the total number of plans that were generated.

In this work we used a large number of automatically generated plans for comparison of radiotherapy beam configurations for young females with ML. To this purpose, an automatic workflow for IMRT/VMAT plan generation, including integrated coplanar or non-coplanar beam angle and beam profile optimization for IMRT, was implemented and validated. The system was used to systematically compare plan quality differences between 24 coplanar and non-coplanar beam configuration approaches for 25 study patients.

6.2 Materials and Methods

6.2.1 Patients and clinical protocol

The study was based on a database with contoured planning CT-scans and manually generated, clinically delivered plans (CLIN) of 26 previously treated female ML patients (21 Hodgkin lymphoma and 4 B cell non-Hodgkin lymphoma). As explained in detail below and in Electronic Appendix A, one patient (patient 0) was excluded from the beam angle configuration comparisons, leaving 25 evaluable patients in this study (patients 1-25).

Visual inspection of planning CT-scans ensured a heterogeneous selection of anatomical presentations in the patient cohort (superior/inferior mediastinum, with/without involvement of supraclavicular or axillar nodes, bulky disease, complex anatomy; see Figure B1 in Supplementary material B). The median patient age was 27 (range: 19-50). The PTV volumes varied from 97 – 1654 cc (median 605 cc). The prescription dose was 30 Gy in 15 fractions, excluding the sequential boost applied for some patients (3 x 2 Gy), which was not considered in this study.

In clinical practice, dosimetric aims were largely based on published recommendations [35, 71, 132, 177, 178]. At least 95% of the target (ideally 100%) had to be covered by 95% of the prescribed dose (V95% >95%), while respecting the PTV over- and under-dose criteria; V110% <1% and V<90% <5 cc (preferably <2 cc), respectively. OAR requirements

were the following, where a preferred value is indicated in parentheses: breast Dmean <5 Gy (<2 Gy), heart Dmean <26 Gy (<10 Gy), lungs Dmean <15 Gy (<13.5 Gy), lungs V5Gy <55% (<50%) and lungs V20Gy <30%. None of the planning requirements was truly a hard constraint (except for PTV V95%), i.e. depending on patient anatomy, violations were sometimes accepted. The 60% isodose was clinically evaluated (visually, not quantitatively), especially related to dose in the back/neck muscles. Five patients were treated with a coplanar partial-arc VMAT plan, and 20 patients were treated with a coplanar IMRT plan with on average 6.0 manually selected mediastinal beams (range: 4-8), mainly from (or close to) anterior and posterior directions (butterfly). For patients with neck involvement, 1-4 beams from (close to) lateral directions were added for neck irradiation only.

6.2.2 Automated plan generation

An automated planning workflow for young ML patients was developed following the clinical planning aims described above. The core of the system was Erasmus-iCycle, an in-house developed multi-criteria optimizer featuring integrated beam angle and profile optimization [22]. Erasmus-iCycle was coupled to the GPUMCD Monte Carlo dose engine [70], which is also implemented in our Monaco clinical TPS (Elekta AB, Stockholm, Sweden). Pareto-optimal plans with clinically favorable trade-offs between all treatment requirements were realized with the optimization protocol ('wish-list', [22]) reported and explained in Supplementary material B. All plans for all patients were automatically generated with the same wish-list without any manual fine-tuning.

For coplanar beam angle optimization (BAO), the candidate beam set consisted of 36 equiangular beams. For non-coplanar BAO, a set of 194 candidate beam directions was defined (including the 36 coplanar beams), avoiding collisions between the patient/couch and the gantry as verified at the linac. Also in the non-coplanar beam set, the angle resolution was around 10°. The applied beam energy was 6 MV.

6.2.3 Compared beam configurations

For all 25 study patients, the following 24 autoplans were generated to systematically investigate the impact of beam angle configuration on plan quality (see also Fig. 6.1):

a) CP_x: coplanar plans with x = 5-15 beams with computer-optimized, patient-specific directions

b) NCP_x: non-coplanar plans with x = 5-15 beams with computer-optimized, patient-specific directions.

c) VMAT: IMRT plan with 21 coplanar equiangular beams, reproducing full-arc VMAT

dose distribution [186].

d) B-VMAT: non-coplanar class solution, consisting of 20 IMRT beams equally spread in three 60° arcs, two centered at gantry angle = 0°, with couch = 0° and couch = 90°, and one centered at gantry angle = 180° with couch = 0°, mimicking the butterfly geometry described by Fiandra et al. [50].

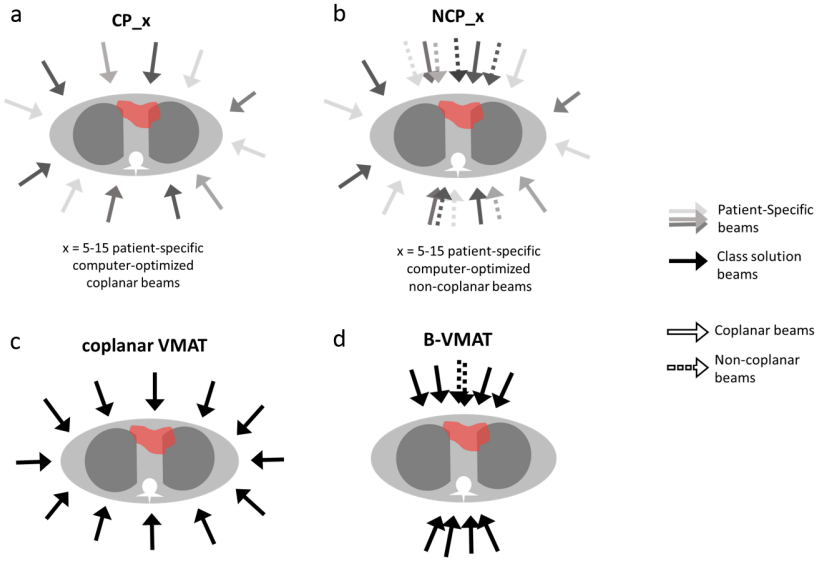

Figure 6.1: Schematic presentation of the investigated beam configurations. CP = coplanar, NCP = non-coplanar, B-VMAT = Butterfly-VMAT.

6

6.2.4 Plan evaluations and comparisons

Plans were mainly evaluated and compared using PTV and OAR planning goals applied in clinical planning (above). On top of that we also reported on breast(s) V4Gy [50], PTV V107%, conformity index (CI, defined as patient V95% / PTV volume), and patient V5Gy (cc) and V20Gy (cc), where the patient is defined by the external skin structure. PTV V110%, mentioned in the clinical planning protocol, was always far below the requested 1%, and was therefore not reported. Two-sided Wilcoxon signed-rank tests were used for statistical analyses, with p-values lower than 0.05 indicating statistical significance in plan parameter differences.

6.3 Results

6.3.1 Quality of autoplans

Prior to the comparisons of beam angle configurations, several analyses were performed to ensure that the autoplans used for these comparisons were clinically acceptable and of high quality. Details of these studies are presented in Electronic appendix A. The main observations were: 1) Of 645 generated autoplans, 98.8% was clinically acceptable. Non-acceptable plans all belonged to a particular patient (patient 0), who was excluded from further analyses, 2) automatically generated plans had overall favorable plan parameters compared to clinically delivered plans, generated with manual planning (Tables 6.A1 and 6.A2 and Figs. 6.A1 and 6.A2), 3) involved clinicians rated positively the automatically generated plans.

6.3.2 Comparisons of beam configurations

All applied 600 autoplans for patients 1-25 showed highly comparable PTV doses (standard deviations for V95%, V<90%, and V107% were 0.2%, 0.4 cc, and 0.3%). Therefore, only OAR doses are reported in this section.

Fig. 6.3 shows population average plan parameters for VMAT, B-VMAT and CP_x and NCP_x (x=5-15) (p-values for all mutual comparisons are reported in Fig. 6.B3 in Supplementary material B). Below, the main observations are summarized:

- *Beam number x in NCP_x and CP_x:* Both for CP_x and NCP_x plan quality increased with increasing x. For some parameters there was some levelling off for x≥11 beams, but not for all. Improvements obtained by adding a beam were highly statistically significant for high-dose plan parameters, i.e. lungs and patient V20Gy, heart Dmean and lungs Dmean. For medium dose parameters (lung V5Gy and breast Dmean) differences were almost always statistically significant. Improvements in left breast V4Gy were not statistically significant.
- *NCP_x vs. CP_x:* For equal beam numbers, x, NCP was always better than CP. Figs.6.4 a and b show that plan improvements with NCP_15 compared to CP_15 were observed for all patients, although the gain was clearly patient and plan parameter dependent. Differences in mean values were often considered clinically significant.
- *NCP_x vs. VMAT:* NCP_x≥10 was better than or equal to VMAT for all OAR plan parameters. For many parameters, equality was achieved for much less beams.

- *NCP_x vs. B-VMAT:* NCP_x was overall superior for lungs and patient V20Gy and for conformality (CI) (higher doses), and, for larger x, also for heart Dmean and lungs Dmean. Figs. 6.4 c and d show that differences are strongly patient- and parameter dependent. Possibly patients that may benefit most from NCP over B-VMAT in terms of heart or lungs doses are those with targets extending to the lower mediastinum (e.g. pt. 4, Fig. 6.B3) and/or the supraclavicular region bilaterally (pts. 3, 5, 11), or with asymmetrical target relative to the midline (e.g. unilateral axilla, pt. 16). Overall, B-VMAT had lower left breast Dmean and V4Gy, lungs V5Gy and patient V5Gy (lower dose parameters). However, some patients did benefit from the individualized beam choice in terms of breast dose, such as patients with axillar involvement (e.g. pts. 8 and 24) and with asymmetrical targets relative to the midline (e.g. pt. 12).

- *VMAT vs. B-VMAT:* Lungs V20Gy, patient V20Gy and CI (higher dose parameters) were on average lowest with VMAT. B-VMAT was on average superior for all other plan parameters. This is consistent with the findings by Fiandra et al. [50]. Figs. 6.4 e and f show strong patient- and plan parameter dependences of differences between VMAT and B-VMAT.

- *VMAT vs. CP_x:* For small x, VMAT was clearly superior. For larger x, differences were dependent on plan parameter.

- *Breast:* Non-coplanar approaches scored best. B-VMAT was overall the clear winner, followed by NCP with 12 beams or more (NCP_x≥12). Superiority of B-VMAT could be related to geometrical constraints as defined by the butterfly geometry, limiting the dose delivered to the breasts.

- *Heart:* Non-coplanar approaches were best. NCP_x≥10 plans had on average a lower heart Dmean than B-VMAT. The superior heart sparing with NCP_15 and B-VMAT is illustrated for patient 3 in Fig. 6.3.

- *Lung:* NCP_≥13 was overall best for Dmean and V20Gy. B-VMAT was overall best for V5Gy but resulted in high V20Gy.

- *Low vs high dose in lungs and patient (V5Gy vs V20Gy):* compared to B-VMAT, NCP improved lung and patient V20Gy (mostly $p<0.001$), at the cost of lungs and patient V5Gy (mostly $p\leq0.001$) and breast V4Gy (only significant for right breast). This can also be observed in the dose distributions in Fig. 6.3, where B-VMAT was less conformal around the tumor (red and yellow isodose lines), but showed less spread of low doses (light green and azure isodose lines in sagittal view), compared to CP_15 and NCP_15.

- *Dose conformality:* On average (Fig. 6.2), conformality was best for VMAT (lowest

CI), closely followed by NCP_15 and CP_15. B-VMAT was clearly the worst.

- *Overall observations:* in Fig. 6.4 patients are sorted according to decreasing heart Dmean in NCP_15 plans. A clear reduction in differences among techniques is visible for patients with decreasing heart Dmean, showing a dependence on patient anatomy (Fig. 6.B3) when selecting the optimal technique. E.g. patient 25 showed smaller differences between techniques, making the less complex CP or VMAT the favorable choice.

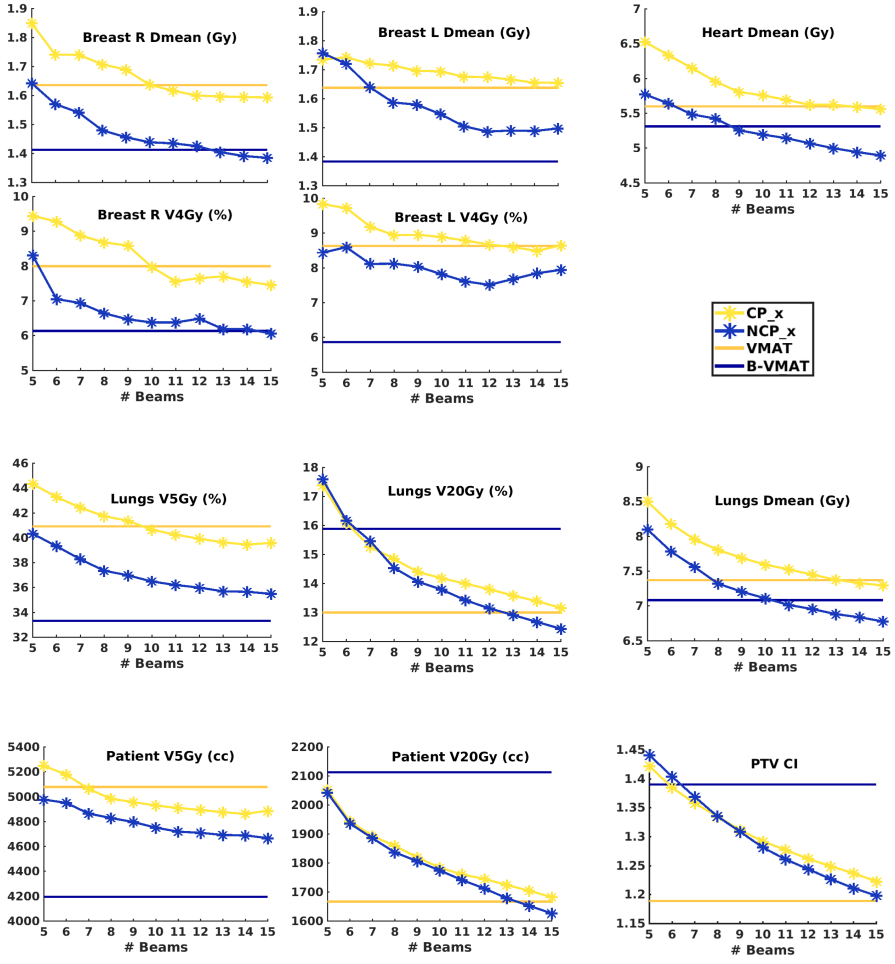

Figure 6.2: Population mean dosimetric plan parameters for CP_x and NCP_x as a function of the number of beams per plan (x). The dashed horizontal lines indicate the population mean values for VMAT and B-VMAT. P-values for beam configuration comparisons are presented in Supplementary material B.

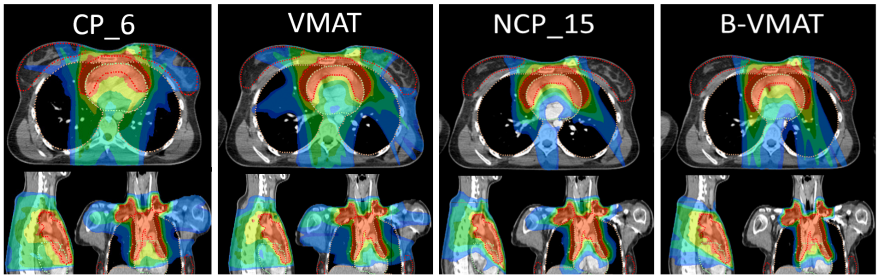

Figure 6.3: Dose distributions for patient 3. CP_6 was added as on average 6 beams were used clinically. CP_15 was similar to VMAT and was therefore not added. The isodose lines are percentages relative to the prescribe dose, i.e. 100% = 30 Gy, with color legend as light blue = 16.7% (5 Gy as OAR constraints), azure = 20%, light green = 40%, dark green = 60%, yellow = 80%, red = 95%.

6.3.3 Comparisons of beam configurations

For NCP_15 and CP_15, patient group analyses were performed on selected beam directions. The results are presented in Electronic appendix C.

6.4 Discussion

To the best of our knowledge, in all published studies comparing beam configurations for treatment of mediastinal lymphoma patients, treatment plans were generated with manual trial-and-error planning, including selection of beam angles. It is well-known that manually generated plans may suffer from inter-and intra-planner quality variations, aggravated by the complex finding of optimal beam configurations. In this paper we present the first study using autoplanning with integrated beam angle optimization to systematically explore advantages and disadvantages of various coplanar and non-coplanar beam configuration approaches for young female mediastinal lymphoma patients. Due to this automation, plan generation became fully independent of planners, and the analyses could be based on a large number of high-quality plans (600 plans in total: 24 beam configuration approaches, 25 patients).

All applied autoplans satisfied the clinical PTV coverage requirement, i.e. V95%≥95% while also the other PTV and OAR aims were sufficiently fulfilled. Autoplanning outperformed manual planning in terms of plan parameters, and treating clinicians rated positively the quality of autoplans (Supplementary material A).

In clinical planning, beam energies of 6, 10, and 18 MV were used, often also in combinations. For autoplanning in this study only 6 MV was used to avoid prolonged optimization times due to inclusion of beam energy optimization. Nevertheless, the obtained plan quality was high. There was not an overall superior beam configuration approach for the patient population, i.e. being on average best for all plan parameters. Performances of the various approaches were dependent on the considered OAR and the endpoint. There were also large inter-patient variations in the gain of one technique compared to another. However, overall there was a clear tendency towards improved plans with non-coplanar configurations (B-VMAT and NCP_x≥12). NCP_x≥12 was

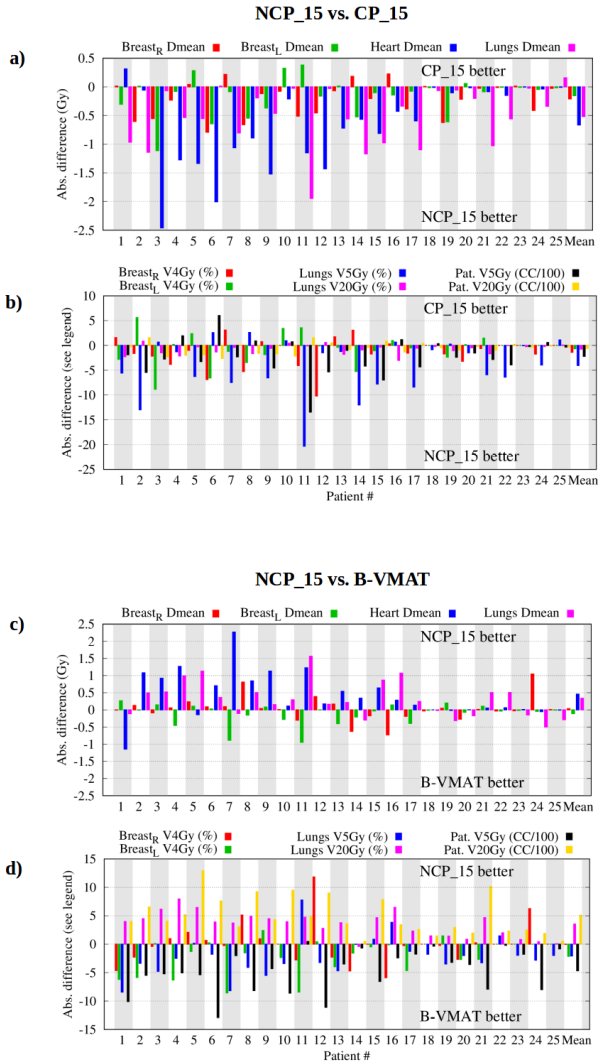

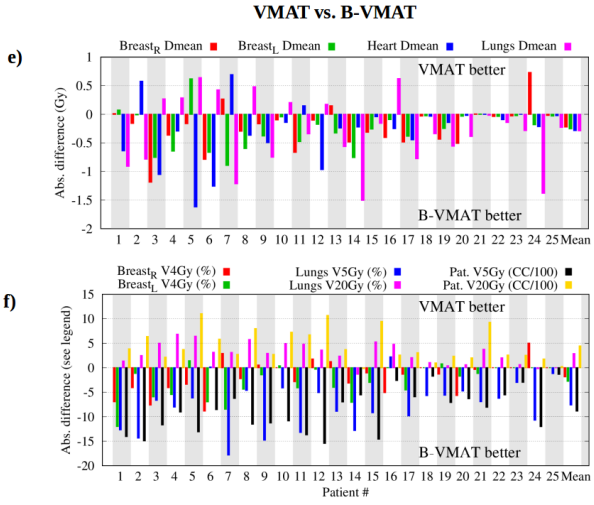

Figure 6.4: Beam configuration comparisons showing large inter-patient and inter-parameter variations in differences in plan parameter values. Patients were ordered according to descending heart Dmean in the NCP_15 plans.

on average better in producing highly conformal plans with reduced high doses in the lungs and patient and also a reduced heart Dmean, while B-VMAT had reduced low-dose spread, related to the confinement of beam angles to the butterfly geometry.

Levis et al. [99] have recently reported on a new-generation butterfly VMAT, where the coplanar part consists of a standard full-arc VMAT (FaB-VMAT). While this approach may solve some of the issues pointed out here for the B-VMAT approach (lack of conformity in the high doses), it might not be superior to NCP_15 for selected patients. In fact, the authors report a loss in breast dosimetry with FaB-VMAT for bulky tumors, compared to B-VMAT.

In this study, we have retrospectively used autoplanning to explore dosimetric differences between various beam configuration approaches. The observed large organ-dependency and inter-patient variations in dosimetric differences between various beam set-ups are incentives for prospective use of automated planning for all new patients to further personalize radiotherapy for lymphoma patients. This study is also an incentive for manufactures of treatment planning systems to extend their systems with advanced options for patient-specific beam angle optimization.

6.5 Conclusion

Using autoplanning including computerized coplanar and non-coplanar beam configuration optimization, 24 beam configuration approaches were compared for 25 young female mediastinal lymphoma patients. The quality of the applied autoplans was superior to that of manually generated, clinically delivered plans. Non-coplanar beam configurations were overall favorable, but significant patient-specific and plan-parameter-dependent dosimetric advantages and disadvantages of different beam configurations were observed, suggesting a need for prospective generation of multiple plans per patient to optimally personalize radiotherapy treatment.

A Supplementary material

Quality of autoplans

Three types of analyses were performed to ensure that the autoplans used for beam angle comparisons were of high quality: global plan parameter evaluations for the generated autoplans (section A1), detailed plan parameter comparisons between manually generated clinical plans (CLIN) and corresponding autoplans (section A2), and physicians' evaluations of autoplans considering full 3D dose distributions, DVHs, and DVH parameters (section A3).

As explained in the manuscript, the study started with 26 patients. In total 645 autoplans were generated for these patients: 26x24 (624) plans for the 24 beam configurations defined in Fig. 6.1, and 21 so-called AUTOclin plans, defined and used below in section A2. For reasons explained in section A1, only patients 1-25 were in the end used for the beam configuration comparisons in the body of the paper (excluding patient 0), i.e. 25x24=600 autoplans were used. Patient 0 was also excluded from the investigations below involving AUTOclin plans (section A2), leaving 20 plans for those analyses, and all other analyses in this and other Supplementary materials.

Two-sided Wilcoxon signed-rank tests were used for statistical analyses with p-values lower than 0.05 indicating statistical significance in plan parameter differences.

A.1 Global plan parameter evaluations for autoplans and exclusion of patient o

Of the 645 generated autoplans, 637 (98.8%) satisfied the clinical PTV coverage requirement, i.e. V95%≥95%. The 8 autoplans with insufficient PTV coverage were from the same patient (patient o in Fig. 6.B3 in Supplementary material B), all with relatively low numbers of coplanar beams (CP_5-11 and CLINauto). In the IMRT plan used for treatment of this patient, sufficient PTV coverage was obtained at the cost of exceptionally high breast and heart doses: breast Dmean = 11.9/6.3 Gy left/right, and heart Dmean = 23.2 Gy (by far the highest in the group). In the wish-list (Table 6.B3 in Supplementary material B), a hard constraint for breast Dmean was set to 5 Gy, reflecting the clinical protocol (M&M). Therefore, the automated planning workflow did not allow generation of plans with the exceptionally high breast doses as present in the CLIN plan, resulting in a really low autoplan PTV coverage when low numbers of beams were used. Because of the unacceptability of generated autoplans, patient o was excluded from all further analyses in the paper, including the supplements. (Interestingly, the non-coplanar autoplans NCP_14 and NCP_15 for patient o fulfilled all clinical plan criteria, including PTV and breast, so much better than CLIN).

		25 CLIN plans		**600 autoplans**	
Structure	**Parameter**	**Mean**	Range	**Mean**	Range
PTV	V95% (%)	**98.1**	95.0 - 99.7	**99.5**	97.1 - 99.9
	V<90% (cc)	**2.9**	0.0 - 19.0	**0.5**	0.0 - 6.6
	V107% (%)	**0.9**	0.0 - 2.6	**0.2**	0.0 - 5.4
	CI	**1.2**	1.1 - 1.6	**1.2**	1.1 - 1.5
BreastR	Dmean (Gy)	**1.9**	0.1 - 6.2	**1.6**	0.2 - 5.2
	V4Gy (%)	**10.7**	0.0 - 35.5	**7.4**	0.0 - 33.6
BreastL	Dmean (Gy)	**1.9**	0.0 - 5.4	**1.6**	0.1 - 5.1
	V4Gy (%)	**10.0**	0.0 - 37.7	**8.4**	0.0 - 38.2
Heart	Dmean (Gy)	**6.5**	0.2 - 20.0	**5.6**	0.2 - 20.4
Lungs	Dmean (Gy)	**8.3**	2.1 - 14.3	**7.4**	1.8 - 16.8
	V5Gy (%)	**44.2**	10.6 - 79.5	**38.9**	7.4 - 88.2
	V20Gy (%)	**15.7**	3.0 - 30.4	**14.4**	2.6 - 39.2
Patient	V5Gy (cc)	**5135.6**	1191.8 - 10186.8	**4861.3**	960.5 - 10816.9
	V20Gy (cc)	**1869.8**	271.1 - 4873.7	**1809.6**	259.5 - 5056.6

Table 6.A1: Comparisons of mean (and ranges) autoplan parameters with corresponding mean (and ranges) CLIN plan parameters for patients 1-25. For calculation of the mean autoplan parameters, all 24 plans per patient, used for the beam configuration studies, were considered. Mean autoplan parameters compared favorably with mean CLIN parameters.

Table 6.A1 compares mean autoplan parameters with the corresponding mean parameters for the CLIN plans. All averaged PTV dose parameters of the autoplans were

favorable compared to those of the CLIN plans. The values for mean/minimum PTV coverage went up from 98.1%/95.0% to 99.5%/97.1%. A remarkable reduction in PTV V<90% was observed, with mean/maximum values decreasing from 2.9 cc/19.0 cc to 0.5 cc/6.6 cc. Autoplans were also superior to CLIN in all mean OAR plan parameters. For lungs and patient, observed maximum values in the autoplans were slightly higher than those in the CLIN plans (compare ranges). This could be related to the improved PTV dose, but statistics might also contribute here: the more plans generated, the higher the chance on outliers (25 CLIN plans vs. 600 autoplans).

A.2 Detailed plan parameter comparisons between clinical plans and autoplans.

For the 20 patients that were clinically treated with IMRT (i.e. excluding patient 0), the CLIN plan was compared to the CLINauto plan, an automatically generated IMRT plan with the same (manually selected) beam configuration as CLIN (Table A2). Significant improvements (statistically and clinically) with autoplanning were observed for PTV V95%, PTV V<90%, PTV V107%, lungs and patient V5Gy, and right breast V4Gy. On average, PTV V95% was 1.4% higher (maximum: 3.3%) and PTV underdose (V<90%) was 2 cc less (maximum: 10 cc). This came at the expense of slightly enhanced lung and patient V20Gy and CI, the latter clearly related with higher PTV coverage. Due to substantially improved PTV dose in the CLINauto plans, the latter plans were overall preferred over the CLIN plans. The last columns in Table 6.A2 show impressive plan quality improvements for NCP_15 compared to CLIN, related to the application of 15 non-coplanar IMRT beams with computer-optimized, individualized beam configurations, instead of 4-8 manually selected beams.

Figures 6.A1 and 6.A2 show for the individual patients, PTV and OAR plan parameters.

A.3 Physicians' evaluations of CP_9, NCP_15, VMAT, and B-VMAT autoplans

The in total 100 evaluated autoplans for patients 1-25 were considered of high quality by both physicians. For one physician, all evaluated autoplans were acceptable. In first instance, the other physician had doubts on 7 coplanar autoplans (3x CP_9, 4x VMAT) because of lungs V5Gy exceeding 55%. However, this parameter turned out to be in the range 61%-79.5% in the corresponding clinical plans and were accepted. The latter physician also had doubts on two non-coplanar plans with dose spread into the liver (resulting mean liver doses: 3.6 Gy and 2.5 Gy).

Structure	Parameters	CLIN	CLINauto - CLIN	p	NCP_15 - CLIN	p
PTV	V95% (%)	98.2 (96.3, 99.7)	1.4 (0.1, 3.3)	<0.001	1.1 (-0.4, 3.1)	<0.001
	V<90% (cc)	2.2 (0, 10.6)	-2 (-10.4, 0.1)	<0.001	-1.5 (-9, 1.1)	0.040
	V107% (%)	1 (0, 2.6)	-0.8 (-2.3, 0.2)	<0.001	-0.8 (-2.3, 0.2)	<0.001
	CI	1.3 (1.1, 1.6)	0.2 (0, 0.3)	<0.001	-0.1 (-0.4, 0.1)	0.006
BreastR	Dmean (Gy)	1.4 (0.1, 6.2)	-0.2 (-1, 0.6)	0.145	-0.4 (-1.6, 0.7)	0.033
	V4Gy (%)	8.1 (0, 35.4)	-2.4 (-10.2, 2.6)	0.011	-3.6 (-20.6, 4.6)	0.022
BreastL	Dmean (Gy)	1.6 (0, 5.3)	-0.1 (-3, 0.5)	0.627	-0.4 (-3.4, 1)	0.145
	V4Gy (%)	8.9 (0, 37.6)	-1.7 (-27.5, 3.2)	0.379	-2 (-26.8, 7.8)	0.352
Heart	Dmean (Gy)	5.8 (0.2, 17.1)	0.1 (-1.8, 1.9)	0.391	-1.6 (-5.8, 1.7)	0.001
Lungs	Dmean (Gy)	8 (2.1, 14.3)	0 (-1.6, 1.2)	1.000	-1.6 (-3.3, 0)	<0.001
	V5Gy (%)	42.8 (10.6, 79.5)	-2.6 (-10.9, 2.8)	0.004	-9.6 (-23.9, 1.3)	<0.001
	V20Gy (%)	14.9 (3, 30)	2 (-1.3, 6.1)	<0.001	-3.4 (-8.5, 1.7)	<0.001
Patient	V5Gy (cc)	4665.7 (1192.9, 7917.9)	-187 (-950.8, 246.3)	0.033	-438.4 (-1777.8, 539.1)	0.007
	V20Gy (cc)	1665.5 (271.3, 4060.9)	323.3 (-3.7, 777.1)	<0.001	-221.6 (-900.5, 192.1)	0.009

Table 6.A2: Average and range (min, max) plan parameters for 20 clinical IMRT plans (CLIN), and differences with CLINauto (IMRT with same beam angles as CLIN) and with NCP_15 (IMRT with 15 beams with computer-optimized patient-specific beams). Colors indicate statistical significance (p<0.05), green: automation superior, red: CLIN superior, white: difference not significant.

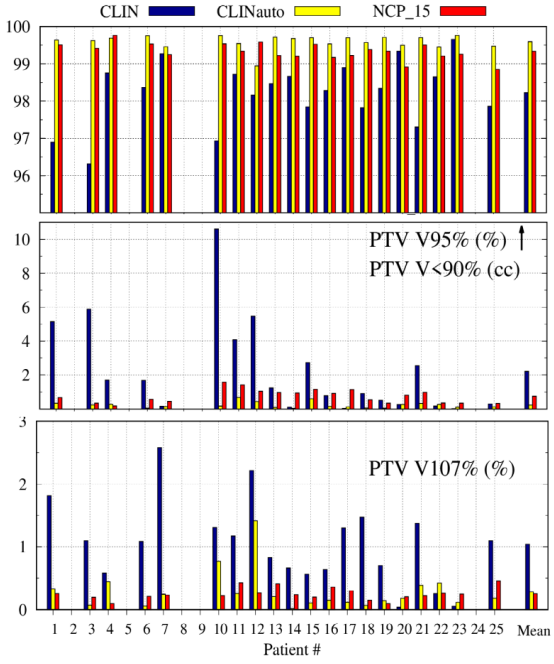

Figure 6.A1: PTV plan parameters for 20 patients treated with IMRT: CLIN (blue), CLINauto (yellow) and NCP_15 (red).

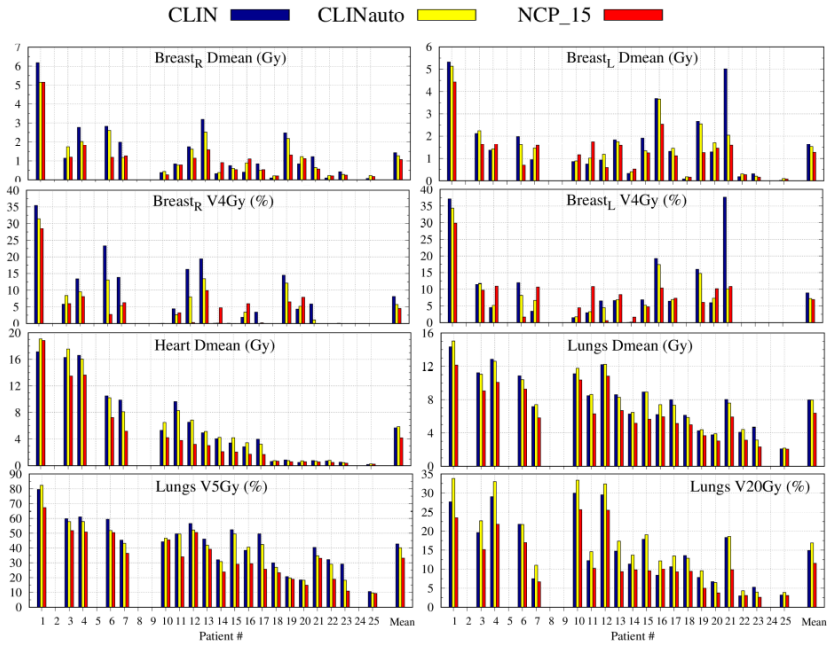

Figure 6.A2: OAR plan parameters for 20 patients treated with IMRT: CLIN (blue), CLINauto (yellow) and NCP_15 (red).

B Supplementary material

B.1 Patient cohort

B.2 Wish-list for mediastinal lymphoma autoplanning with Erasmus-iCycle

Autoplanning with Erasmus-iCycle is based on a patient-group-specific wish-list [22]. Hard constraints and prioritized objectives in the wish-list steer the optimizer in the multi-criterial plan generation. Constraints are always met, while objectives are goals that are optimized as much as possible, following the objective priorities and within the imposed hard constraints. Objectives are optimized sequentially, starting with the highest priority objective (priority 1). After each objective optimization, a constraint is

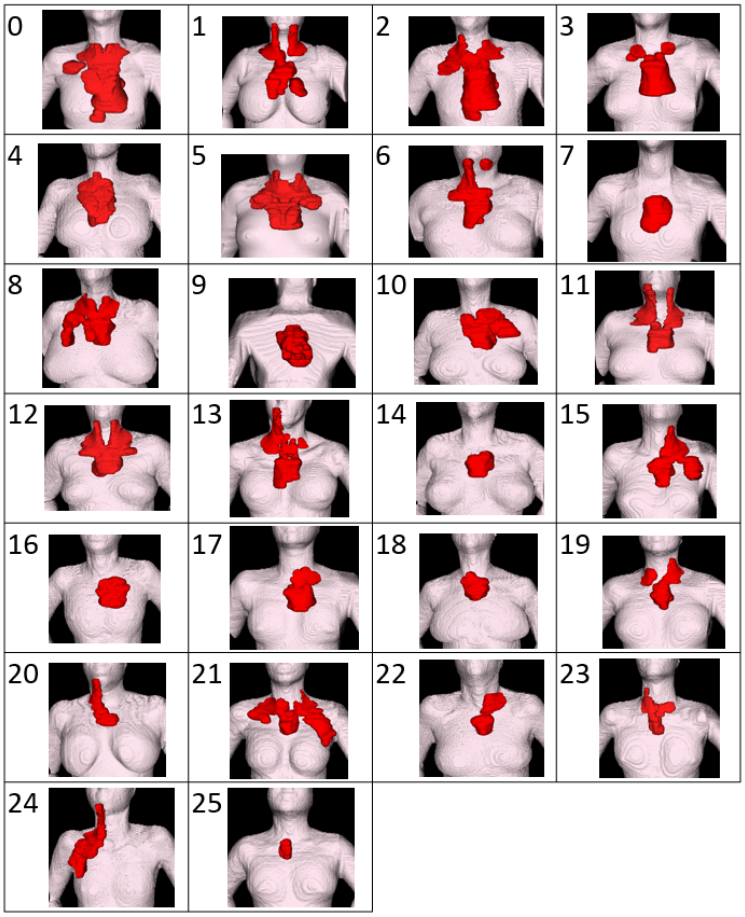

Figure 6.B3: Study patients ordered according to descending heart Dmean in the NCP_15 plans. Patient 0 was excluded from all analyses because of unacceptable autoplans (see Electronic appendix A). red: PTV, pink: patient.

added to the optimization problem, which is used for optimizing lower priority objectives without losing on obtained higher priority objective values [21, 22, 73, 145, 157, 185, 186].

The wish-list created in this study for young female mediastinal lymphoma patients, using the wish-list creation methodology as explained in the Electronic appendix of [69], is shown in Table B1. It contains constraints on (a) the PTV Dmean and Dmax to control tumor dose homogeneity, (b) shells at 0.3-5 cm distance from the PTV, to control dose fall off, (c) breast Dmean, and (d) entrance dose. With the LTCP cost function (logarithmic tumor control probability [1]) as first priority, plan generation always started with optimizing PTV coverage within the constraints, which was also clinically the most im-

portant objective. Next, the PTV minimum dose (priority 2) was optimized, again in line with clinical planning. Priority 3 tried to limit the maximum dose in a 2 cm ring around the PTV, while priority 4 aimed at reducing dose (to about 60% of the prescribed dose at 5 cm) in a larger volume, including the back muscles. With priorities 5-11, OAR doses were optimized, balancing dose delivery to breasts, heart and lungs. Mean doses and EUDs were used as cost functions. EUDs with a=0.5 were used to control the low-dose bath in lungs and breasts. As last objective, the dose at 1 cm from the PTV (shell) was reduced to further minimize dose outside the PTV where possible.

Constraints

Structure	Type	Limit
PTV	maximum	32.1 Gy
PTV	mean	30.6 Gy
Breast L	mean	5 Gy
Breast R	mean	5 Gy
Shell 3 mm from PTV	maximum	30 Gy
Shell 1 cm from PTV	maximum	28.5 Gy
Shell 3 cm from PTV	maximum	27 Gy
Shell 5 cm from PTV	maximum	22.5 Gy
Entrance dose*	maximum	18 Gy

Objectives

Priority	Structure	Type	Goal	Sufficient	Parameters
1	PTV	LTCP	0.2	0.2	Dc=28.5 Gy, α=0.8
2	PTV	minimum	28.5 Gy		
3	Ring 2 cm around PTV**	maximum	28.5 Gy		
4	Patient - PTV exp 5 cm***	maximum	21 Gy		
5	Lungs - PTV	EUD	6 Gy	6 Gy	a=0.5
6	Lungs - PTV	EUD	22 Gy	22 Gy	a=8
7	Breast L	EUD	0.9 Gy		a=0.5
7	Breast R	EUD	0.9 Gy		a=0.5
8	Heart - PTV	mean	0 Gy		
9	Lungs - PTV	mean	0 Gy		
10	Heart - PTV	EUD	0 Gy		a=8
11	Breast L	EUD	0 Gy		a=8
11	Breast R	EUD	0 Gy		a=8
12	Shell 1 cm from PTV	maximum	27 Gy		

Table 6.B3: Wish-list used in autoplanning for all patients and beam configurations. *: dose in first 2 cm inwards the patient contour, subtracting PTV expanded by 7 cm. **= PTV expanded with 2 cm – PTV, ***= patient – (PTV expanded by 5 cm). LTCP = Logarithmic tumor control probability, Dc = 95% * prescribed dose and α = cell sensitivity. EUD = Equivalent Uniform Dose, a = volume parameter. The use of goal and sufficient parameters is explained in [Breedveld 2012].

B.3 Mutual dosimetric comparisons of all 24 investigated beam configurations (related to Fig. 3 in the body of the manuscript)

Data available online

C Supplementary material

Selected beam angles

The population distributions of selected beam directions for NCP_15 and CP_15 are shown in Fig. 6.C4. The rectangles in the left panel of Fig. 6.C4 show the coplanar and non-coplanar beam directions used for B-VMAT. Non-coplanar beams resulting from a couch angle of 90° and gantry angles between 10° and 30°, entering the patient from anterior-inferior directions, were frequently present in NCP_15 plans. These entrance angles have a heart sparing/avoidance effect (see also sagittal views in Fig. 6.3 in the body of the paper). The (couch, gantry) directions around (-70°,-30°) and around (-45°,-15°) were also often present in the NCP_15 plans. A clear prevalence of anterior beams was found in both NCP_15 and CP_15 with gantry angles between ±90°. For all patients, at least one anterior beam was present in the range -10° to 10° for CP_15 plans. Many beams in NCP_15 coincide with the anterior beam directions of B-VMAT On the other hand, the posterior angles of B-VMAT were hardly selected in NCP_15. Apart from the clustered areas, Fig. 6.C4 shows broad distributions of selected beam directions for NCP_15 and CP_15. This is in agreement with the large inter-patient variations in selected directions, see Figs. 6.C5 and 6.C6.

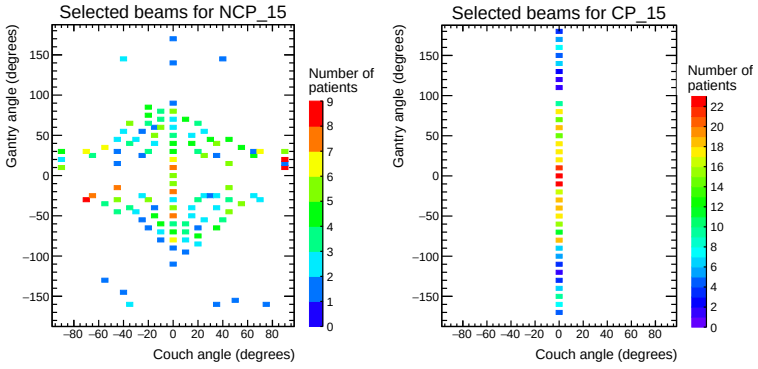

Figure 6.C4: Population distributions of beams selected for NCP_15 (left) and CP_15 (right) for patients 1-25 (375 beams per panel). The black rectangles in the left panel indicate the beams present in B-VMAT.

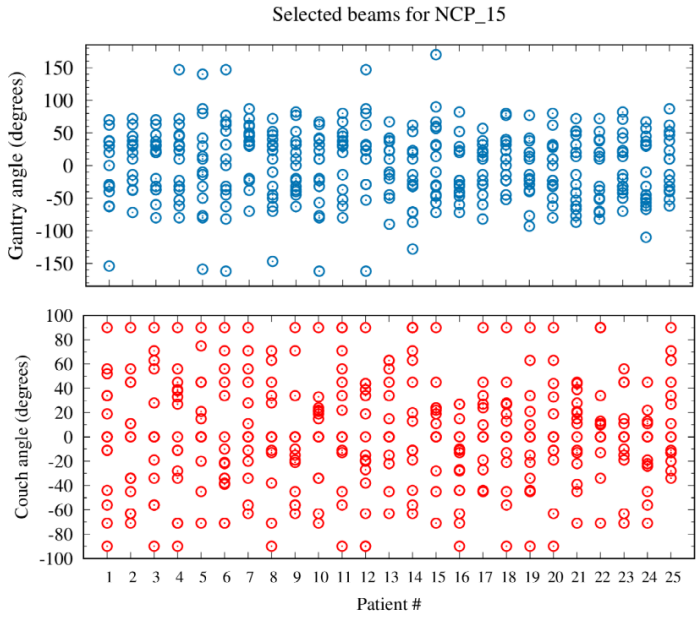

Figure 6.C5: Optimized, patient-specific beam directions for NCP_15 plans for patients 1-25.

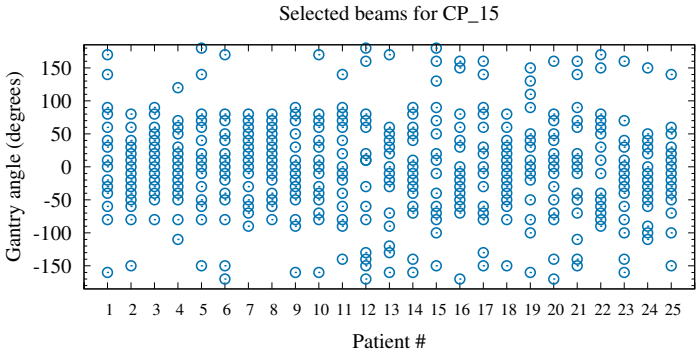

Figure 6.C6: Optimized, patient-specific beam directions for CP_15 plans for patient 1-25.

Complementing prostate SBRT VMAT with a two-beam non-coplanar IMRT class solution to enhance rectum and bladder sparing with minimum increase in treatment time

7

Abdul Wahab Sharfo, Linda Rossi, Maarten Dirkx,
Sebastiaan Breedveld, Shafak Aluwini, Ben Heijmen

Department of Radiation Oncology,
Erasmus MC, Rotterdam

Submitted

Abstract

Background and purpose Enhance rectum and bladder sparing in prostate SBRT with minimum increase in treatment time by complementing VMAT with a two-beam non-coplanar IMRT class solution (CS).

Materials and Methods For twenty patients, an optimizer for automated multi-criterial planning with integrated beam angle optimization (BAO) was used to generate VMAT plans, supplemented with five non-coplanar IMRT beams with individualized orientations (VMAT+5). A CS with two most preferred directions in VMAT+5 was then defined for VMAT+CS. VMAT+CS was compared with automatically generated i) dual-arc coplanar VMAT plans (VMAT), ii) VMAT+5 plans, and iii) IMRT plans with 30 patient-specific non-coplanar beam orientations (30-NCP). Differences in PTV doses, OAR sparing, and computation and treatment delivery times were quantified.

Results Compared to VMAT, VMAT+CS significantly reduced rectum and bladder doses, and the dose bath. Mean relative differences in rectum D_{mean}, D_{1cc}, V_{40GyEq} and V_{60GyEq} were 19.4±10.6%, 4.2±2.7%, 34.9±20.3%, and 39.7±23.2%, respectively (all $p<0.001$). Total delivery times with VMAT+CS only increased by 1.9±0.7 min compared to VMAT (9.1±0.7 min). The dosimetric quality of VMAT+CS plans was equivalent to VMAT+5, while optimization times were reduced by a factor of 25 due to avoidance of BAO. Compared to VMAT+CS, the 30-NCP plans were only favorable in terms of dose bath, at the cost of much enhanced optimization and delivery times.

Conclusion The proposed two-beam non-coplanar class solution to complement coplanar VMAT resulted in substantial plan quality improvements with minor increases in treatment delivery times. In addition, patient-specific non-coplanar beam angle optimization was superfluous.

7.1 Introduction

Stereotactic body radiation therapy (SBRT) is becoming the standard treatment radiotherapy option for several primary and metastatic tumors [61, 63, 76, 96, 121, 152, 182, 193]. In prostate SBRT, volumetric modulated arc therapy (VMAT) has been promoted because of its short treatment delivery time [4, 78, 102]. On the other hand, several studies have shown that use of non-coplanar beam arrangements minimizes doses in the normal tissues compared to coplanar VMAT, at the cost of enhanced treatment delivery times [43, 143, 145]. To overcome the prolonged treatment times of non-coplanar IMRT beam arrangements, recent work has been focusing on increasing the delivery efficiency by employing non-coplanar arcs instead. This showed promise due to a drastic reduction in the treatment time, while obtaining a high plan quality [26, 83, 84, 106]. Recently, we proposed a novel treatment approach for liver SBRT, designated VMAT+, complementing VMAT with a few non-coplanar IMRT beams with computer-optimized, patient-specific orientations to enhance plan quality, while keeping delivery time low [157]. However, plan optimization times for VMAT+ were long because of the need for individualized beam angle optimization (BAO).

In this study, we used our in-house developed algorithm for automated multi-criterial planning with integrated BAO to explore opportunities for enhancing prostate SBRT dose distributions by complementing dual-arc coplanar VMAT with non-coplanar IMRT beams. To keep the total delivery time limited, the investigated maximum number of complementary non-coplanar beams was five (VMAT+5). Based on the selected beam orientations in the VMAT+5 plans, a class solution (CS) for the non-coplanar beams was defined. Final VMAT+CS plans were benchmarked against automatically generated i) dual-arc coplanar VMAT plans (VMAT), ii), VMAT+5 plans, and iii) 30-beam non-coplanar IMRT plans with computer-optimized beam orientations (30-NCP). Differences in dosimetric plan parameters, computation and treatment delivery times were analyzed. Dose measurements were performed to verify deliverability of generated plans at the treatment unit.

7.2 Materials and methods

7.2.1 Patient data

Planning CT-scans of 20 randomly selected prostate SBRT patients were included in this study. In all CT-scans the rectum (outer contour), rectal mucosa (3mm wall), bladder,

urethra, femoral heads, scrotum, penis and prostate were delineated. The average planning target volume (PTV) size was 91.2 cc [57.8 – 142.3 cc] (PTV was defined as prostate plus 3 mm isotropic margin). Dose was delivered in 4 fractions of 9.5 Gy, emulating high-dose rate (HDR) brachytherapy with highly heterogeneous dose distributions [5]. Plan acceptability was subject to the dosimetric constraints presented in Table table:VMAT+table1.

Structure	Parameter	Tolerance Limit
PTV	$V_{100\%}$	95%
Rectum	D_{max}	38 Gy
	D_{1cc}	32.3 Gy
Rectum mucosa	D_{max}	28.5 Gy
Bladder	D_{max}	41.8 Gy
	D_{1cc}	38 Gy
Urethra	$D_{5\%}$	45.5 Gy
	$D_{10\%}$	42 Gy
	$D_{50\%}$	40 Gy
Femoral heads	D_{max}	24 Gy

Table 7.1: Clinically applied dose constraints for prostate SBRT.

7.2.2 Automated plan generation

For each patient, the Erasmus-iCycle multi-criterial optimizer was used to automatically generate one treatment plan per investigated technique (VMAT+CS, VMAT, VMAT+5, 30-NCP) that is both Pareto-optimal and clinically favorable [22]. For practical and legal reasons, Erasmus-iCycle plans are not directly used clinically. Instead, the Erasmus-iCycle plan is automatically converted into a clinically deliverable plan by the Monaco treatment planning system (TPS) (Elekta AB, Stockholm, Sweden) [185]. For this purpose, a patient-specific Monaco template is automatically made based on the ErasmusiCycle dose distribution. In case plan generation includes BAO, the optimal angles are established with Erasmus-iCycle, and are then used as fixed angles in the subsequent Monaco plan generation. Many studies have demonstrated superiority of these automatically generated plans compared to manually generated plans [27, 69, 145, 156, 159].

Multi-criterial plan generation with Erasmus-iCycle is based on a tumor site-specific 'wish-list' containing hard constraints to be strictly obeyed and plan objectives with ascribed priorities. For BAO, a set of candidate beam orientations has to be defined as well [22]. In this study, we used a published wish-list for prostate SBRT [145]. For the optimizations with integrated BAO (VMAT+5 and 30-NCP), the non-coplanar beam selection search space consisted of 300 candidate beams, separated by about 10 degrees, and homogeneously distributed across the part of the sphere where collisions between

the patient/couch and the gantry were avoided, as verified at the treatment unit.

All plans in this study were generated for an Elekta Synergy treatment machine equipped with a VersaHD collimator with a leaf width of 5 mm. 10 MV photon beams were used. Dose calculations in Monaco (version 5.10) were performed with a dose grid resolution of 3 mm. The total number of control points in all plans in this study was kept fixed at 300 for all investigated techniques (i.e. VMAT+CS, VMAT, VMAT+, and 30-NCP) to eliminate potential bias. IMRT was delivered with dynamic multi-leaf collimation with a maximum of 10 control points per involved beam, in line with our clinical practice. A 5 degrees collimator angle was used for all arcs/beams, and the maximum dose rate was 600 MU/min. For generation of the VMAT+5 and VMAT+CS plans, VMAT and the non-coplanar IMRT beams were optimized simultaneously, both in Erasmus-iCycle and in Monaco.

7.2.3 Workflow for generation of the non-coplanar beam angle class solution (CS)

The final CS to supplement dual-arc VMAT in VMAT+CS treatments was developed in a stepwise approach, based on automatically generated plans:

1. For each of the 20 study patients, the optimal VMAT+5 plan with individualized beam angles was generated.
2. Based on an analysis of the angular distribution of the selected 20x5 non-coplanar beams, candidate class solutions, CSi, were defined as described in the Results section, all including a small number of frequently selected beam directions, and accounting for the left-right symmetry in the patients' anatomies.
3. For a subgroup of 6 randomly selected patients, VMAT+CSi plans were generated for all CSi. These plans were then compared with corresponding VMAT plans, and the CSi resulting in the most favorable plan quality increases relative to VMAT (focusing on rectum dose parameters) was selected as final CS.

7.2.4 Dosimetric comparisons of VMAT+CS plan parameters with VMAT, VMAT+5 and 30-NCP

Automatically generated VMAT+CS, VMAT, VMAT+5 and 30-NCP plans were compared for the 20 study patients. Prior to the analyses, all generated 80 plans were normalized to have identical PTV dose coverage (V_{38Gy}=95%, as requested in clinical practice). Next, compliance with the clinically applied dose constraints (Table 7.1) was verified for all plans. Finally, plan parameter differences were analyzed. Paired two-sided Wilcoxon

signed-rank tests were performed to assess clinical significance of observed differences ($p<0.05$).

7.2.5 Plan deliverability, treatment time and MU for VMAT and VMAT+CS

For a subgroup of 5 patients with the largest plan quality gains achieved with VMAT+CS compared to VMAT, both VMAT and VMAT+CS plans were delivered at an Elekta Synergy linac (Elekta AB, Sweden) while irradiating a PTW 2D-Array seven29™ and Octavius™ phantom (PTW, Freiburg, Germany). The measurements were compared to Monaco TPS predictions using a commercial QA software package (PTW VeriSoft version 6.2) with 5% cut-off, 3% global maximum dose and 1 mm distance to agreement (3%/1 mm) criteria, and 95% Gamma passing rate threshold. For delivery time comparisons, we separately measured i) beam-on-times, ii) gantry-travel-times (times to rotate the gantry from one fixed angle to another while the beam is off), and iii) couch-travel-times (times required to rotate the treatment couch in between beams, including time needed for entering the room). Additionally, the VMAT and VMAT+CS plans were compared regarding the total number of monitor units (MU).

7.3 Results

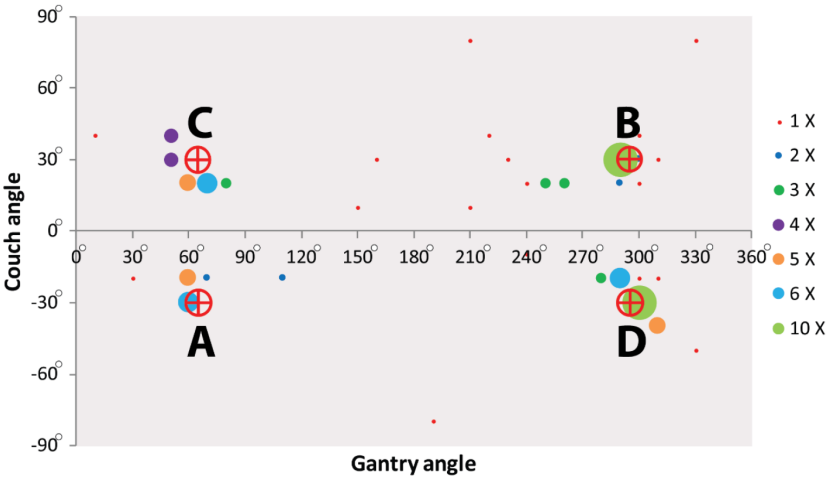

Figure 7.1: Angular distribution of the 100 non-coplanar IMRT beams in the VMAT+5 plans of the 20 study patients. Based on these results four principle beam directions A = (65°,-30°), B = (295°, 30°), C = (65°, 30°) and D = (295°,-30°) were derived to develop the final class solution for VMAT+CS.

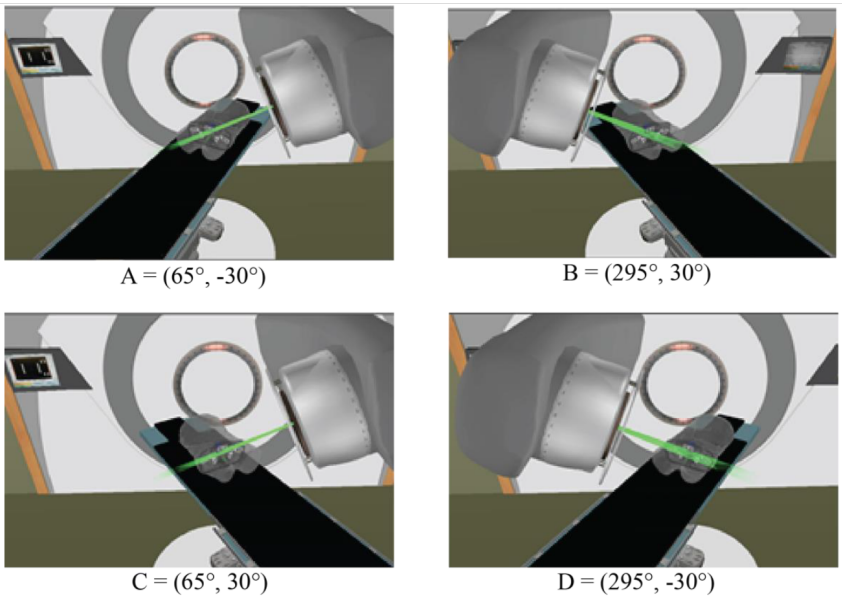

Figure 7.2: Four principle beam directions, characterized by (gantry angle, couch angle), from Fig. 7.1, used to develop the final class solution for VMAT+CS. This final CS consisted of directions C and D.

7.3.1 Establishment of the final CS to define VMAT+CS

Based on the four clusters of frequently selected angles in the generated VMAT+5 plans (Fig. 7.1), four principal directions (gantry angle, couch angle) for class solution definition were derived: A = (65°,-30°), B = (295°, 30°), C = (65°, 30°) and D = (295°,-30°). These are visually displayed in Fig. 7.2. Based on these directions, three candidate CSi were defined: CS1, containing all four directions, CS2 consisting of directions A and B, and CS3 with directions C and D. Clearly, VMAT+CS3 resulted in the most favorable plan quality improvements for the rectum dose parameters compared to VMAT (Fig. 7.A1 See Supplementary Material). Therefore, CS3 was selected as the final CS for further evaluation of VMAT+CS with respect to VMAT, VMAT+5 and 30-NCP for all 20 study patients.

7.3.2 Comparisons of VMAT+CS plan parameters with VMAT, VMAT+5 and 30-NCP

All 20x4 plans included in the analysis fulfilled the clinically applied dose constraints. In general, all plans with non-coplanar beam arrangements (VMAT+CS, VMAT+5, and 30-NCP) resulted in substantial reductions in doses in healthy tissues and dose bath com-

pared to VMAT (Fig. 7.4 and Table 7.2). Differences between VMAT+CS and VMAT+5 were generally small and clinically negligible, while the former had less non-coplanar beams (yielding smaller overall treatment delivery time), and did not require individualized beam-angle-optimization (yielding reduced optimization time). Remarkably, also the differences between VMAT+CS and 30-NCP, the latter with much enhanced degrees of freedom in plan optimization, were relatively small. Actually, in rectum and bladder D_{mean} there was even a small advantage for VMAT+CS. For rectum D_{1cc}, V_{40GyEq}, V_{60GyEq}, bladder D_{1cc} and all urethra parameters, differences between VMAT+CS and 30-NCP were considered clinically irrelevant. There was a significant improvement in dose bath with 30-NCP, but clear disadvantages of this technique are the long optimization times (around 100 hours per patient) and the very long delivery times (see below).

	VMAT+CS	**VMAT-(VMAT+CS)**		**(VMAT+5) – (VMAT+CS)**		**30NCP – (VMAT+CS)**	
	Mean ± SD [range]	**Mean ± SD [range]**	p-value	**Mean ± SD [range]**	p-value	**Mean ± SD [range]**	p-value
PTV							
$V_{100\%}$ (%)	95.0 ± 0.0 [94.9, 95.1]	0.0 ± 0.1 [-0.1, 0.1]	1	0.0 ± 0.0 [-0.1, 0.0]	1	0.0 ± 0.0 [-0.1, 0.1]	1
$D_{98\%}$ (Gy)	35.1 ± 0.7 [33.8, 36.3]	1.1 ± 1.5 [-1.0, 1.5]	**0.004**	-0.1 ± 1.6 [-2.8, 3.8]	0.245	0.6 ± 1.7 [-1.5, 4.3]	0.368
CI	1.11 ± 0.04 [1.04, 1.20]	-1.6 ± 1.9 [-6.8, 2.5]	**0.001**	-0.5 ± 2.3 [-5.1, 3.4]	0.522	-1.5 ± 1.9 [-4.7, 2.0]	**0.006**
Rectum							
D_{mean} (Gy)	5.4 ± 1.0 [3.7, 7.5]	19.4 ± 10.6 [-9.3, 35.0]	**< 0.001**	4.6 ± 10.9 [-16.5, 23.0]	0.097	11.5 ± 11.2 [-17.4, 32.9]	**0.001**
D_{1cc} (Gy)	27.6 ± 2.6 [23.7, 32.8]	4.2 ± 2.7 [-1.0, 9.8]	**< 0.001**	0.5 ± 2.8 [-3.5, 6.5]	0.312	0.4 ± 2.1 [-4.3, 4.9]	0.596
V_{40GyEq} (%)	3.5 ± 1.3 [1.8, 6.1]	34.9 ± 20.3 [-8.1, 78.0]	**< 0.001**	6.1 ± 18.5 [-20.1, 52.0]	0.231	7.6 ± 13.5 [-21.2, 32.8]	**0.03**
V_{60GyEq} (%)	1.1 ± 0.7 [0.2, 2.8]	39.7 ± 23.2 [4.6, 97.5]	**< 0.001**	1.1 ± 19.9 [-33.2, 36.6]	0.784	-0.2 ± 13.6 [-25.8, 27.8]	0.49
Rectum Mucosa							
D_{max} (Gy)	26.2 ± 2.6 [20.9, 31.6]	6.3 ± 3.9 [-1.9, 14.7]	**< 0.001**	-0.3 ± 4.0 [-9.3, 8.0]	0.763	0.6 ± 3.6 [-8.2, 7.0]	0.577
Bladder							
D_{mean} (Gy)	6.6 ± 1.3 [4.5, 8.8]	17.9 ± 11.0 [-1.8, 45.6]	**< 0.001**	-1.5 ± 7.7 [-15.2, 18.6]	0.841	9.8 ± 15.7 [-28.0, 48.6]	**0.006**
D_{1cc} (Gy)	36.7 ± 1.2 [34.1, 38.5]	0.3 ± 1.1 [-1.5, 2.7]	0.409	-1.0 ± 1.0 [-3.0, 1.3]	**0.036**	-1.1 ± 1.8 [-6.4, 1.1]	**0.017**
Urethra							
$D_{5\%}$ (Gy)	40.1 ± 0.8 [38.6, 41.5]	1.1 ± 1.4 [-1.1, 4.0]	**0.003**	-0.4 ± 1.6 [-4.0, 2.4]	0.261	-0.2 ± 1.3 [-2.7, 2.7]	0.409
$D_{10\%}$ (Gy)	39.6 ± 0.7 [38.4, 41.1]	1.1 ± 1.0 [-0.6, 3.8]	**< 0.001**	-0.2 ± 1.1 [-2.4, 2.3]	0.571	-0.1 ± 1.0 [-2.4, 2.1]	0.596
$D_{50\%}$ (Gy)	38.0 ± 0.5 [37, 38.9]	0.4 ± 0.9 [-1.7, 2.3]	**0.036**	-0.2 ± 0.8 [-1.5, 1.9]	0.927	-0.3 ± 1.1 [-2.5, 1.6]	0.312
Left femur head							
D_{max} (Gy)	13.8 ± 1.6 [10.7, 17.9]	10.9 ± 8.4 [-8.8, 23.3]	**< 0.001**	1.6 ± 8.3 [-15.5, 19.3]	0.133	-34.2 ± 15.6 [-65.4, -6.8]	**< 0.001**
Right femur head							
D_{max} (Gy)	14.0 ± 1.7 [10.7, 17.5]	7.4 ± 5.3 [-3.4, 16.9]	**< 0.001**	-1.3 ± 4.7 [-9.2, 7.3]	0.701	-32.3 ± 13.9 [-50.0, -7.0]	**< 0.001**
Patient							
V_{2Gy} (cc)	5325 ± 1007 [4151, 7790]	9.3 ± 5.7 [-1.6, 20.5]	**< 0.001**	18.6 ± 6.8 [6.3, 30.3]	**0.008**	32.9 ± 6.9 [14.7, 42.2]	**< 0.001**
V_{5Gy} (cc)	3444 ± 687 [2692, 5134]	4.1 ± 4.4 [-3.1, 12.4]	**0.001**	-0.6 ± 5.2 [-9.6, 14.9]	0.546	-7.2 ± 5.5 [-17.9, 4.5]	**< 0.001**
V_{10Gy} (cc)	1332 ± 339 [924, 2022]	19.0 ± 7.3 [4.2, 30.4]	**< 0.001**	1.4 ± 7.0 [-10.3, 13.3]	**0.008**	-12.2 ± 7.6 [-26.0, 0.3]	**< 0.001**
V_{20Gy} (cc)	317 ± 83 [213, 481]	6.7 ± 3.3 [0.1, 12.3]	**< 0.001**	1.2 ± 2.4 [-3.2, 5.6]	**0.003**	-5.1 ± 3.2 [-10.5, 1.0]	**< 0.001**
V_{30Gy} (cc)	156 ± 44 [102, 246]	1.1 ± 1.6 [-2.5, 5.9]	**0.001**	0.5 ± 1.3 [-1.5, 4.1]	0.09	-1.6 ± 2.2 [-5.5, 3.2]	**0.008**

Table 7.2: Comparison of dosimetric plan parameters of VMAT+CS with VMAT, VMAT+5, and 30-NCP plans for all study patients. While the VMAT+CS column contains absolute values of the plan parameters, the VMAT, VMAT+5 and 30-NCP columns show percentage differences with respect to VMAT+CS. Positive differences hint at an advantage of VMAT+CS.

7.3.3 Plan deliverability, treatment time and MU for VMAT and VMAT+CS

All delivered VMAT and VMAT+CS plans passed the QA tests (gamma passing rate >95%) with an average gamma passing rate of 98.3%±1.0% [97.5%, 100%] for VMAT plans and 98.3%±0.7% [97.5%, 99.4%] for VMAT+CS plans. Compared to VMAT, the average total delivery time of VMAT+CS plans increased from 9.1±0.7 min to 11.0±0.3 min (see Fig. 7.3 for details). VMAT+CS plans required 3% less MU (4055±191 compared to 4186±398), which was not significant (p=0.375).

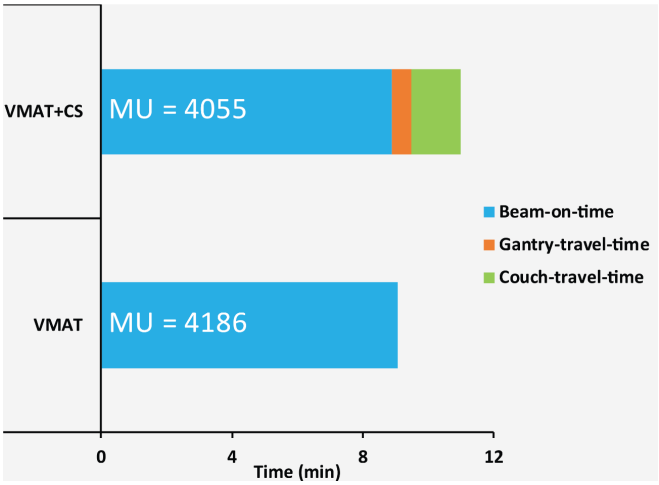

Figure 7.3: Average measured beam-on-times, gantry-travel-times and couch-travel-times for five VMAT and VMAT+CS plans. The numbers in the bars represent mean delivered MUs.

7.3.4 Optimization time reduction

Using a class solution instead of individualized beam angle selection in VMAT+5 resulted in a substantial reduction in optimization time by a factor of 25. Optimization for VMAT+CS plans in Erasmus-iCycle took on average 1 hour.

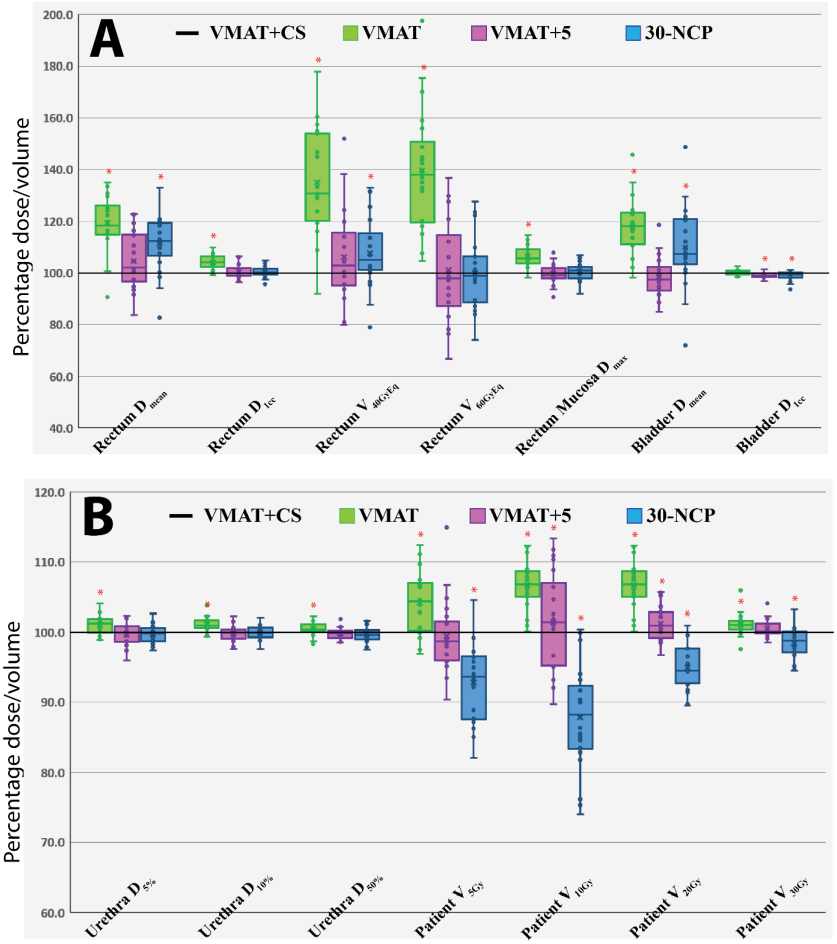

Figure 7.4: Healthy tissue dose parameters for VMAT, VMAT+5, and 30-NCP plans relative to VMAT+CS (VMAT+CS always 100%) for all study patients. All plans were normalized to deliver the clinically required PTV coverage (V_{38Gy}=95%). The central line of each box represents the median value, and its upper and lower edge the 25th and 75th percentiles, respectively. The whiskers extend to the minimum and maximum values, or to 1.5 times the inter-quartile range from the top/bottom of the box. Hollow points are the discrete data points of the 20 study patients ('○'). Positive values indicate lower doses for VMAT+CS. *: difference with VMAT+CS is statistically significant.

7.4 Discussion

In this study, we have developed and evaluated a novel treatment approach for prostate SBRT at a C-arm linac, consisting of dual-arc coplanar VMAT supplemented with a non-coplanar beam-angle class solution (CS) consisting of two IMRT beams (VMAT+CS). Initial aim of the study was to explore opportunities for enhancement of the plan quality for prostate SBRT, as obtained with VMAT, by adding non-coplanar beams. To keep the treatment delivery time short, no more than 5 non-coplanar beams were added. The study was inspired by the success for liver SBRT, where substantial plan quality enhancement compared to VMAT could be obtained by adding 1-5 non-coplanar beams with patient-specific, computer-optimized orientations (VMAT+) [157]. For the prostate case studied in this paper, the distribution of selected non-coplanar orientations for VMAT+5 in the twenty study patients pointed at a possibility for the use of a CS, which was then successfully further explored. A fixed set of two non-coplanar orientations (CS) resulted for all patients in substantial plan quality enhancements compared to VMAT, while the increase in treatment time was very moderate (from 9.1 min to 11.0 min).

Remarkably, the quality of VMAT+CS plans was highly similar to that of VMAT+5 plans, the latter with more, and also patient-specific beam orientations. Most likely, because the pelvic anatomies of prostate cancer patients are highly similar, high quality plans could be generated for all patients with a fixed set of two non-coplanar beams supplementing VMAT. Interestingly, also the quality of plans with 30 non-coplanar beams with individually optimized orientations (30-NCP) was highly similar to that of VMAT+CS, while optimization and treatment times were largely enhanced. Apparently, adding only two well-selected orientations to the patient plans was enough for a substantial gain in plan quality. Adding more non-coplanar beams and patient-specific optimization of the orientations of the non-coplanar beams did not result in significantly better plans, especially when also considering the involved increases in optimization and delivery times.

Recently, Rossi et al. [145] showed a clear advantage for non-coplanar CyberKnife planning compared to coplanar VMAT for prostate SBRT. Also in that study, all plans were fully automatically generated, using the same autoplanning system and configuration as applied in this study. Also the patient group was the same. Interestingly, the quality of the VMAT+CS plans generated here is very similar to that of the previously generated CyberKnife plans. On the other hand, delivery times with the CyberKnife were much longer (45 min vs. 11 min in this study). There is a high similarity here with the above comparison between VMAT+CS and 30-NCP; apparently in prostate SBRT there is no need for using a large amount of non-coplanar beams to get a very high plan quality.

Currently, we have not yet an idea whether the CS developed for the planning protocol used in our center would also work for SBRT planning approaches in other centres. This is a topic of further research. However, as a small side study, we tested the developed CS for 15 prostate cancer patients treated with our regular 20 x 3 Gy scheme for homogeneous target dose delivery (non SBRT). Also for this conventional delivery scheme, VMAT+CS showed an improvement in plan quality compared to VMAT (<10% in rectum, anus and bladder mean doses, data not presented), but no improvements in the high rectum and bladder doses. Possibly, the applied larger PTV margins and/or higher PTV dose homogeneity (with shallower dose fall-off towards the healthy tissues) reduced the impact of the added CS beams.

Addition of a few, well-selected non-coplanar beams to VMAT (the VMAT+ approach) has now turned out to be successful for both liver SBRT and prostate SBRT. New studies on other tumor sites are part of a future project. We are able to do this type of work due to availability of our in-house developed optimizer for fully automated and integrated multi-criterial beam angle selection and IMRT beam profile optimization. The success of our work on VMAT+ is an indication for the need of advanced algorithms for integrated beam angle and beam profile optimization in commercial treatment planning systems. In this context, one should keep in mind that with the VMAT+CS approach, BAO is not needed for new patients. However, development of the CS was only possible with the use of integrated optimization of beam angles and profiles.

To the best of our knowledge, this paper and our paper on liver SBRT [157] are the only papers that use autoplanning to systematically investigate the addition of non-coplanar IMRT beams to fast coplanar VMAT for enhancement of the plan quality achieved with VMAT, while keeping treatments fast. Several recent publications [11, 31, 162, 168, 195] investigated the use of non-coplanar arcs to enhance plan quality without prohibitively prolonged treatment times. Selection of the non-coplanar arcs was performed manually. Clark et al. [31] and Thomas et al. [168] showed that three non-coplanar arcs combined with one coplanar arc produced clinically equivalent conformity and dose spillage compared with GammaKnife for multiple cranial brain metastases while increasing the delivery efficiency due to its reduced treatment time. Since, this class solution has been incorporated in the Eclipse treatment planning system as HyperArc and has further proven to improve delivery efficiency and reduce dose to normal brain tissue when compared to coplanar VMAT [130]. More specific studies are needed to compare such approaches with the proposed VMAT+.

In conclusion, using an algorithm for fully automated, integrated multi-criterial beam profile and beam angle optimization, we have derived a two-beam non-coplanar class solution to supplement VMAT for prostate SBRT. Adding the CS beams to conventional coplanar VMAT resulted in substantial improvement in treatment plan quality with a

minimal increase in treatment delivery time. Due to the use of a non-coplanar beam-angle class solution, time-consuming individualized beam angle optimization can be avoided.

Supplementary material

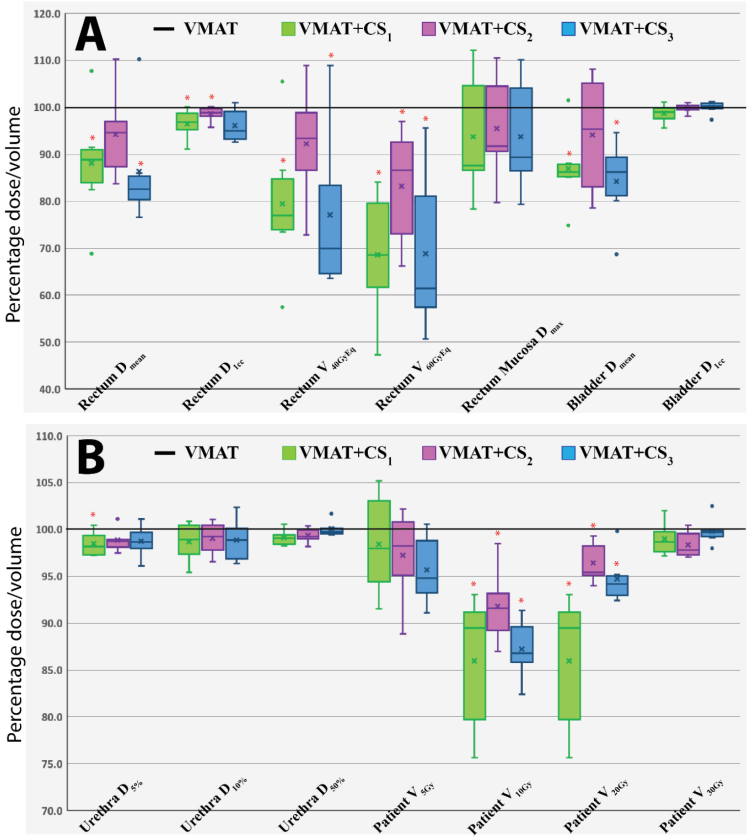

Figure 7.A1: Healthy tissue dose parameters for VMAT+CS1, VMAT+CS2, and VMAT+CS3 plans relative to VMAT (VMAT always 100%) for the 6 randomly selected patients used to compare the class solutions. All plans were normalized to deliver the clinically required PTV coverage (V_{38Gy}=95%). The central line of each box represents the median value, and its upper and lower edge the 25th and 75th percentiles, respectively. The x mark inside the box represents the mean value. The whiskers extend to the minimum and maximum values, or to 1.5 times the inter-quartile range from the top/bottom of the box. Values outside this range are plotted individually as outliers ('○'). *: difference with VMAT is statistically significant.

Chapter 8

Discussion

In this thesis, automated treatment planning has been intensively used and investigated, focusing on comparisons of coplanar and non-coplanar beam configurations and on plan quality improvements relative to manual planning. In this Discussion chapter, the focus will be on challenges that automated planning brings along in clinics and in research, disputes on the use of non-coplanar beam geometries, and the benefits of automated planning in treatment technique comparisons. To conclude, possibilities for future research are discussed.

8.1 Challenges in autoplanning configuration

Configuration of an autoplanning workflow is a new concept in radiotherapy (RT). In conventional manual planning, each plan is produced by itself in a trial-and-error approach, allowing multiple iterations with human interventions to fix undesired aspects of intermediate dose distributions. Plan generation based on patient-group templates is in the direction of autoplanning. These templates can enhance plan quality uniformity and can speed up the planning process. However, in almost all cases, manual fine-tuning of a template-based plan is necessary.

Ideally, autoplanning results for all patients in the final acceptable high-quality plan, which should then also be Pareto-optimal. More realistically, for the vast majority of patients there should be no need for manual fine-tuning of the autoplan. To come at this point, proper configuration of the autoplanning algorithm is crucial.

In Erasmus-iCycle, configuration means generation of a wish-list [22]. The process of

wish-list tuning is globally described in the Electronic supplement of [69]. A proper wish-list can ensure that plans are generated in line with scientific knowledge, as well as local treatment traditions, e.g. regarding the required level of overall high-dose conformality vs. sparing of specific OARs. The configurations performed for the studies in this thesis have resulted in the following observations:

i) Each wish-list determines the plan quality for an entire patient group. If the configuration is suboptimal, the quality of all plans will be suboptimal, effectively introducing a systematic problem. There is never a guarantee that the best possible wish-list will be found, also because the best possible plan quality is generally not well defined. Comparison with manually generated, clinically delivered plans is a basic measure to ensure that at least the clinical quality is obtained. However, as demonstrated in several studies (also in this thesis, chapters 4, 5 and 6), extensive tuning generally results in a wish-list that can beat clinical plan quality. Tuning of wish-lists is a complex, interactive procedure. As for manual planning for individual patients, it is not always clear when to stop. Previous experience in generation of wish-lists is likely to ease the task and may result in a better result. Important is also that enough time is reserved to obtain the best possible result.

ii) A well-established treatment planning protocol, agreed upon by the treating clinicians, is crucial for proper wish-list tuning. However, these protocols can generally only partly describe how optimal plans should look like, as it is virtually impossible to fully quantify requirements for conformality, dose spikes, the dose bath, hot/cold spots, and balances between all treatment objectives. It may also happen that during wish-list generation, dose distributions occur with characteristics that have not been encountered in previous manual planning, making that the clinical planning protocol cannot be strictly used as a guideline. As mentioned before, with proper wish-list tuning, the quality of autoplans generated with Erasmus-iCycle can supersede that of manual plans. However, the clinical planning protocol does generally not contain enough information to decide on how to best use the extra room for quality enhancement, e.g. how should it be divided between target and OARs, or how should it be divided among OARs, should it be used to enhance conformality, etc. To overcome the unavoidable limitations of planning protocols, it is essential to regularly discuss during the tuning process intermediate planning results with the full planning team, including the radiation oncologists. The comments of the clinicians can be used in further tuning iterations to shape plans according to their needs.

iii) Current planning protocols generally allow flexibility in the performed manual planning to accommodate variations in planning objectives in a group of treating clinicians. Autoplanning by itself does not have this flexibility. Therefore, configuration of the autoplanning algorithm is often preceded by discussions between clinicians to better agree

on what is actually desired. Agreement can also be obtained during the tuning process, in discussions on how to improve the plans relative to current clinical planning. The latter discussions may be easier as autoplanning may improve quality for all clinicians. No agreement may in the end result in manual fine-tuning of part of the autoplans. Fine-tuned autoplans are generally of higher quality than plans that were created with manual planning from scratch. Moreover, fine-tuning is often a lot faster.

iv) During wish-list tuning it may appear that, compared to manual planning, a substantial quality gain can be obtained for an objective at the cost of a seemingly minor loss for another. This may result in lengthy discussions because of difficulty in accepting a loss in quality compared to what one is used to since a long time, even if the loss is small and the gain on other aspects is large.

v) Non-convex cost functions such as dose-volume constraints can result in unstable behaviour of optimizers when generating treatment plans. In manual planning, the planner can observe this and try to correct for it. In autoplanning, such unpredictable, unstable behavior can result in suboptimal plans. Therefore, in this thesis, non-convex cost functions were avoided as much as possible in wish-list creation. A drawback of this approach is that there may be a gap between functions used to optimize a plan, and parameters used to clinically evaluate plans. E.g. in Chapter 4, D_{1cc} dose-volume requirements for both rectum and bladder were optimized using EUD cost functions in autoplanning.

vi) In current practice, every new patient is considered as a new planning problem, to be solved in a collaboration between the planner and the treating radiation oncologist. Obviously, there is time reserved for this per patient approach. For autoplanning, a different workflow is required; prior to treatment of any patient, substantial time investments are needed for wish-list creation. After this investment, much less time is needed for individual patients, as high-quality plans are automatically generated. The upfront time investments are not part of the still mostly applied clinical workflow based on manual planning, and it may be challenging to find time for the necessary meetings.

vii) Depending on the case complexity, automated plan generation may take longer than manual planning. In return, there is often a higher plan quality, and there is no manual workload involved. In clinical practice in our center, it is accepted that the plan is available the day after starting the autoplanning run. Often it is available on the same day. A cluster of servers is available for autoplanning 7 days per week, 24 hours per day, and the planner receives an email when the plan is ready, avoiding the need of active waiting and checking.

8.2 Non-coplanar beam setups in clinical reality

In clinical practice, the spread/use and therefore the potential positive impact of non-coplanar planning can be restricted. This can e.g. be related to 1) reluctance in moving away from the more conventional coplanar setup that was used for many years, 2) doses delivered to healthy tissues that are fully spared with coplanar approaches, 3) lack of commercial treatment planning systems (TPS) for advanced non-coplanar BAO for treatment at regular C-arm linacs, 4) increase in computation and/or treatment time, and 5) potentially reduced delivery.

With the introduction of the robotic CyberKnife treatment unit, some of the perceived issues with non-coplanar treatment could be resolved. It allows easy delivery of non-coplanar beams without intensively moving the patient. Instead, the linac head moves around the patient.

Nowadays, the dosimetric advantages of non-coplanar geometries have been broadly acknowledged for intracranial tumors, where the solid angle with candidate beams can be made large, as for many directions there is no risk of gantry-couch/patient collisions [133]. For extracranial treatment, the matter seems more controversial [161]. There are studies showing clear benefit of non-coplanar treatment; reduction of OAR doses [41–44, 86, 143, 145, 184], improved conformality [153], reduced low-intermediate doses [45, 144], and opportunity for dose escalation [126, 146]. Other studies did not show a clear dosimetrical benefit of non-coplanar setups, maintaining the enhanced complexity in planning and delivery compared to coplanar geometry [30, 40, 160].

However, often the latter studies included few patients (8-10) and planning was performed manually, including the complex selection of non-coplanar beam setups. E.g. non-coplanar IMRT with 6 manually selected beams was compared to VMAT and Tomotherapy [160].

Conceptually, the coplanar beams form a subset of the full non-coplanar space. The increased degree of freedom in planning by considering also non-coplanar beams can theoretically only result in plans that are as least as good as coplanar plans. Manual selection of non-coplanar beams may hamper observation of plan quality enhancements [22, 95]. With the fully automated, integrated multi-criterial beam angle and profile optimization in Erasmus-iCycle, clear dosimetric advantages of optimized non-coplanar beam setups were observed for prostate cancer patients (Chapters 2, 4 and 7), vestibular schwannoma (Chapter 5) and mediastinal lymphoma patients (Chapter 6).

(Largely) enhanced delivery times may be a prohibitive condition for the widespread employment of non-coplanar beam setups. It makes treatments more expensive and can

also result in reduced delivery accuracy. However, active research and effort have been directed towards developing non-coplanar techniques [163]. Recently, the CyberKnife was equipped with an MLC, resulting in 36% shorter treatment time compared to treatment with the variable aperture IRIS collimator [79]. In a research setting, continuous radiation delivery between CyberKnife nodes (CyberArc) has been explored, reducing delivery time by a factor of 1.5 or 2, depending on the plan, without plan quality deterioration [83]. For C-arm linacs, fully dynamic treatments, including gantry and couch motion during dose delivery, have been explored [192]. Sharfo et al. proposed the VMAT+ treatment approach, combining coplanar VMAT with a few non-coplanar IMRT beams [157]. For liver SBRT, VMAT+ resulted in largely enhanced dosimetric plan quality compared to VMAT, with only modest increases in treatment time. In Chapter 7, VMAT+ was investigated for prostate SBRT and a non-coplanar beam angle class solution, consisting of only two IMRT beams with fixed directions, was proposed for complementing VMAT. Again, plan quality increased substantially compared to VMAT at the cost of only a moderate increase in treatment time.

8.3 Reducing bias in treatment planning studies that compare treatment techniques

Treatment planning entails solving a large and complex multi-criterial optimization problem, with an infinite number of suboptimal solutions. Current conventional, manual planning is an interactive trial-and-error procedure, in which the planner tries to steer the TPS towards an acceptable and hopefully high-quality plan. However, the final plan quality is highly dependent on the planner's skills, experience, and endurance, and on allotted time. Moreover, the definition of plan optimality is to a large extent based on the judgement of the planner, even in case of an existing detailed planning protocol, and plan quality is also influenced by the planners' judgements on whether or not more iterations can result in a better plan. Apart from inter-planner variations in treatment plans, there are also the well-known intra-planner variations, i.e. for the same patient, the achieved quality may be different for different planning attempts. As every patient deserves the best possible treatment, without being dependent on luck regarding the assigned planner and the available planning time, planning should be optimized and standardized as much as possible by reducing the impact of planners. Planning automation has shown major opportunities for plan quality improvement compared to manual planning, together with workload reductions [38, 64–66, 69, 73, 114, 144, 145, 158, 185, 186].

Also in planning studies for comparing treatment techniques, manual planning can potentially lead to suboptimal results.

In order to assess whether a treatment technique is better than another, ideally the final conclusion is only related to intrinsic technique differences. In particular, there should be no bias introduced by the performed treatment planning.

In bias-free technique comparisons based on planning, repeated planning should ideally always result in exactly the same plans. In manual planning, one can be far from this ideal situation (see above). Variations in plan quality can result in inconsistent treatment technique comparisons, especially when variations in planning are in the order of the quality differences between the investigated techniques.

When treatment techniques are compared based on manually generated plans, a bias can also be introduced by differences in planning experience for the investigated techniques, or a wish that one of the techniques will be superior. The latter may also occur if the planner is aware of a desired output, and makes best efforts to avoid study bias. As manual generation of high-quality treatment plans is time consuming, published treatment planning studies are generally based on limited numbers of treatment plans. As patient anatomies may be highly diverse, this can potentially also result in study bias in treatment technique comparisons.

Apart from manual planning, also more technical issues can result in suboptimal technique comparisons. E.g. if delivery techniques are compared with different TPSs, there is the risk of bias, as the TPSs used for the different techniques may not be equally powerful.

Irreproducibility, inconsistency and suboptimality can also occur when (mathematical) optimality conditions are not reached or converge to a local optimum as with the use of non-convex cost functions (above), but this can also happen if cost functions are not minimized to the full extent to reduce calculation times.

In this thesis, Erasmus-iCycle was used for treatment technique comparisons. In all comparisons, exactly the same wish-list was used for all treatment plans and all techniques, preventing a lot of the above described issues with bias, plan quality definition and reproducibility related to manual planning. However, wish-list generation is basically a tuning process with many decisions to be made by the treatment team (see also section 8.1 above). Importantly, all involved treatment techniques have to be evaluated in the tuning process to avoid/reduce bias. Apart from consistency in plan generation, autoplanning with Erasmus-iCycle also drastically reduces the involved planning workload. Therefore, the technique comparisons performed in this thesis could be based on large numbers of treatment plans; 1500, 1060, 645 and 740 plans were generated for the studies described in Chapters 2, 3, 6 and 7.

By using the same optimizer for all treatment techniques, the often observed bias in published technique comparisons related to different TPSs for different techniques

could be avoided. However, to investigate deliverable plans, in Chapters 4, 5 and 7, fluence-optimized Erasmus-iCycle plans were converted into deliverable plans, by an automatic mimicking of these plans in a commercial TPS. Care was taken that this mimicking went equally well for all techniques to avoid introduction of bias. In Chapter 4, comparing CyberKnife with VMAT for prostate SBRT, the mimicking was performed with different commercial TPSs, requiring an even larger focus on prevention of bias.

8.4 Future work

Validation of beam angle optimization (BAO) with Erasmus-iCycle

In this thesis, BAO as implemented in Erasmus-iCycle was used to investigate opportunities for plan quality enhancement, and to compare coplanar and non-coplanar beam configurations. BAO showed robust and consistent behaviour; plan quality increased with increasing numbers of beams, and non-coplanar set-ups resulted in higher quality than coplanar. Also the difficulty in defining a beam angle class solution in Chapter 3 points at a high quality of the plans generated with BAO as implemented in Erasmus-iCycle.

Erasmus-iCycle was also compared to another BAO algorithm not showing significant differences [181].

Based on available evidence at this time, it can be concluded that BAO in Erasmus-iCycle behaves as expected and that it generally results in high-quality plans. On the other hand, except from [181], formal plan quality assessments have not yet been performed, and it would be good to do it. Such validation studies could e.g. be performed by investigating variations in beam geometries from the ones selected by Erasmus-iCycle. To this purpose, low weight beams, or the first selected beams could be removed, followed by an automated selection of new beams from the pool of candidate beams. Similarly, a local neighbourhood search could be performed, where a neighbour beam is added to the beam geometry instead of a beam selected by BAO. For the VMAT+ approach ([157] and Chapter 7), selected non-coplanar beam geometries could be compared with exhaustive search.

An interesting study would also be to compare Erasmus-iCycle BAO with the non-coplanar beam orientation optimization used in studies on the 4π treatment approach [41, 42].

Further exploration of the VMAT+ concept

In [159] and Chapter 7, clear dosimetric benefits were found for complementing coplanar VMAT with a small set of non-coplanar beams. This novel VMAT+ treatment approach allowed to substantially increase plan quality with respect to VMAT with only minor increases in treatment time.

This is an important finding for the clinical routine, as plan quality could be substantially improved without the use of many non-coplanar beams that would result in drastic increases in delivery times

Therefore, there is an incentive to investigate the VMAT+ approach for more tumor sites, including exploration of opportunities for the use of non-coplanar beam angle class solutions with low numbers of beams to avoid the need for individualized BAO (see Chapter 7). Treatment sites as mediastinal lymphoma (showing benefit of non-coplanar configurations, Chapter 6), challenging head and neck cases, lung tumors, or intracranial tumors would be good candidates for exploration of VMAT+.

Semi-automated wish-list generation

Automated planning with Erasmus-iCycle can be a powerful approach for improving and standardizing plan quality and for reducing the planning workload. As described in section 8.1 it does not come without challenges; plan generation is based on a wish-list that is created in a complex trial-and-error tuning procedure, while a sub-optimal wish-list translates into sub-optimal quality of all generated autoplans.

Currently, many trail-and-error iterations are performed in wish-list creation, together with intensive discussions with the treating physicians in order to maximize the probably that the best possible wish-list will be generated. The current tuning of wish-lists entails large time investments while there is no guarantee for finding the best wish-list.

More 'automation of the automation' would be desirable and could be a topic of further research, as discussed below.

Many plan requirements are equally present in different treatment protocols. For example, in most of the protocols the PTV coverage comes as first priority within OAR constraints, and it is defined as $V_{95\% \text{ or } 98\% \text{ or } 99\%}$ = 100%PD or 95%PD. This recurrent clinical protocol requirement can be translated with fixed cost functions, known by experience to be efficient.

Moreover, the tuning of some cost function parameters could possibly be automated, letting the optimizer i) try automatically generate plans with a certain parameter value for a group of patients, ii) automatically evaluate the planning results, iii) adapting the

parameter values and iv) go back to i).

Another approach for partial automation of wish-list creation could be the development and use of well-structured questionnaires to be filled out by planning team. Different dose distributions, generated with a starting-point wish-list or several version of a wish-list, could be shown to the team, while asking questions on things they would like to change or not, adapting the wish-list(s) consequently and so on.

Automated planning for personalized care

Nowadays, the applied treatment technique is generally fixed per tumor group, e.g. treatment with VMAT at a C-arm linac or robotic therapy with a CyberKnife. However, technique selection could also be made patient-specific, by comparing for each patient treatment plans for the available treatment options. With automated planning this could be performed with a minimum of bias and workload. Such patient-specific technique comparisons could further personalize patient care. Currently, admission of a patient to the scarce and more expensive proton therapy is in The Netherlands already based on a comparison of a generated proton plan with a competing photon plan. Only in case of sufficient gain, the patient is referred to proton therapy.

At the same time, every patient comes with his/her own background and anatomy. Therefore, even within a fixed treatment technique, generation of several plans with different trade-offs between the treatment objectives could potentially contribute to improved patient care. In case of a comorbidity leading to an enhanced risk of radiation-induced side effects (e.g. diabetes in prostate cancer patients, resulting in a substantially enhanced risk for rectal toxicity), several plans could be generated to explore trade-offs between the target and the OARs. Technically, this type of approaches with multiple plans per patient are now feasible and clinical testing is warranted.

Prioritized planning for coping with GTV delineation uncertainty and microscopic disease

Currently, the biggest geometrical uncertainties in radiotherapy are related to segmentation of the Gross Target Volume (GTV) and establishment of margins for microscopic disease to define the Clinical Target Volume (CTV). Involved decisions are nowadays binary, i.e. tissues are either inside the structures and then considered as tumor during treatment plan generation, or they are outside and are then considered as healthy tissue to be maximally spared. In many situations uncertainties on the GTV and CTV boundaries may be large [183].

The multi-criteria prioritized optimization nature of Erasmus-iCycle could probably help in moving away from this binary thinking, by defining ring structures around the

delineated GTV contours and in areas with potential microscopic disease. By proper selection of priorities of the objective functions used to steer dose delivery in these rings, patient-specific balances could be made between radiation-induced toxicity and risk of tumor miss. This could e.g. be used to enlarge the high dose volumes in areas where high dose would not result in enhanced toxicity. Investigations to explore this approach for several tumor types are warranted.

Summary

In conventional, manual planning for IMRT, a planner has to make many choices to drive the treatment planning system (TPS) towards generation of a high-quality plan. In an interactive trial-and-error procedure, he/she has to carefully select the number of beams, the beam directions, as well as the cost functions with their weights to define an optimization problem that will result in a high-quality plan. Each problem definition results in a treatment plan with unique trade-offs between all treatment objectives, and definition of the optimization problem that results in optimal trade-offs is highly complex. As a consequence, the quality of a radiotherapy treatment plan may be highly dependent on the skills of the involved planner and on allotted planning time. This is the case in a single plan generation for a patient, but it can also affect research studies where plan comparisons are performed to compare treatment techniques.

Automated planning with our in-house Erasmus-iCycle optimizer has demonstrated possibilities for consistent generation of high-quality plans, while fully avoiding manual planning workload. As a unique feature, this system features integrated beam profile and beam angle optimization (BAO).

In this thesis, Erasmus-iCycle was used to systematically investigate the impact of beam configurations on plan quality, and to investigate plan quality improvements relative to conventional manual planning.

In Chapter 2, the BAO option was used to investigate relationships between plan quality and the beam angle search space, i.e. the set of candidate beam directions that may be selected for generating an optimal plan. Ten prostate SBRT patients were included in the study. Autoplans with up to 30 beams with individualized directions were generated for 5 different candidate beam sets, one coplanar and four non-coplanar. The candidate sets sets were: i) a coplanar set, covering the whole 360° range (CP), ii) all directions (mainly anterior) available in the robotic CyberKnife treatment unit (CK), iii) a fully non-coplanar sphere (F-NCP), i.e. also including posterior beams that were not present in

CK, and iv)/v) CK^{+} and CK^{++}, as subsets of F-NCP, with higher beam density than the CK beam set (CK^{+}), or covering a (bigger) laterally extended beam area (CK^{++}). In total 1500 plans were generated.

Generated plans were clinically acceptable, according to an assessment of involved clinicians. All plans were generated with highly similar PTV coverages, allowing plan comparisons to be based on OAR dose parameters, with the rectum considered most important.

OAR sparing improved with all NCP configurations compared to CP, especially for the rectum. F-NCP performed the best, with reductions in rectum D_{mean}, V_{40GyEq}, V_{60GyEq} and $D_{2\%}$ of 25%, 35%, 37%, and 8%, respectively, compared to CP. CK performed slightly worse than F-NCP, which could be compensated by the laterally extended beam area in CK++. Addition of posterior beams ($CK^{++} \rightarrow$ F-NCP) or enhancement of the beam density (CK $\rightarrow CK^{+}$) did not lead to further improvements.

Increasing the number of selected beams significantly improved plan quality. For coplanar plans, for instance, rectum D_{mean}, V_{40GyEq}, V_{60GyEq} and $D_{2\%}$ could be improved by 39%, 57%, 64%, and 13%, respectively, when using 25 beams instead of 11 beams. Using more than 25 beams did not result in relevant further plan improvements.

With the clear benefit of non-coplanar Cyberknife beams for prostate SBRT as observed in Chapter 3, the possibility of creating a non-coplanar beam angle class solution (CS) for Cyberknife was explored to replace the time-consuming individualized BAO, while not losing in plan quality.

CS generation was performed in 3 steps, based on 10 training patients. First, Erasmus-iCycle was used to generate plans with 15, 20, and 25 non-coplanar individualized beams. Secondly, based on the beams selected in these plans, 6 recipes for creation of beam angle CSs were investigated for all three beam numbers. Finally, Erasmus-iCycle was used to generate plans for the fixed (6x3) CSs, both for the 10 training patients and for 20 independent validation patients. A total of 1060 plans was generated.

Out of the 6 tested CS recipes, only 1 resulted in 15-, 20-, and 25-beam non-coplanar CSs without plan deterioration compared with individualized BAO. Negligible differences were found between 25-beam CS plans and 25-beam BAO plans, with mean differences in rectum rectum D_{1cc}, V_{60GyEq}, V_{40GyEq}, and D_{mean} of 0.2 ± 0.4 Gy, 0.1 ± 0.2%-points, 0.2 ± 0.3%-points, and 0.1 ± 0.2 Gy, respectively.

Differences between 15- and 20-beam CS and BAO plans were also negligible. On the other hand, computation times with the CSs were reduced by a factor of 14 to 25, due to the avoidance of costly BAO.

In Chapter 4, the first system for fully automated generation of clinically deliverable CyberKnife treatment plans (autoROBOT) was developed and evaluated for prostate SBRT. To this purpose, Erasmus-iCycle was coupled to the commercial CyberKnife TPS. The system was first validated by comparing automatically generated CyberKnife plans with manually generated plans. Next, for 20 patients, autoROBOT plans were compared to VMAT plans, that were also automatically generated (autoVMAT). Both autoROBOT and autoVMAT plans with CTV-PTV margins of 3 mm (as used in clinical prostate SBRT CyberKnife routine) were generated. In addition, 5 mm CTV-PTV margin autoVMAT plans were generated (a margin often applied for VMAT).

Compared to manual planning, autoROBOT improved rectum D_{1cc} (16%), V_{60GyEq} (75%) and D_{mean} (41%), and bladder D_{mean} (37%) (all $p \leq 0.002$), with equal PTV coverage. Compared to autoVMAT with equal 3 mm margin, autoROBOT reduced rectum D_{1cc} by 5% ($p = 0.002$), rectum V_{60GyEq} by 33% ($p = 0.001$), and rectum D_{mean} by 4% ($p = 0.05$), respectively, with comparable PTV coverage and other OAR sparing. For autoVMAT with 5 mm margin, 18/20 plans had a PTV coverage lower than requested (<95%) and all plans had higher rectum doses than autoROBOT (mean percentage differences of 13%, 69% and 32% for D_{1cc}, V_{60GyEq}, and D_{mean}, respectively (all $p<0.001$)).

In Chapter 5, a similar workflow was developed for automated planning in robotic CyberKnife radiosurgery of benign vestibular schwannoma tumors, to explore possibilities for reducing dose outside the PTV to potentially reduce risk of secondary tumor induction.

The goal of automated planning was to reduce the dose bath, including the occurrence of high dose spikes leaking from the PTV into normal tissues, without worsening PTV coverage, OAR doses, or treatment time. CyberKnife autoplans were generated for 20 patients, treated with 1x12 Gy, and compared with manually generated CyberKnife plans.

Autoplans performed as good as manual plans for all OAR sparing (largest mean difference for all OARs: $\Delta D_{2\%}$ = 0.2 Gy), while highly reducing the dose bath. With autoplans, patient volumes receiving more than 1 or 6 Gy, were reduced by (mean/maximum reduction) 23.6/53.8% and 9.6/28.5% with autoplans compared to manual plans ($p<0.001$). Autoplans also reduced dose spikes, with mean/maximum reductions of 22.8/37.2% and 14.2/40.4% in $D_{2\%}$ for shells at 1 and 7 cm distance from the PTV, respectively ($p<0.001$).

The study showed that automated planning highly outperformed manual planning, reducing 'for-free' the dose bath outside the PTV, without deteriorating PTV coverage or OAR sparing, or significantly increasing treatment time.

In Chapter 6, Erasmus-iCycle was challenged with planning for young female mediastinal lymphoma patients with large variations in tumor location, shape and size. The purpose of this work was to implement an automated planning workflow to obtain adequate target coverage with maximum sparing of breasts, heart, and lungs, and to investigate the impact of beam configuration on plan quality.

Twenty-four coplanar and non-coplanar beam configuration approaches were considered, partly based on individualized beam angle optimization, and partly on beam angle class solutions. Twenty-six patients were included in the study. The automated planning workflow was first validated by comparing clinically delivered, manually generated plans (CLIN) with automatically generated plans. Next, for the beam configuration investigations, autoplans were generated with i) coplanar configurations with computer-optimized patient-specific beam directions (CP_x with x = 5-15), ii) non-coplanar configurations with patient-specific beam directions (NCP_x with x = 5-15), iii) the VMAT coplanar beam angle class solution, and iv) the non-coplanar Butterfly VMAT (B-VMAT) class solution.

Of the 645 generated autoplans, 98.8% were suited for clinical use. Compared to the CLIN plans, autoplans had significantly enhanced PTV dose delivery and, especially for non-coplanar autoplans with 10-15 individualized beams, also large OAR dose reductions could be obtained. None of the investigated 24 beam configuration approaches was best for all patients, but overall non-coplanar configurations (B-VMAT and NCP_x$\geq$12) performed clearly the best. NCP_x$\geq$12 produced on average highly conformal plans with favourable high dose plan parameters for the lungs and the patient, and also a low heart D_{mean}. B-VMAT had reduced low-dose spread in lungs and left breast, with the practical advantages of a faster delivery and the elimination of patient-specific BAO. Generation of multiple plans for each new patient for a per-patient selection of the optimal beam configuration, based on both plan quality differences and practical considerations as delivery time, could importantly contribute to personalization of the treatment of these patients.

In Chapter 7, autoplanning with Erasmus-iCycle was used to explore the use of VMAT+, i.e. coplanar VMAT supplemented with a few ($\leq$5) non-coplanar beams, for enhancing OAR sparing in prostate SBRT with minimal increase in treatment time compared to VMAT. The work was inspired by successes reported for VMAT+ in liver SBRT [157]. Initially, VMAT+5 plans, complementing VMAT with five non-coplanar IMRT beams with computer-optimized, patient-specific directions, were generated for the 20 study patients, showing large preferences for a few principal directions in the beam angle search space. Two most preferred directions were used to define a 2-beam non-coplanar beam angle class solution (CS) for complementing VMAT, resulting in the VMAT+CS treatment approach.

VMAT+CS autoplans were then compared to i) VMAT, ii) VMAT+5, and iii) IMRT with 30 individualized non-coplanar beam directions (30-NCP). Plan comparisons were performed in terms of PTV dose, OAR sparing, and computation and treatment delivery times.

Compared to VMAT, plan quality was significantly improved with the non-coplanar VMAT+CS. For equal PTV dose, rectum D_{mean}, D_{1cc}, V_{60GyEq} and V_{40GyEq} were reduced by 19.4 ± 10.6%, 4.2 ± 2.7%, 39.7 ± 23.2% and 34.9 ± 0.3%, respectively (all $p<0.001$). Total delivery times only increased by 1.9 ± 0.7 min compared to VMAT (9.1±0.7 min). VMAT+CS performed equivalently to VMAT+5 regarding plan quality, while reducing optimization times by a factor of 25 due to avoidance of BAO. VMAT+CS had larger dose bath than 30-NCP, but with equal quality regarding all other plan parameters and with highly reduced optimization and delivery times.

In Chapter 8, challenges and opportunities of autoplanning with Erasmus-iCycle, and of the use of non-coplanar beam configurations are discussed. The chapter concludes with an outlook on future research opportunities.

Samenvatting

Wanneer een patiënt is gediagnosticeerd met kanker, en met radiotherapie (bestralingstherapie) behandeld gaat worden, moet er een zogenaamd bestralingsplan worden gemaakt. Een bestralingsplan beschrijft in essentie de configuratie van het bestralingsapparaat, en de daaruit volgende dosisverdeling in de patiënt. Het doel is om de tumor zo goed mogelijk met een hoge dosis te bestralen, en de (onvermijdelijke) dosis aan het omliggende gezonde weefsel zo laag mogelijk te houden.

Conventioneel wordt een bestralingsplan 'handmatig' gemaakt, waarbij een planner interactief werkt met het 'treatment planning system' (TPS), software die het maken van een bestralingsplan ondersteund. Hierin moeten veel keuzes gemaakt worden om een plan van hoge kwaliteit te produceren. Dit is in de praktijk een interactieve 'trial-and-error' procedure waarbij het aantal bestralingsbundels, de bundelhoeken en de benodigde doelfuncties met hun parameters moeten worden vastgesteld. Bij het maken van het plan moet rekening gehouden worden met meerdere, vaak tegenstrijdige doelen van de bestraling (bijv. hoge tumordosis, maar tegelijkertijd lage dosis in gevoelige weefsels rondom de tumor), wat het plannen extra uitdagend maakt. Door de inherente complexiteit is bij handmatig plannen de kwaliteit van het uiteindelijke bestralingsplan sterk afhankelijk van de planner en de beschikbare tijd. Dit is het geval wanneer een plan gemaakt wordt voor een specifieke patiënt, maar het heeft ook invloed op breder onderzoek waarin een groot aantal plannen gemaakt moet worden om bijvoorbeeld verschillende bestralingstechnieken kwalitatief met elkaar te vergelijken. Onderzoek heeft aangetoond dat automatisch plannen met Erasmus-iCycle, een TPS ontwikkeld in Rotterdam, een belangrijke rol kan spelen in het substantieel verbeteren van de plankwaliteit ten opzichte van handmatige planning, terwijl daarnaast de werklast van het handmatig plannen ook grotendeels vervalt. Een unieke optie van Erasmus-iCycle is dat bij IMRT niet enkel de dosisprofielen, maar gelijktijdig ook de bundelhoeken geoptimaliseerd kunnen worden.

In dit proefschrift is Erasmus-iCycle gebruikt om systematisch de invloed van bun-

delhoeken op plankwaliteit te onderzoeken. Daarnaast is onderzoek gedaan naar verbetering van plankwaliteit met het toegepaste automatisch plannen ten opzichte van handmatige planning zoals klinisch gebruikelijk is.

In hoofdstuk 2 werd de bundelhoekoptimalisatie optie ('beam angle optimization', BAO) van Erasmus-iCycle gebruikt om voor stereotactische prostaatbestraling (SBRT) onderzoek te doen naar het verband tussen plankwaliteit en karakteristieken van het bundelhoekzoekgebied, ofwel de kandidaatbundelhoeken die geselecteerd konden worden voor het genereren van een optimaal plan. In totaal werden 1500 plannen gemaakt voor 10 patiënten met verschillende coplanaire en niet-coplaniare bundelconfiguraties en verschillende bundelaantallen.

Er werd een duidelijk voordeel gevonden voor niet-coplanaire configuraties ten aanzien van de sparing van gezonde weefsels. Voor het rectum, het kritieke orgaan met de hoogste prioriteit, leidde een volledig niet-coplanaire configuratie tot reducties in $D_{gemiddeld}$, V_{40GyEq}, V_{60GyEq} en $D_{2\%}$ van respectievelijk 25%, 35% 37% en 8%, vergeleken met coplanair. De plankwaliteit nam significant toe met het verhogen van het aantal bundels. Voor coplanaire plannen konden bijvoorbeeld de rectum $D_{gemiddeld}$, V_{40GyEq}, V_{60GyEq} en $D_{2\%}$ verbeterd worden met respectievelijk 39%, 57%, 64% en 13%, wanneer 25 in plaats van 11 bundels werden gebruikt. Anderzijds resulteerde het gebruik van meer dan 25 bundels niet in relevante verbeteringen van de plannen.

Met de aangetoonde voordelen van niet-coplanaire bundels in prostaat SBRT werd in hoofdstuk 3 de mogelijkheid tot het creëren van een niet-coplanaire bundelhoek 'class solution' (CS) onderzocht om de tijdrovende individuele BAO te vervangen zonder significant verlies in plankwaliteit. Erasmus-iCycle werd gebruikt om 1060 plannen te genereren voor 30 patiënten. Zes verschillende recepten voor het maken van een CS werden onderzocht voor plannen met 15, 20 en 25 bundels.

Van de geteste CS recepten resulteerde er slechts 1 in CSs met 15, 20 en 25 bundels waarvoor planverslechteringen ten opzichte van BAO verwaarloosbaar waren. Voor 25 bundels werden gemiddelde verschillen in rectum D_{1cc}, V_{60GyEq}, V_{40GyEq} en $D_{gemiddeld}$ gevonden van respectievelijk 0.2 ± 0.4 Gy, 0.1 ± 0.2%-punt, 0.2 ± 0.3%-punt en 0.1 ± 0.2 Gy. Het grote voordeel van het gebruik van een CS in plaats van BAO was dat bij gelijkblijvende plankwaliteit de rekentijden omlaag gingen met een factor 14-25.

In hoofdstuk 4 wordt het eerste systeem voor volledig automatische generatie van klinisch bruikbare CyberKnife plannen (autoROBOT) gepresenteerd. Hiervoor werd het Erasmus-iCycle TPS gekoppeld aan het commerciële CyberKnife TPS. Het systeem werd

geëvalueerd voor prostaat SBRT. autoROBOT plangeneratie werd eerst gevalideerd door vergelijking met handmatig gegenereerde, klinisch gebruikte plannen. Daarna werd voor 20 patiënten het autoROBOT plan vergeleken met twee automatisch gegenereerde VMAT plannen (autoVMAT): één voor een CTV-PTV marge van 3 mm (zoals gebruikt in de kliniek voor behandeling met de CyberKnife, en ook gebruikt voor autoROBOT) en één voor een marge van 5 mm (zoals vaak gebruikt wordt voor VMAT SBRT).

Vergeleken met handmatig gegenereerde plannen verbeterde autoROBOT de rectum D_{1cc} (16%), V_{60GyEq} (75%) en $D_{gemiddeld}$ (41%), en blaas Dgemiddeld (37%) (alle p<0.002), met gelijkwaardige PTV dekking. Vergeleken met autoVMAT met een marge van 3 mm reduceerde autoROBOT de rectum D_{1cc} met 5% (p = 0.002), rectum V_{60GyEq} met 33% (p = 0.001) en de gemiddelde rectumdosis met 4% (p = 0.05) met vergelijkbare PTV dekking en sparing van andere gezonde weefsels. Voor autoVMAT met 5 mm marge hadden 18/20 plannen een PTV dekking lager dan klinisch vereist. Daarnaast hadden deze plannen hogere rectum doses dan autoROBOT (gemiddelde procentuele verschillen van 13%, 69% and 32% voor D_{1cc}, V_{60GyEq}, en $D_{gemiddeld}$, respectievelijk (alle p<0.001)).

In hoofdstuk 5 wordt een soortgelijk systeem beschreven voor het automatisch genereren van CyberKnife plannen voor radiochirurgie van goedaardige vestibulair schwannoom tumoren. De focus van het onderzoek lag op de vraag of met automatisch plannen het dosisbad verminderd kon worden om daarmee de kans op het ontwikkelen van een stralingsgeïnduceerde tumor te verkleinen, zonder te verliezen op plan kwaliteit voor de tumor en de kritieke gezonde weefsels, of een toename in de bestralingstijd.

Door automatisch te plannen kon het dosisbad inderdaad substantieel verkleind worden zonder in te leveren op de andere criteria. Patiëntvolumes die meer dan 1 of 6 Gy ontvingen konden verlaagd worden met (gemiddelde/maximale reductie) 23.6/53.8% en 9.6/28.5%, vergeleken met handmatige planning (p<0.001). Automatisch gegenereerde plannen verminderden ook de hoge dosis uitlopers vanuit de tumor richting de gezonde weefsels ('spikes'), met gemiddelde/maximale reducties van 22.8/37.2% en 14.2/40.4% in $D_{2\%}$ voor dosis op respectievelijk 1 en 7 cm afstand van het PTV (p<0.001).

Uiteindelijk werd dus aangetoond dat automatisch plannen het handmatig plannen werd overtrofen door een 'gratis' reductie van het dosisbad buiten het PTV, ofwel zonder verslechtering van PTV dekking of sparing van kritieke structuren, of significante toename in bestralingstijd.

In hoofdstuk 6 werd Erasmus-iCycle gebruikt om verschillende bundelgeometrieën te vergelijken voor de uitdagende en anatomisch zeer heterogene groep van 26 jonge, vrouwelijke patiënten met een mediastinaal lymfoom. Eerst werd Erasmus-iCycle gecon-

figureerd voor het automatisch genereren van plannen met voldoende dekking van de tumor en maximale sparing van de mamma's, het hart en de longen. Vervolgens werd met dit systeem de invloed van bundelhoekconfiguraties op de plankwaliteit onderzocht.

Er werden 24 coplanaire en niet-coplanaire bundelhoekconfiguraties vergeleken, deels verkregen met patiënt-specifieke BAO en deels gedefinieerd middels 'class solutions'. Allereerst werd de automatische plangeneratie gevalideerd door te vergelijken met handmatig gemaakte plannen die gebruikt waren voor de bestraling van de patiënten (CLIN). Vervolgens werd het systeem gebruikt om voor iedere patiënt voor elk van de 24 onderzochte bundelhoekconfiguraties automatisch een plan te genereren.

Van de 645 automatisch gegenereerde plannen was 98.8% geschikt voor klinisch gebruik. Vergeleken met de CLIN plannen hadden de automatisch gegenereerde plannen een significant verbeterde tumordekking, en voor niet-coplanaire configuraties met 10-15 geïndividualiseerde bundels, ook grote dosisreducties in de kritieke organen. Geen enkele van de 24 onderzochte bundelhoekconfiguraties was duidelijk het best voor alle patiënten, maar over het algemeen waren niet-coplanaire configuraties duidelijk het gunstigst. Niet-coplanaire, patient-specifieke configuraties met 12 bundels of meer resulteerden gemiddeld in conformere plannen met gunstige hoge-dosis voor de longen en de patiënt als geheel en ook in een lagere gemiddelde hartdosis. Met 'Butterfly-VMAT' was de afgifte van lage doses in longen en linkerborst relatief laag met daarnaast de praktische voordelen van een snelle dosisafgifte en een plangeneratie waarvoor de bundelhoeken niet per patiënt geoptimaliseerd hoeven te worden. Geconcludeerd werd dat het genereren van meerdere plannen per patiënt voor geïndividualiseerde selectie van de optimale bundelhoekconfiguratie in belangrijke mate kan bijdragen aan de behandelkwaliteit van jonge, vrouwelijke patiënten met een mediastinaal lymfoom.

In hoofdstuk 7 werd automatisch plannen met Erasmus-iCycle gebruikt om voor prostaat SBRT te onderzoeken of VMAT+, gedefineerd als coplanaire VMAT met enkele toegevoegde (<5) niet-coplanaire IMRT bundels, gebruikt kan worden voor het verbeteren van de sparing van kritieke gezonde organen met een minimale toename in behandeltijd in vergelijking met VMAT. Dit werk werd geïnspireerd door recente successen van VMAT+ voor lever SBRT [157]. Aanvankelijk werd met Erasmus-iCycle voor 20 patiënten een VMAT+5 plan gegenereerd met geïndividualiseerde hoeken voor de 5 toegevoegde IMRT bundels. Uit analyse van de in totaal 100 gekozen bundelhoeken bleek er een sterke voorkeur te zijn voor een paar hoofdrichtingen. Twee van die richtingen werden gekozen als bundelhoek 'class solution' (CS) voor de gehele patiëntgroep voor het aanvullen van VMAT (VMAT+CS). Automatisch gegenereerde VMAT+CS plannen werden vervolgens vergeleken met automatisch genereerde i) VMAT, ii) VMAT+5 en iii) 30-NCP: IMRT met 30 geïndividu-

aliseerde niet-coplanaire hoeken.

De plankwaliteit van VMAT+CS was significant beter dan voor VMAT; voor gelijke PTV dosis werden rectum $D_{gemiddeld}$, D_{1cc}, V_{60GyEq} en V_{40GyEq} gereduceerd met 19.4 ± 10.6%, 4.2 ± 2.7%, 39.7 ± 23.2% and 34.9 ± 0.3% (alle p<0.001). De totale bestralingstijd (inclusief benodigde tafeldraaiingen voor VMAT+CS) steeg met slechts 1.9 ± 0.7 min vergeleken met VMAT (9.1 ± 0.7 min). De plankwaliteit van VMAT+CS was vergelijkbaar met die van VMAT+5, terwijl de optimalisatietijd een factor 25 lager was door het vermijden van patiëntspecifieke BAO. Het dosisbad van VMAT+CS was groter dan dat van 30-NCP, met verder vergelijkbare plankwaliteit, maar met substantieel lagere optimalisatie- en behandeltijden.

Tenslotte worden er in hoofdstuk 8 uitdagingen en kansen van het automatisch plannen met Erasmus-iCycle, en van het gebruik van niet-coplanaire bundelhoekconfiguraties bediscussieerd. Dit hoofdstuk wordt afgesloten met suggesties voor toekomstig onderzoek.

References

[1] Alber M., and Reemtsen R. Intensity modulated radiotherapy treatment planning by use of a barrier-penalty multiplier method. *Optim. Methods Softw. 22* (2007), 391–411. 22, 72, 104

[2] Aleman B., van den Belt-Dusebout A., and De Bruin M. Late cardiotoxicity after treatment for hodgkin lymphoma. *Blood. 5*, 109 (2008), 1878–1886. 89

[3] Aleman D. M., Romeijn H. E., and Dempsey J. F. A response surface approach to beam orientation optimization in intensity modulated radiation therapy treatment planning. *INFORMS J. Comput. 21* (2009), 62–76. 19

[4] Alongi F., Cozzi L., Arcangeli S., Iftode C., Comito T., Villa E., Lobefalo F., Navarria P., Reggiori G., Mancosu P., Clerici E., Fogliata A., Tomatis S., Taverna G., Graziotti P., and Scorsetti M. Linac based SBRT for prostate cancer in 5 fractions with VMAT and flattening filter free beams: preliminary report of a phase II study. *Radiat Oncol 8* (Jul 2013), 171. 111

[5] Aluwini S., van Rooij P., Hoogeman M., Bangma C., Kirkels W. J., Incrocci L., , and Kolkman-Deurloo I.-K. Cyberknife stereotactic radiotherapy as monotherapy for low- to intermediate-stage prostate cancer: early experience, feasibility and tolerance. *J. Endourol. 24*, 5 (2010), 865–869. 19, 112

[6] Aluwini S., van Rooij P., Hoogeman M., Kirkels W., Kolkman-Deurloo I.-K., and Bangma C. Stereotactic body radiotherapy with a focal boost to the MRI-visible tumor as monotherapy for low- and intermediate-risk prostate cancer: Early results. *Radiat Oncol 24*, 8 (2013), 1–7. 41, 59

[7] Arcangeli G., Fowler J., Gomellini S., Arcangeli S., Saracino B., Petrongari M., Benassi M., and Strigari L. Acute and late toxicity in a randomized trial of conventional versus hypofractionated three-dimensional conformal radiotherapy for prostate cancer. *Int. J. Radiat. Oncol. Biol. Phys. 79*, 4 (2011), 1013–21. 19, 41

[8] Armstrong G. T., Liu Q., Yasui Y., Huang S., Ness K. K., Leisenring W., Hudson M. M., Donaldson S. S., King A. A., Stovall M., Krull K. R., Robison L. L., and Packer R. J. Long-term outcomes among adult survivors of childhood central nervous system malignancies in the Childhood Cancer Survivor Study. *J. Natl. Cancer Inst. 101*, 13 (Jul 2009), 946–958. 77

[9] Arthurs B. J., Fairbanks R. K., Demakas J. J., Lamoreaux W. T., Giddings N. A., Mackay A. R., Cooke B. S., Elaimy A. L., and Lee C. M. A review of treatment modalities for vestibular schwannoma. *Neurosurg Rev 34*, 3 (Jul 2011), 265–277. 77

[10] Asmerom G., Bourne D., Chappelow J., Goggin L. M., Heitz R., Jordan P., Kilby W., Laing T., C R Maurer J., and Noll J. M. The design and physical characterization of a multileaf collimator for robotic radiosurgery. *Biomed Phys Eng Express. 01* (2016), 7003. 71

[11] Audet C., Poffenbarger B. A., Chang P., Jackson P. S., Lundahl R. E., Ryu S. I., and Ray G. R. Evaluation of volumetric modulated arc therapy for cranial radiosurgery using multiple noncoplanar arcs. *Med Phys 38*, 11 (Nov 2011), 5863–5872. 120

[12] Berry S. L., Boczkowski A., Ma R., Mechalakos J., and Hunt M. Interobserver variability in radiation therapy plan output: Results of a single-institution study. *Pract Radiat Oncol 6*, 6 (2016), 442–449. 69

[13] Berry S. L., Ma R., Boczkowski A., Jackson A., Zhang P., and Hunt M. Evaluating intercampus plan consistency using a knowledge based planning model. *Radiother Oncol 120*, 2 (Aug 2016), 349–355. 69

[14] Bhattasali O., Chen L. N., Woo J., Park J. W., Kim J. S., Moures R., Yung T., Lei S., Collins B. T., Kowalczyk K., Suy S., Dritschilo A., Lynch J. H., and Collins S. P. Patient-reported outcomes following stereotactic body radiation therapy for clinically localized prostate cancer. *Radiat Oncol 9* (Feb 2014), 52. 41

[15] Bijman R., Rossi L., Janssen T., de Ruiter P., Carbaat C., van Triest B., Breedveld S., Sonke J. J., and Heijmen B. First system for fully-automated multi-criterial treatment planning for a high-magnetic field MR-Linac applied to rectal cancer. *Acta Oncol* (May 2020), 1–7. 171

[16] Bijman R., Rossi L., Sharfo A., Heemsbergen W., Incrocci L., Breedveld S., and Heijmen B. Automated Radiotherapy Planning for Patient-Specific Exploration of the Trade-Off Between Tumor Dose Coverage and Predicted Radiation-Induced Toxicity—A Proof of Principle Study for Prostate Cancer. *Front. Oncol. 10* (2020), 943. 171

[17] Blomgren H., Lax I., Naslund I., and Svanstrom R. Stereotactic high dose fraction radiation therapy of extracranial tumours using an accelerator. *Acta Oncol. 34*, 6 (1995), 861–870. 19

[18] Boike T., Lotan Y., Cho L., Brindle J., DeRose P., Xie X., Yan J., Foster R., Pistenmaa D., Perkins A., Cooley S., and Timmerman R. Phase I dose-escalation study of stereotactic body radiation therapy for low- and intermediate-risk prostate cancer. *J Clin Oncol. 29*, 15 (2011), 2020–6. 59

[19] Boylan C., and Rowbottom C. A bias-free, automated planning tool for technique comparison in radiotherapy - application to nasopharyngeal carcinoma treatments. *J Appl Clin Med Phys 15*, 1 (Jan 2014), 4530. 41, 77

[20] Braunstein S., and Ma L. Stereotactic radiosurgery for vestibular schwannomas. *Cancer Manag Res 10* (2018), 3733–3740. 77

[21] Breedveld S., Storchi P., and Heijmen B. The equivalence of multi-criteria methods for radiotherapy plan optimization. *Phys. Med. Biol. 54* (2009), 7199–7209. 22, 33, 72, 104

[22] Breedveld S., Storchi P., Voet P., and Heijmen B. iCycle: Integrated, multicriterial beam angle, and profile optimization for generation of coplanar and noncoplanar IMRT plans. *Med. Phys. 39* (2012), 951–963. 13, 19, 20, 22, 33, 36, 41, 42, 59, 60, 61, 68, 72, 77, 78, 79, 91, 103, 104, 112, 123, 126

[23] Breedveld S., Storchi P. R. M., Keijzer M., Heemink A. W., and Heijmen B. J. M. A novel approach to multi-criteria inverse planning for IMRT. *Phys. Med. Biol. 52* (2007), 6339–6353. 13, 20

[24] Brenner D., and Hall E. Fractionation and protraction for radiotherapy of prostate carcinoma. *Int. J. Radiat. Oncol. Biol. Phys. 43*, 5 (1999), 1095–101. 19, 41, 59

[25] Buergy D., Sharfo A. W., Heijmen B. J., Voet P. W., Breedveld S., Wenz F., Lohr F., and Stieler F. Fully automated treatment planning of spinal metastases - A comparison to manual planning of Volumetric Modulated Arc Therapy for conventionally fractionated irradiation. *Radiat Oncol 12*, 1 (Jan 2017), 33. 13

[26] Burghelea M., Verellen D., Poels K., Hung C., Nakamura M., Dhont J., Gevaert T., Van den Begin R., Collen C., Matsuo Y., Kishi T., Simon V., Hiraoka M., and de Ridder M. Initial characterization, dosimetric benchmark and performance validation of Dynamic Wave Arc. *Radiat Oncol 11* (Apr 2016), 63. 111

[27] Buschmann M., Sharfo A. W. M., Penninkhof J., Seppenwoolde Y., Goldner G., Georg D., Breedveld S., and Heijmen B. J. M. Automated volumetric modulated arc therapy

planning for whole pelvic prostate radiotherapy. *Strahlenther Onkol 194*, 4 (04 2018), 333–342. 112

[28] Campbell B. A., Hornby C., Cunninghame J., Burns M., MacManus M., Ryan G., Lau E., Seymour J. F., and Wirth A. Minimising critical organ irradiation in limited stage Hodgkin lymphoma: a dosimetric study of the benefit of involved node radiotherapy. *Ann. Oncol. 23*, 5 (May 2012), 1259–1266. 89

[29] Cavedon C., Meliado G., Rossi L., Camera L., Baglio I., Caumo F., and Montemezzi S. High-field MR spectroscopy in the multiparametric MRI evaluation of breast lesions. *Phys Med 32*, 12 (Dec 2016), 1707–1711. 172

[30] Chan M. K., Kwong D. L., Law G. M., Tam E., Tong A., Lee V., and Ng S. C. Dosimetric evaluation of four-dimensional dose distributions of CyberKnife and volumetric-modulated arc radiotherapy in stereotactic body lung radiotherapy. *J Appl Clin Med Phys 14*, 4 (Jul 2013), 4229. 126

[31] Clark G. M., Popple R. A., Prendergast B. M., Spencer S. A., Thomas E. M., Stewart J. G., Guthrie B. L., Markert J. M., and Fiveash J. B. Plan quality and treatment planning technique for single isocenter cranial radiosurgery with volumetric modulated arc therapy. *Pract Radiat Oncol 2*, 4 (2012), 306–313. 120

[32] Cozzi L., Dinshaw K. A., Shrivastava S. K., Mahantshetty U., Engineer R., Deshpande D. D., Jamema S. V., Vanetti E., Clivio A., Nicolini G., and Fogliata A. A treatment planning study comparing volumetric arc modulation with RapidArc and fixed field IMRT for cervix uteri radiotherapy. *Radiother Oncol 89*, 2 (Nov 2008), 180–191. 84

[33] Craft D., and Bortfeld T. How many plans are needed in an IMRT multi-objective plan database? *Phys. Med. Biol. 53* (2008), 2785–2796. 35

[34] Cusumano D., Fumagalli M. L., Ghielmetti F., Rossi L., Grossi G., Lanzarotti R., Fariselli L., and De Martin E. Sum signal dosimetry: A new approach for high dose quality assurance with Gafchromic EBT3. *J Appl Clin Med Phys 18*, 2 (Mar 2017), 181–190. 172

[35] Cutter D. J., Schaapveld M., Darby S. C., Hauptmann M., van Nimwegen F. A., Krol A. D., Janus C. P., van Leeuwen F. E., and Aleman B. M. Risk of valvular heart disease after treatment for Hodgkin lymphoma. *J. Natl. Cancer Inst. 107*, 4 (Apr 2015). 90

[36] Dabaja B. S., Hoppe B. S., Plastaras J. P., Newhauser W., Rosolova K., Flampouri S., Mohan R., Mikhaeel N. G., Kirova Y., Specht L., and Yahalom J. Proton therapy for adults with mediastinal lymphomas: the International Lymphoma Radiation Oncology Group guidelines. *Blood 132*, 16 (10 2018), 1635–1646. 89

[37] De Bruin M. L., Sparidans J., van't Veer M. B., Noordijk E. M., Louwman M. W., Zijlstra J. M., van den Berg H., Russell N. S., Broeks A., Baaijens M. H., Aleman B. M., and van Leeuwen F. E. Breast cancer risk in female survivors of Hodgkin's lymphoma: lower risk after smaller radiation volumes. *J. Clin. Oncol. 27*, 26 (Sep 2009), 4239–4246. 89

[38] Della Gala G., Dirkx M. L. P., Hoekstra N., Fransen D., Lanconelli N., van de Pol M., Heijmen B. J. M., and Petit S. F. Fully automated VMAT treatment planning for advanced-stage NSCLC patients. *Strahlenther Onkol 193*, 5 (May 2017), 402–409. 13, 60, 68, 127

[39] Demanes D., Rodriguez R., Schour L., Brandt D., and Altieri G. High-dose-rate intensity-modulated brachytherapy with external beam radiotherapy for prostate cancer: California endocurietherapy's 10-year results. *Int. J. Radiat. Oncol. Biol. Phys. 61*, 5 (2005), 1306–16. 19

[40] Ding C., Chang C. H., Haslam J., Timmerman R., and Solberg T. A dosimetric comparison of stereotactic body radiation therapy techniques for lung cancer: robotic versus conventional linac-based systems. *J Appl Clin Med Phys 11*, 3 (Jun 2010), 3223. 126

[41] Dong P., Lee P., Ruan D., Long T., Romeijn E., Low D. A., Kupelian P., Abraham J., Yang Y., and Sheng K. 4π noncoplanar stereotactic body radiation therapy for centrally located or larger lung tumors. *Int. J. Radiat. Oncol. Biol. Phys. 86*, 3 (Jul 2013), 407–413. 126, 129

[42] Dong P., Lee P., Ruan D., Long T., Romeijn E., Yang Y., Low D., Kupelian P., and Sheng K. 4π non-coplanar liver SBRT: a novel delivery technique. *Int. J. Radiat. Oncol. Biol. Phys. 85*, 5 (Apr 2013), 1360–1366. 129

[43] Dong P., Nguyen D., Ruan D., King C., Long T., Romeijn E., Low D. A., Kupelian P., Steinberg M., Yang Y., and Sheng K. Feasibility of prostate robotic radiation therapy on conventional C-arm linacs. *Pract Radiat Oncol. 4*, 4 (2014), 254–260. 59, 70, 111

[44] Dong P., Nguyen D., Ruan D., King C., Long T., Romeijn E., Low D. A., Kupelian P., Steinberg M., Yang Y., and Sheng K. Feasibility of prostate robotic radiation therapy on conventional C-arm linacs. *Pract Radiat Oncol 4*, 4 (2014), 254–260. 126

[45] Dunlop A., Welsh L., McQuaid D., Dean J., Gulliford S., Hansen V., Bhide S., Nutting C., Harrington K., and Newbold K. Brain-sparing methods for IMRT of head and neck cancer. *PLoS ONE 10*, 3 (2015), e0120141. 126

[46] Dutta D., Balaji Subramanian S., Murli V., Sudahar H., Gopalakrishna Kurup P. G., and Potharaju M. Dosimetric comparison of Linac-based (BrainLAB) and robotic

radiosurgery (CyberKnife) stereotactic system plans for acoustic schwannoma. *J. Neurooncol. 106*, 3 (Feb 2012), 637–642. 77

[47] Echner G. G., Kilby W., Lee M., Earnst E., Sayeh S., Schlaefer A., Rhein B., Dooley J. R., Lang C., Blanck O., Lessard E., Maurer C. R., and Schlegel W. The design, physical properties and clinical utility of an iris collimator for robotic radiosurgery. *Phys Med Biol 54*, 18 (Sep 2009), 5359–5380. 78

[48] Edvardsson A., Kugele M., Alkner S., Enmark M., Nilsson J., Kristensen I., Kjellen E., Engelholm S., and Ceberg S. Comparative treatment planning study for mediastinal Hodgkin's lymphoma: impact on normal tissue dose using deep inspiration breath hold proton and photon therapy. *Acta Oncol 58*, 1 (Jan 2019), 95–104. 84

[49] Eichenauer D. A., Becker I., Monsef I., Chadwick N., de Sanctis V., Federico M., Fortpied C., Gianni A. M., Henry-Amar M., Hoskin P., Johnson P., Luminari S., Bellei M., Pulsoni A., Sydes M. R., Valagussa P., Viviani S., Engert A., and Franklin J. Secondary malignant neoplasms, progression-free survival and overall survival in patients treated for Hodgkin lymphoma: a systematic review and meta-analysis of randomized clinical trials. *Haematologica 102*, 10 (10 2017), 1748–1757. 89

[50] Fiandra C., Filippi A. R., Catuzzo P., Botticella A., Ciammella P., Franco P., Borca V. C., Ragona R., Tofani S., and Ricardi U. Different IMRT solutions vs. 3D-conformal radiotherapy in early stage Hodgkin's Lymphoma: dosimetric comparison and clinical considerations. *Radiat Oncol 7* (Nov 2012), 186. 89, 92, 94

[51] Fiandra C., Rossi L., Alparone A., Zara S., Vecchi C., Sardo A., Bartoncini S., Loi G., Pisani C., Gino E., Ruo Redda M. G., Marco Deotto G., Tini P., Comi S., Zerini D., Ametrano G., Borzillo V., Strigari L., Strolin S., Savini A., Romeo A., Reccanello S., Rumeileh I. A., Ciscognetti N., Guerrisi F., Balestra G., Ricardi U., and Heijmen B. Automatic genetic planning for volumetric modulated arc therapy: A large multicentre validation for prostate cancer. *Radiother Oncol 148* (Apr 2020), 126–132. 171

[52] Filippi A. R., Ragona R., Piva C., Scafa D., Fiandra C., Fusella M., Giglioli F. R., Lohr F., and Ricardi U. Optimized volumetric modulated arc therapy versus 3D-CRT for early stage mediastinal Hodgkin lymphoma without axillary involvement: a comparison of second cancers and heart disease risk. *Int. J. Radiat. Oncol. Biol. Phys. 92*, 1 (May 2015), 161–168. 89

[53] Fogliata A., Belosi F., Clivio A., Navarria P., Nicolini G., Scorsetti M., Vanetti E., and Cozzi L. On the pre-clinical validation of a commercial model-based optimisation engine: application to volumetric modulated arc therapy for patients with lung or prostate cancer. *Radiother Oncol 113*, 3 (Dec 2014), 385–391. 69

[54] Fowler J., Chappell R., and Ritter M. Is alpha/beta for prostate tumors really low? *Int. J. Radiat. Oncol. Biol. Phys. 50*, 4 (2001), 1021–1031. 19

[55] Freeman D., and King C. Stereotactic body radiotherapy for low-risk prostate cancer: five-year outcomes. *Radiother. Oncol. 6*, 1 (2011), 3. 41, 59

[56] Freeman D. E., Friedland J. L., and Masterson-McGary M. E. Stereotactic radiosurgery for low-intermediate risk prostate cancer: An emerging treatment approach. *Am. J. Clin. Oncol. 33* (2010), 208. 19

[57] Fuller D., Mardirossian G., Wong D., and McKellar H. Prospective evaluation of CyberKnife stereotactic body radiotherapy for low- and intermediate-risk prostate cancer: Emulating HDR brachytherapy dose distribution, 2010. 41, 59

[58] Fuller D. B., Naitoh J., Lee C., Hardy S., and Jin H. Virtual HDR CyberKnife treatment for localized prostatic carcinoma: dosimetry comparison with HDR brachytherapy and preliminary clinical observations. *Int. J. Radiat. Oncol. Biol. Phys. 70*, 5 (2008), 1588–1597. 19

[59] Fürweger C., Prins P., Coskan H., and Heijmen B. Characteristics and performance of the first commercial multileaf collimator for a robotic radiosurgery system. *Med. Phys. 43*, 5 (2016), 2063. 71

[60] Gevaert T., Levivier M., Lacornerie T., Verellen D., Engels B., Reynaert N., Tournel K., Duchateau M., Reynders T., Depuydt T., Collen C., Lartigau E., and De Ridder M. Dosimetric comparison of different treatment modalities for stereotactic radiosurgery of arteriovenous malformations and acoustic neuromas. *Radiother Oncol 106*, 2 (Feb 2013), 192–197. 77

[61] Glicksman R. M., Tjong M. C., Neves-Junior W. F. P., Spratt D. E., Chua K. L. M., Mansouri A., Chua M. L. K., Berlin A., Winter J. D., Dahele M., Slotman B. J., Bilsky M., Shultz D. B., Maldaun M., Szerlip N., Lo S. S., Yamada Y., Vera-Badillo F. E., Marta G. N., and Moraes F. Y. Stereotactic Ablative Radiotherapy for the Management of Spinal Metastases: A Review. *JAMA Oncol* (Jan 2020). 111

[62] Grills I., Martinez A., Hollander M., Huang R., Goldman K., Chen P., and Gustafson G. High dose rate brachytherapy as prostate cancer monotherapy reduces toxicity compared to low dose rate palladium seeds. *J. Urol. 171*, 3 (2004), 1098–104. 19

[63] Guckenberger M., Andratschke N., Dieckmann K., Hoogeman M. S., Hoyer M., Hurkmans C., Tanadini-Lang S., Lartigau E., Méndez Romero A., Senan S., and Verellen D. ESTRO ACROP consensus guideline on implementation and practice of stereotactic body radiotherapy for peripherally located early stage non-small cell lung cancer. *Radiother Oncol 124*, 1 (07 2017), 11–17. 111

[64] Hansen C. R., Bertelsen A., Hazell I., Zukauskaite R., Gyldenkerne N., Johansen J., Eriksen J. G., and Brink C. Automatic treatment planning improves the clinical quality of head and neck cancer treatment plans. *Clinical and Translational Radiation Oncology 1* (2016), 2–8. 69, 127

[65] Hansen C. R., Nielsen M., Bertelsen A. S., Hazell I., Holtved E., Zukauskaite R., Bjerregaard J. K., Brink C., and Bernchou U. Automatic treatment planning facilitates fast generation of high-quality treatment plans for esophageal cancer. *Acta Oncol 56*, 11 (Nov 2017), 1495–1500. 83

[66] Hazell I., Bzdusek K., Kumar P., Hansen C. R., Bertelsen A., Eriksen J. G., Johansen J., and Brink C. Automatic planning of head and neck treatment plans. *J Appl Clin Med Phys 17*, 1 (01 2016), 272–282. 127

[67] Heijkoop S., Langerak T., Quint S., Bondar L., Mens J., Heijmen B., and Hoogeman M. Clinical implementation of an online adaptive plan-of-the-day protocol for nonrigid motion management in locally advanced cervical cancer imrt. *Int. J. Radiat. Oncol. Biol. Phys. 90* (2014), 673–9. 13, 60

[68] Heijmen B., Voet P., and Dirkx M. Fully automatic imrt and vmat treatment planning in routine clinical practice. *Phys Med 301 S* (2014), 2. cited By 1. 41, 42

[69] Heijmen B., Voet P., Fransen D., Penninkhof J., Milder M., Akhiat H., Bonomo P., Casati M., Georg D., Goldner G., Henry A., Lilley J., Lohr F., Marrazzo L., Pallotta S., Pellegrini R., Seppenwoolde Y., Simontacchi G., Steil V., Stieler F., Wilson S., and Breedveld S. Fully automated, multi-criterial planning for Volumetric Modulated Arc Therapy - An international multi-center validation for prostate cancer. *Radiother Oncol 128*, 2 (08 2018), 343–348. 13, 104, 112, 124, 127

[70] Hissoiny S., Ozell B., and Després P. GPUMCD, a new GPU-oriented monte carlo dose calculation platform. *Med. Phys. 38* (2011), 754–764. 91

[71] Hoskin P. J., Diez P., Williams M., Lucraft H., and Bayne M. Recommendations for the use of radiotherapy in nodal lymphoma. *Clin Oncol (R Coll Radiol) 25*, 1 (Jan 2013), 49–58. 90

[72] Huss M., Barsoum P., Dodoo E., Sinclair G., and Toma-Dasu I. Fractionated SRT using VMAT and Gamma Knife for brain metastases and gliomas–a planning study. *J Appl Clin Med Phys 16*, 6 (11 2015), 3–16. 84

[73] Hussein M., Heijmen B. J. M., Verellen D., and Nisbet A. Automation in intensity modulated radiotherapy treatment planning-a review of recent innovations. *Br J Radiol 91*, 1092 (Dec 2018), 20180270. 13, 104, 127

[74] Jabbari S., Weinberg V., Kaprealian T., Hsu I., Ma L., Chuang C., Descovich M., Shiao S., Shinohara K., Roach M., and Gottschalk A. Stereotactic body radiotherapy as monotherapy or post-external beam radiotherapy boost for prostate cancer: technique, early toxicity, and PSA response. *Int. J. Radiat. Oncol. Biol. Phys. 82*, 1 (2012), 228–34. 19, 41, 59

[75] Jang S., Lalonde R., Ozhasoglu C., Burton S., Heron D., and Huq M. Dosimetric comparison between cone/Iris-based and InCise MLC-based CyberKnife plans for single and multiple brain metastases. *J Appl Clin Med Phys. 17* (2016), 184–199. 71

[76] Jang W. I., Bae S. H., Kim M. S., Han C. J., Park S. C., Kim S. B., Cho E. H., Choi C. W., Kim K. S., Hwang S., Kim J. H., Chang A. R., Park Y., Kim E. S., Kim W. C., Jo S., and Park H. J. A phase 2 multicenter study of stereotactic body radiotherapy for hepatocellular carcinoma: Safety and efficacy. *Cancer 126*, 2 (Jan 2020), 363–372. 111

[77] Jeraj R., Keall P. J., and Siebers J. V. The effect of dose calculation accuracy on inverse treatment planning. *Phys. Med. Biol. 47* (2002), 391–407. 36

[78] Kang S. W., Chung J. B., Kim J. S., Kim I. A., Eom K. Y., Song C., Lee J. W., Kim J. Y., and Suh T. S. Optimal planning strategy among various arc arrangements for prostate stereotactic body radiotherapy with volumetric modulated arc therapy technique. *Radiol Oncol 51*, 1 (Mar 2017), 112–120. 111

[79] Kathriarachchi V., Shang C., Evans G., Leventouri T., and Kalantzis G. Dosimetric and radiobiological comparison of CyberKnife M6 InCise multileaf collimator over Iris variable collimator in prostate stereotactic body radiation therapy. *J Med Phys. 41* (2016), 2135–143. 71, 127

[80] Katz A., and Santoro M. Cyberknife radiosurgery for early carcinoma of the prostate: A three year experience. *Int. J. Radiat. Oncol. Biol. Phys. 75*, 3 (2009), S312–S313. 19, 41

[81] Katz A. J., Santoro M., Diblasio F., and Ashley R. Stereotactic body radiotherapy for localized prostate cancer: disease control and quality of life at 6 years. *Radiation Oncology 8* (2013), 118. 41, 59

[82] Keall P., Ng J., Juneja P., O'Brien R., Huang C., Colvill E., Caillet V., Simpson E., Poulsen P., Kneebone A., Eade T., and Booth J. Real-time 3D image guidance using a standard LINAC: Measured motion, accuracy, and precision of the first prospective clinical trial of kilovoltage intrafraction monitoring-guided gating for prostate cancer radiation therapy. *Int. J. Radiat. Oncol. Biol. Phys. 94* (2016), 1015–21. 59, 71

[83] Kearney V., Cheung J. P., McGuinness C., and Solberg T. D. CyberArc: a non-coplanar-arc optimization algorithm for CyberKnife. *Phys Med Biol 62*, 14 (Jun 2017), 5777–5789. 111, 127

[84] Kearney V., Descovich M., Sudhyadhom A., Cheung J. P., McGuinness C., and Solberg T. D. A continuous arc delivery optimization algorithm for CyberKnife m6. *Med Phys* (Jun 2018). 111

[85] Kilby W., Dooley J. R., Kuduvalli G., Sayeh S., and Maurer, C. R. J. The cyberknife robotic radiosurgery system in 2010. *Technol. Cancer Res. Treat. 9*, 5 (2010), 433–452. 19

[86] Kim S. T., An H. J., Kim J. I., Yoo J. R., Kim H. J., and Park J. M. Non-coplanar VMAT plans for lung SABR to reduce dose to the heart: a planning study. *Br J Radiol 93*, 1105 (Jan 2020), 20190596. 126

[87] King C., Brooks J., Gill H., and Presti J. J. Long-term outcomes from a prospective trial of stereotactic body radiotherapy for low-risk prostate cancer. *Int. J. Radiat. Oncol. Biol. Phys. 82*, 2 (2011), 877–82. 19, 41

[88] King C., and Fowler J. A simple analytic derivation suggests that prostate cancer alpha/beta ratio is low. *Int. J. Radiat. Oncol. Biol. Phys. 51*, 1 (2001), 213–214. 19

[89] King C., Freeman D., Kaplan I., Fuller D., Bolzicco G., Collins S., Meier R., Wang J., Kupelian P., Steinberg M., and Katz A. Stereotactic body radiotherapy for localized prostate cancer: Pooled analysis from a multi-institutional consortium of prospective phase II trials. *Radiother Oncol 109* (2013), 217–221. 41, 59

[90] King C., Lehmann J., Adler J., and Hai J. Cyberknife radiotherapy for localized prostate cancer: rationale and technical feasibility. *Technol. Cancer Res. Treat. 2*, 1 (2003), 25–30. 19, 41

[91] Koh E. S., Tran T. H., Heydarian M., Sachs R. K., Tsang R. W., Brenner D. J., Pintilie M., Xu T., Chung J., Paul N., and Hodgson D. C. A comparison of mantle versus involved-field radiotherapy for Hodgkin's lymphoma: reduction in normal tissue dose and second cancer risk. *Radiat Oncol 2* (Mar 2007), 13. 89

[92] Krayenbuehl J., Di Martino M., Guckenberger M., and Andratschke N. Improved plan quality with automated radiotherapy planning for whole brain with hippocampus sparing: a comparison to the RTOG 0933 trial. *Radiat Oncol 12*, 1 (Oct 2017), 161. 77, 83

[93] Krayenbuehl J., Norton I., Studer G., and Guckenberger M. Evaluation of an automated knowledge based treatment planning system for head and neck. *Radiother. Oncol. 10* (2015), 226. 59

[94] Kupelian P., Willoughby T., Mahadevan A., Djemil T., Weinstein G., Jani S., Enke C., Solberg T., Flores N., Liu D., Beyer D., and Levine L. Multi-institutional clinical experience with the Calypso system in localization and continuous, real-time monitoring of the prostate gland during external radiotherapy. *Int. J. Radiat. Oncol. Biol. Phys. 67* (2007), 1088–1098. 59

[95] Landers A., O'Connor D., Ruan D., and Sheng K. Automated 4π radiotherapy treatment planning with evolving knowledge-base. *Med Phys 46*, 9 (Sep 2019), 3833–3843. 126

[96] Lee J., Shin I. S., Yoon W. S., Koom W. S., and Rim C. H. Comparisons between radiofrequency ablation and stereotactic body radiotherapy for liver malignancies: Meta-analyses and a systematic review. *Radiother Oncol 145* (Jan 2020), 63–70. 111

[97] Lee Y., Joo J. H., and Choi G. M. Effect of al- or ga-additive on ionic conductivity of thin-film gd-doped ceria. *Solid State Ionics 249-250* (2013), 165 – 170. 53

[98] Leinders S. M., Breedveld S., Romero A. M., Schaart D., Seppenwoolde Y., and Heijmen B. Adaptive liver stereotactic body radiation therapy: Automated daily plan reoptimization prevents dose delivery degradation caused by anatomy deformations. *Int. J. Radiat. Oncol. Biol. Phys. 87* (2013), 1016–1021. 41

[99] Levis M., Filippi A. R., Fiandra C., De Luca V., Bartoncini S., Vella D., Ragona R., and Ricardi U. Inclusion of heart substructures in the optimization process of volumetric modulated arc therapy techniques may reduce the risk of heart disease in Hodgkin's lymphoma patients. *Radiother Oncol 138* (09 2019), 52–58. 98

[100] Li R., and Xing L. An adaptive planning strategy for station parameter optimized radiation therapy (SPORT): Segmentally boosted VMAT. *Med. Phys. 40* (2013), 050701. 41

[101] Li T., Wu Q., Zhang Y., Vergalasova I., Lee W. R., Yin F. F., and Wu Q. J. Strategies for automatic online treatment plan reoptimization using clinical treatment planning system: a planning parameters study. *Med Phys 40*, 11 (Nov 2013), 111711. 41

[102] Lin Y., Lin K., Ho H., Lin H., Lin L., Lee S., and Chui C. Treatment plan comparison between stereotactic body radiation therapy techniques for prostate cancer: Non-isocentric cyberknife versus isocentric rapidarc. *Physica Medica 30* (2014), 654–661. 59, 70, 111

[103] Linthout N., Verellen D., Tournel K., Reynders T., Duchateau M., and Storme G. Assessment of secondary patient motion induced by automated couch movement during on-line 6 dimensional repositioning in prostate cancer treatment. *Radiother. Oncol. 83* (2007), 168–174. 70

[104] Loi M., Duijm M., Baker S., Rossi L., Grunhagen D., Verhoef C., and Nuyttens J. Stereotactic body radiotherapy for oligometastatic soft tissue sarcoma. *Radiol Med 123*, 11 (Nov 2018), 871–878. 172

[105] Luca P. D., and et al. ICRU Report 83: prescribing, recording and reporting photon-beam intensity-modulated radiation therapy (IMRT). *J ICRU 1*, 10 (2010), 1–160. 23

[106] Lyu Q., Yu V. Y., Ruan D., Neph R., O'Connor D., and Sheng K. A novel optimization framework for VMAT with dynamic gantry couch rotation. *Phys Med Biol 63*, 12 (06 2018), 125013. 111

[107] MacDougall N., Dean C., and Muirhead R. Stereotactic body radiotherapy in prostate cancer: is rapidarc a better solution than Cyberknife? *Clinical Oncology 26* (2014), 4–9. 59, 70

[108] Madsen B., Hsi R., Pham H., Fowler J., Esagui L., and Corman J. Stereotactic hypofractionated accurate radiotherapy of the prostate (sharp), 33.5 Gy in five fractions for localized disease: first clinical trial results. *Int. J. Radiat. Oncol. Biol. Phys. 67* (2007), 1009–1105. 59

[109] Maraldo M. V., Brodin N. P., Aznar M. C., Vogelius I. R., Munck af Rosenschöld P., Petersen P. M., and Specht L. Estimated risk of cardiovascular disease and secondary cancers with modern highly conformal radiotherapy for early-stage mediastinal Hodgkin lymphoma. *Ann. Oncol. 24*, 8 (Aug 2013), 2113–2118. 89

[110] Maraldo M. V., Brodin N. P., Vogelius I. R., Aznar M. C., Munck Af Rosenschöld P., Petersen P. M., and Specht L. Risk of developing cardiovascular disease after involved node radiotherapy versus mantle field for Hodgkin lymphoma. *Int. J. Radiat. Oncol. Biol. Phys. 83*, 4 (Jul 2012), 1232–1237. 89

[111] Maraldo M. V., Dabaja B. S., Filippi A. R., Illidge T., Tsang R., Ricardi U., Petersen P. M., Schut D. A., Garcia J., Headley J., Parent A., Guibord B., Ragona R., and Specht L. Radiation therapy planning for early-stage Hodgkin lymphoma: experience of the International Lymphoma Radiation Oncology Group. *Int. J. Radiat. Oncol. Biol. Phys. 92*, 1 (May 2015), 144–152. 89

[112] Maraldo M. V., Giusti F., Vogelius I. R., Lundemann M., van der Kaaij M. A., Ramadan S., Meulemans B., Henry-Amar M., Aleman B. M., Raemaekers J., Meijnders P., Moser E. C., Kluin-Nelemans H. C., Feugier P., Casasnovas O., Fortpied C., and Specht L. Cardiovascular disease after treatment for Hodgkin's lymphoma: an analysis of nine collaborative EORTC-LYSA trials. *Lancet Haematol 2*, 11 (Nov 2015), 492–502. 89

[113] Maraldo M. V., and Specht L. A decade of comparative dose planning studies for early-stage Hodgkin lymphoma: what can we learn? *Int. J. Radiat. Oncol. Biol. Phys. 90*, 5 (Dec 2014), 1126–1135. 89

[114] Marrazzo L., Meattini I., Arilli C., Calusi S., Casati M., Talamonti C., Livi L., and Pallotta S. Auto-planning for VMAT accelerated partial breast irradiation. *Radiother Oncol 132* (03 2019), 85–92. 127

[115] McGuinness C., Gottschalk A., Lessard E., Nakamura J., Pinnaduwage D., Pouliot J., Sims C., and Descovich M. Investigating the clinical advantages of a robotic linac equipped with a multileaf collimator in the treatment of brain and prostate cancer patients. *J Appl Clin Med Phys. 16* (2015), 284–95. 71

[116] McIntosh C., Welch M., McNiven A., Jaffray D. A., and Purdie T. G. Fully automated treatment planning for head and neck radiotherapy using a voxel-based dose prediction and dose mimicking method. *Phys Med Biol 62*, 15 (Jul 2017), 5926–5944. 77

[117] Michalski J., Gay H., Jackson A., Tucker S., and Deasy J. Radiation dose-volume effects in radiation-induced rectal injury. *Int. J. Radiat. Oncol. Biol. Phys. 76*, 3 (2010), S123–9. 23, 35, 45, 62

[118] Minniti G., Traish D., Ashley S., Gonsalves A., and Brada M. Risk of second brain tumor after conservative surgery and radiotherapy for pituitary adenoma: update after an additional 10 years. *J. Clin. Endocrinol. Metab. 90*, 2 (Feb 2005), 800–804. 77

[119] Miralbell R., Roberts S., Zubizarreta E., and Hendry J. Dose-fractionation sensitivity of prostate cancer deduced from radiotherapy outcomes of 5,969 patients in seven international institutional datasets: α/β=1.4 (0.9-2.2) Gy. *Int. J. Radiat. Oncol. Biol. Phys. 82*, 1 (2012), e17–e24. 19

[120] Monz M., Küfer K.-H., Bortfeld T. R., and Thieke C. Pareto navigation - algorithmic foundation of interactive multi-criteria IMRT planning. *Phys. Med. Biol. 53* (2008), 985–998. 35

[121] Morgan S. C., Hoffman K., Loblaw D. A., Buyyounouski M. K., Patton C., Barocas D., Bentzen S., Chang M., Efstathiou J., Greany P., Halvorsen P., Koontz B. F., Lawton C., Leyrer C. M., Lin D., Ray M., and Sandler H. Hypofractionated Radiation Therapy for Localized Prostate Cancer: Executive Summary of an ASTRO, ASCO, and AUA Evidence-Based Guideline. *Pract Radiat Oncol 8*, 6 (2018), 354–360. 111

[122] Murphy E. S., and Suh J. H. Radiotherapy for vestibular schwannomas: a critical review. *Int. J. Radiat. Oncol. Biol. Phys. 79*, 4 (Mar 2011), 985–997. 77

[123] Murray L., Cosgrove V., Lilley J., Sykes J., Thompson C., Franks K., Sebag-Montefiore D., and Henry A. Developing a class solution for prostate stereotactic ablative body radiotherapy (sabr) using volumetric modulated arc therapy (vmat). *Radiotherapy and Oncology 110*, 2 (2014), 298–302. cited By 16. 53

[124] Nelms B. E., Robinson G., Markham J., Velasco K., Boyd S., Narayan S., Wheeler J., and Sobczak M. L. Variation in external beam treatment plan quality: An inter-institutional study of planners and planning systems. *Pract Radiat Oncol 2*, 4 (2012), 296–305. 69

[125] Ng A., Patricia Bernardo M., Weller E., Backstrand K., Silver B., Marcus K., Tarbell N., Stevenson M., Friedberg J., and Mauch P. Second malignancy after Hodgkin disease treated with radiation therapy with or without chemotherapy: long-term risks and risk factors. *Blood 6*, 100 (2002), 1989–1996. 89

[126] Nguyen D., Rwigema J. C., Yu V. Y., Kaprealian T., Kupelian P., Selch M., Lee P., Low D. A., and Sheng K. Feasibility of extreme dose escalation for glioblastoma multiforme using 4π radiotherapy. *Radiat Oncol 9* (Nov 2014), 239. 126

[127] Niemierko A. A generalized concept of equivalent uniform dose (EUD). *Med. Phys. 26* (1999), 1100. 73

[128] Nishio S., Morioka T., Inamura T., Takeshita I., Fukui M., Sasaki M., Nakamura K., and Wakisaka S. Radiation-induced brain tumours: potential late complications of radiation therapy for brain tumours. *Acta Neurochir (Wien) 140*, 8 (1998), 763–770. 77

[129] Norkus D., Miller A., Kurtinaitis J., Haverkamp U., Popov S., Prott F., and Valuckas K. A randomized trial comparing hypofractionated and conventionally fractionated three-dimensional external-beam radiotherapy for localized prostate adenocarcinoma : a report on acute toxicity. *Strahlenther. Onkol. 185*, 11 (2009), 715–21. 19

[130] Ohira S., Ueda Y., Akino Y., Hashimoto M., Masaoka A., Hirata T., Miyazaki M., Koizumi M., and Teshima T. HyperArc VMAT planning for single and multiple brain metastases stereotactic radiosurgery: a new treatment planning approach. *Radiat Oncol 13*, 1 (Jan 2018), 13. 120

[131] Park J. M., Park S. Y., Wu H. G., and Kim J. I. Improvement of VMAT plan quality for head and neck cancer with high resolution fluences generated by couch shift between arcs. *Phys Med 46* (Feb 2018), 1–6. 84

[132] Pinnix C. C., Smith G. L., Milgrom S., Osborne E. M., Reddy J. P., Akhtari M., Reed V., Arzu I., Allen P. K., Wogan C. F., Fanale M. A., Oki Y., Turturro F., Romaguera J., Fayad

L., Fowler N., Westin J., Nastoupil L., Hagemeister F. B., Rodriguez M. A., Ahmed S., Nieto Y., and Dabaja B. Predictors of radiation pneumonitis in patients receiving intensity modulated radiation therapy for Hodgkin and non-Hodgkin lymphoma. *Int. J. Radiat. Oncol. Biol. Phys. 92*, 1 (May 2015), 175–182. 89, 90

[133] Podgorsak E. B., Pike G. B., Olivier A., Pla M., and Souhami L. Radiosurgery with high energy photon beams: a comparison among techniques. *Int. J. Radiat. Oncol. Biol. Phys. 16*, 3 (Mar 1989), 857–865. 126

[134] Pollack A., Hanlon A., Horwitz E., Feigenberg S., Konski A., Movsas B., Greenberg R., Uzzo R., Ma C., McNeeley S., Buyyounouski M., and Price R. J. Dosimetry and preliminary acute toxicity in the first 100 men treated for prostate cancer on a randomized hypofractionation dose escalation trial. *Int. J. Radiat. Oncol. Biol. Phys. 64*, 2 (2006), 518–526. 19, 41

[135] De Pooter J. A., Méndez Romero A., Wunderink W., Storchi P. R. M., and Heijmen B. J. M. Automated non-coplanar beam direction optimization improves IMRT in SBRT of liver metastasis. *Radiother. Oncol. 88* (2008), 376–381. 19, 41, 42

[136] Pugachev A., and Xing L. Computer-assisted selection of coplanar beam orientations in intensity-modulated radiation therapy. *Phys. Med. Biol. 46* (2001), 2467–2476. 19

[137] Purdie T., Dinniwell R., and Fyles A. Automation and intensity modulated radiation therapy for individualized high-quality tangent breast treatment plans. *Int. J. Radiat. Oncol. Biol. Phys. 90* (2014), 688–695. 59

[138] Quan E., Chang J., Liao Z., Xia T., Yuan Z., Liu H., Li X., Wages C., Mohan R., and Zhang X. Automated volumetric modulated Arc therapy treatment planning for stage III lung cancer: how does it compare with intensity-modulated radiotherapy? *Int. J. Radiat. Oncol. Biol. Phys. 84* (2012), e69–76. 59

[139] Ricardi U., Maraldo M. V., Levis M., and Parikh R. R. Proton Therapy For Lymphomas: Current State Of The Art. *Onco Targets Ther 12* (2019), 8033–8046. 89

[140] Ron E., Modan B., Boice J. D., Alfandary E., Stovall M., Chetrit A., and Katz L. Tumors of the brain and nervous system after radiotherapy in childhood. *N. Engl. J. Med. 319*, 16 (Oct 1988), 1033–1039. 77

[141] Rossi L., Bijman R., Schillemans W., Aluwini S., Cavedon C., Witte M., Incrocci L., and Heijmen B. Texture analysis of 3D dose distributions for predictive modelling of toxicity rates in radiotherapy. *Radiother Oncol 129*, 3 (12 2018), 548–553. 172

[142] Rossi L., Breedveld S., Aluwini S., and Heijmen B. Non-coplanar beam angle class solutions to replace time-consuming patient-specific beam angle optimization in robotic prostate SBRT. *Int. J. Radiat. Oncol. Biol. Phys. 92* (2015), 762–770. 172

[143] Rossi L., Breedveld S., Heijmen B. J. M., Voet P. W. J., Lanconelli N., and Aluwini S. On the beam direction search space in computerized non-coplanar beam angle optimization for IMRT - prostate SBRT. *Phys. Med. Biol. 57* (2012), 5441–5458. 41, 42, 43, 51, 59, 60, 77, 79, 111, 126, 172

[144] Rossi L., Méndez Romero A., Milder M., de Klerck E., Breedveld S., and Heijmen B. Individualized automated planning for dose bath reduction in robotic radiosurgery for benign tumors. *PLoS ONE 14*, 2 (2019), e0210279. 13, 126, 127, 172

[145] Rossi L., Sharfo A. W., Aluwini S., Dirkx M., Breedveld S., and Heijmen B. First fully automated planning solution for robotic radiosurgery - comparison with automatically planned volumetric arc therapy for prostate cancer. *Acta Oncol 57*, 11 (Nov 2018), 1490–1498. 13, 77, 78, 104, 111, 112, 119, 126, 127, 172

[146] Rwigema J. C., Nguyen D., Heron D. E., Chen A. M., Lee P., Wang P. C., Vargo J. A., Low D. A., Huq M. S., Tenn S., Steinberg M. L., Kupelian P., and Sheng K. 4π noncoplanar stereotactic body radiation therapy for head-and-neck cancer: potential to improve tumor control and late toxicity. *Int. J. Radiat. Oncol. Biol. Phys. 91*, 2 (Feb 2015), 401–409. 126

[147] Samii M., and Matthies C. Management of 1000 vestibular schwannomas (acoustic neuromas): hearing function in 1000 tumor resections. *Neurosurgery 40*, 2 (Feb 1997), 248–260. 77

[148] van Santvoort J. P. C., and Heijmen B. J. M. Dynamic multileaf collimation without 'tongue-and-groove' underdosage effects. *Phys. Med. Biol. 41* (1996), 2091–2105. 24

[149] Schaapveld M., Aleman B. M., van Eggermond A. M., Janus C. P., Krol A. D., van der Maazen R. W., Roesink J., Raemaekers J. M., de Boer J. P., Zijlstra J. M., van Imhoff G. W., Petersen E. J., Poortmans P. M., Beijert M., Lybeert M. L., Mulder I., Visser O., Louwman M. W., Krul I. M., Lugtenburg P. J., and van Leeuwen F. E. Second Cancer Risk Up to 40 Years after Treatment for Hodgkin's Lymphoma. *N. Engl. J. Med. 373*, 26 (Dec 2015), 2499–2511. 89

[150] Schipaanboord B. W. K., Breedveld S., Rossi L., Keijzer M., and Heijmen B. Automated prioritised 3D dose-based MLC segment generation for step-and-shoot IMRT. *Phys Med Biol 64*, 16 (Aug 2019), 165013. 172

[151] Schlaefer A., and Schweikard A. Stepwise multi-criteria optimization for robotic radiosurgery. *Med Phys 35*, 5 (May 2008), 2094–2103. 78

[152] Schneider B. J., Daly M. E., Kennedy E. B., Antonoff M. B., Broderick S., Feldman J., Jolly S., Meyers B., Rocco G., Rusthoven C., Slotman B. J., Sterman D. H., and Stiles B. M. Stereotactic Body Radiotherapy for Early-Stage Non-Small-Cell Lung Cancer: American Society of Clinical Oncology Endorsement of the American Society for Radiation Oncology Evidence-Based Guideline. *J. Clin. Oncol. 36*, 7 (03 2018), 710–719. 111

[153] Seuntjens J., Lartigau E., Cora S., Ding G., Goetsch S., Nuyttens J., and Roberge D. ICRU Report 91. Prescribing, recording, and reporting of stereotactic treatments with small photon beams. *J ICRU 2*, 1 (2014), 1–160. 126

[154] Shapiro S., and Mealey J. Late anaplastic gliomas in children previously treated for acute lymphoblastic leukemia. *Pediatr Neurosci 15*, 4 (1989), 176–180. 77

[155] Sharfo A., Voet P., Breedveld S., Mens J., Hoogeman M., and Heijmen B. Comparison of VMAT and IMRT strategies for cervical cancer patients using automated planning. *Radiother. Oncol. 114* (2015), 395–401. 13, 60, 68, 78, 83

[156] Sharfo A. W., Breedveld S., Voet P. W., Heijkoop S. T., Mens J. M., Hoogeman M. S., and Heijmen B. J. Validation of Fully Automated VMAT Plan Generation for Library-Based Plan-of-the-Day Cervical Cancer Radiotherapy. *PLoS ONE 11*, 12 (2016), e0169202. 59, 112

[157] Sharfo A. W., Dirkx M. L., Breedveld S., Méndez Romero A., and Heijmen B. J. VMAT plus a few computer-optimized non-coplanar IMRT beams (VMAT+) tested for liver SBRT. *Radiother Oncol 123*, 1 (04 2017), 49–56. 104, 111, 119, 120, 127, 129, 138, 144

[158] Sharfo A. W. M., Dirkx M. L. P., Bijman R. G., Schillemans W., Breedveld S., Aluwini S., Pos F., Incrocci L., and Heijmen B. J. M. Late toxicity in the randomized multicenter HYPRO trial for prostate cancer analyzed with automated treatment planning. *Radiother Oncol 128*, 2 (Aug 2018), 349–356. 127

[159] Sharfo A. W. M., Stieler F., Kupfer O., Heijmen B. J. M., Dirkx M. L. P., Breedveld S., Wenz F., Lohr F., Boda-Heggemann J., and Buergy D. Automated VMAT planning for postoperative adjuvant treatment of advanced gastric cancer. *Radiat Oncol 13*, 1 (Apr 2018), 74. 13, 112, 130

[160] Sheng K., Molloy J. A., Larner J. M., and Read P. W. A dosimetric comparison of non-coplanar IMRT versus Helical Tomotherapy for nasal cavity and paranasal sinus cancer. *Radiother Oncol 82*, 2 (Feb 2007), 174–178. 126

[161] Sheng K., Shepard D. M., and Orton C. G. Point/Counterpoint. Noncoplanar beams improve dosimetry quality for extracranial intensity modulated radiotherapy and should be used more extensively. *Med Phys 42*, 2 (Feb 2015), 531–533. 126

[162] Slosarek K., Bekman B., Wendykier J., Grzadziel A., Fogliata A., and Cozzi L. In silico assessment of the dosimetric quality of a novel, automated radiation treatment planning strategy for linac-based radiosurgery of multiple brain metastases and a comparison with robotic methods. *Radiat Oncol 13*, 1 (Mar 2018), 41. 120

[163] Smyth G., Evans P. M., Bamber J. C., and Bedford J. L. Recent developments in non-coplanar radiotherapy. *Br J Radiol 92*, 1097 (May 2019), 20180908. 127

[164] Storchi P. R. M., and Woudstra E. Calculation of the absorbed dose distribution due to irregularly shaped photon beams using pencil beam kernels derived from basic beam data. *Phys. Med. Biol. 41* (1996), 637–656. 23

[165] Sung K., and Choi Y. E. Dose gradient curve: A new tool for evaluating dose gradient. *PLoS ONE 13*, 4 (2018), e0196664. 84

[166] Swerdlow A. J., Higgins C. D., Smith P., Cunningham D., Hancock B. W., Horwich A., Hoskin P. J., Lister T. A., Radford J. A., Rohatiner A. Z., and Linch D. C. Second cancer risk after chemotherapy for Hodgkin's lymphoma: a collaborative British cohort study. *J. Clin. Oncol. 29*, 31 (Nov 2011), 4096–4104. 89

[167] Thieke C., Nill S., Oelfke U., and Bortfeld T. Acceleration of intensity-modulated radiotherapy dose calculation by importance sampling of the calculation matrices. *Med. Phys. 29* (2002), 676–681. 35

[168] Thomas E. M., Popple R. A., Wu X., Clark G. M., Markert J. M., Guthrie B. L., Yuan Y., Dobelbower M. C., Spencer S. A., and Fiveash J. B. Comparison of plan quality and delivery time between volumetric arc therapy (RapidArc) and Gamma Knife radiosurgery for multiple cranial metastases. *Neurosurgery 75*, 4 (Oct 2014), 409–417. 120

[169] Tol J., Dahele M., Delaney A., Doornaert P., Slotman B., and Verbakel W. Detailed evaluation of an automated approach to interactive optimization for volumetric modulated arc therapy plans. *Med. Phys. 43* (2015), 1818. 59, 77

[170] Tol J., Dahele M., Peltola J., Nord J., Slotman B., and Verbakel W. Automatic interactive optimization for volumetric modulated arc therapy planning. *Radiother. Oncol. 10* (2015), 75. 77

[171] Toltz A., Shin N., Mitrou E., Laude C., Freeman C. R., Seuntjens J., Parker W., and Roberge D. Late radiation toxicity in Hodgkin lymphoma patients: proton therapy's potential. *J Appl Clin Med Phys 16*, 5 (09 2015), 167â€“178. 89

[172] Townsend N., Huth B., Ding W., Garber B., Mooreville M., Arrigo S., Lamond J., and Brady L. Acute toxicity after cyberknife-delivered hypofractionated radiotherapy for treatment of prostate cancer. *Am. J. Clin. Oncol. 34*, 1 (2010), 6–10. 19

[173] Travis L. B., Gospodarowicz M., Curtis R. E., Clarke E. A., Andersson M., Glimelius B., Joensuu T., Lynch C. F., van Leeuwen F. E., Holowaty E., Storm H., Glimelius I., Pukkala E., Stovall M., Fraumeni J. F., Boice J. D., and Gilbert E. Lung cancer following chemotherapy and radiotherapy for Hodgkin's disease. *J. Natl. Cancer Inst. 94*, 3 (Feb 2002), 182–192. 89

[174] Travis L. B., Hill D. A., Dores G. M., Gospodarowicz M., van Leeuwen F. E., Holowaty E., Glimelius B., Andersson M., Wiklund T., Lynch C. F., Van't Veer M. B., Glimelius I., Storm H., Pukkala E., Stovall M., Curtis R., Boice J. D., and Gilbert E. Breast cancer following radiotherapy and chemotherapy among young women with Hodgkin disease. *JAMA 290*, 4 (Jul 2003), 465–475. 89

[175] Tseng Y. D., Cutter D. J., Plastaras J. P., Parikh R. R., Cahlon O., Chuong M. D., Deneckova K., Khan M. K., Lin S. Y., McGee L. A., Shen E. Y., Terezakis S. A., Badiyan S. N., Kirova Y. M., Hoppe R. T., Mendenhall N. P., Pankuch M., Flampouri S., Ricardi U., and Hoppe B. S. Evidence-based Review on the Use of Proton Therapy in Lymphoma From the Particle Therapy Cooperative Group (PTCOG) Lymphoma Subcommittee. *Int. J. Radiat. Oncol. Biol. Phys. 99*, 4 (11 2017), 825–842. 89

[176] van de Water S., Valli L., Aluwini S., Lanconelli N., Heijmen B., and Hoogeman M. Intrafraction prostate translations and rotations during hypofractionated robotic radiation surgery: Dosimetric impact of correction strategies and margins. *Int. J. Radiat. Oncol. Biol. Phys. 88*, 5 (2013), 1154–1160. 59, 60

[177] van Nimwegen F. A., Ntentas G., Darby S. C., Schaapveld M., Hauptmann M., Lugtenburg P. J., Janus C. P. M., Daniels L., van Leeuwen F. E., Cutter D. J., and Aleman B. M. P. Risk of heart failure in survivors of Hodgkin lymphoma: effects of cardiac exposure to radiation and anthracyclines. *Blood 129*, 16 (04 2017), 2257–2265. 89, 90

[178] van Nimwegen F. A., Schaapveld M., Cutter D. J., Janus C. P., Krol A. D., Hauptmann M., Kooijman K., Roesink J., van der Maazen R., Darby S. C., Aleman B. M., and van Leeuwen F. E. Radiation Dose-Response Relationship for Risk of Coronary Heart Disease in Survivors of Hodgkin Lymphoma. *J. Clin. Oncol. 34*, 3 (Jan 2016), 235–243. 90

[179] van Nimwegen F. A., Schaapveld M., Janus C. P., Krol A. D., Petersen E. J., Raemaekers J. M., Kok W. E., Aleman B. M., and van Leeuwen F. E. Cardiovascular disease after Hodgkin lymphoma treatment: 40-year disease risk. *JAMA Intern Med 175*, 6 (Jun 2015), 1007–1017. 89

[180] Vanderstraeten B., Goddeeris B., Vandecasteele K., van Eijkeren M., De Wagter C., and Lievens Y. Automated Instead of Manual Treatment Planning? A Plan Com-

parison Based on Dose-Volume Statistics and Clinical Preference. *Int. J. Radiat. Oncol. Biol. Phys. 102*, 2 (Oct 2018), 443–450. 77

[181] Ventura T., Rocha H., da Costa Ferreira B., Dias J., and Lopes M. D. C. Comparison of two beam angular optimization algorithms guided by automated multicriterial IMRT. *Phys Med 64* (Aug 2019), 210–221. 129

[182] Videtic G. M. M., Donington J., Giuliani M., Heinzerling J., Karas T. Z., Kelsey C. R., Lally B. E., Latzka K., Lo S. S., Moghanaki D., Movsas B., Rimner A., Roach M., Rodrigues G., Shirvani S. M., Simone C. B., Timmerman R., and Daly M. E. Stereotactic body radiation therapy for early-stage non-small cell lung cancer: Executive Summary of an ASTRO Evidence-Based Guideline. *Pract Radiat Oncol 7*, 5 (2017), 295–301. 111

[183] Vinod S. K., Jameson M. G., Min M., and Holloway L. C. Uncertainties in volume delineation in radiation oncology: A systematic review and recommendations for future studies. *Radiother Oncol 121*, 2 (11 2016), 169–179. 131

[184] Voet P., Breedveld S., Dirkx M., Levendag P., and Heijmen B. Integrated multicriterial optimization of beam angles and intensity profiles for coplanar and non-coplanar head and neck IMRT and implications for VMAT. *Med. Phys. 39* (2012), 4858–4865. 19, 22, 36, 41, 42, 126

[185] Voet P., Dirkx M., Breedveld S., Al-Mamgani A., Incrocci L., and Heijmen B. Fully automated VMAT plan generation for prostate cancer patients. *Int. J. Radiat. Oncol. Biol. Phys. 88* (2014), 1175–1179. 13, 41, 59, 60, 68, 69, 77, 78, 79, 83, 104, 112, 127

[186] Voet P., Dirkx M., Breedveld S., Fransen D., Levendag P., and Heijmen B. Towards fully automated multi-criterial plan generation: a prospective clinical study. *Int. J. Radiat. Oncol. Biol. Phys. 85* (2013), 866–872. 13, 36, 41, 42, 60, 68, 92, 104, 127

[187] Voong K. R., McSpadden K., Pinnix C. C., Shihadeh F., Reed V., Salehpour M. R., Arzu I., Wang H., Hodgson D., Garcia J., Aristophanous M., and Dabaja B. S. Dosimetric advantages of a "butterfly" technique for intensity-modulated radiation therapy for young female patients with mediastinal Hodgkin's lymphoma. *Radiat Oncol 9* (Apr 2014), 94. 89

[188] Watanabe S., Yamamoto M., Kawabe T., Koiso T., Yamamoto T., Matsumura A., and Kasuya H. Stereotactic radiosurgery for vestibular schwannomas: average 10-year follow-up results focusing on long-term hearing preservation. *J. Neurosurg. 125*, Suppl 1 (12 2016), 64–72. 77

[189] Van de Water S., Hoogeman M. S., Breedveld S., and Heijmen B. J. M. Shortening treatment time in robotic radiosurgery using a novel node reduction technique. *Med. Phys. 38* (2011), 1397–1405. 19, 24, 61

[190] Van de Water S., Hoogeman M. S., Breedveld S., Nuyttens J. J. M. E., Schaart D. R., and Heijmen B. J. M. Variable circular collimator in robotic radiosurgery: A time-efficient alternative to a mini-multileaf collimator? *Int. J. Radiat. Oncol. Biol. Phys. 81* (2011), 863–870. 71

[191] Weksberg D. C., Palmer M. B., Vu K. N., Rebueno N. C., Sharp H. J., Luo D., Yang J. N., Shiu A. S., Rhines L. D., McAleer M. F., Brown P. D., and Chang E. L. Generalizable class solutions for treatment planning of spinal stereotactic body radiation therapy. *Int. J. Radiat. Oncol. Biol. Phys. 84*, 3 (2012), 847 – 853. 53

[192] Wild E., Bangert M., Nill S., and Oelfke U. Noncoplanar VMAT for nasopharyngeal tumors: Plan quality versus treatment time. *Med Phys 42*, 5 (May 2015), 2157–2168. 127

[193] Wilke L., Andratschke N., Blanck O., Brunner T. B., Combs S. E., Grosu A. L., Moustakis C., Schmitt D., Baus W. W., and Guckenberger M. ICRU report 91 on prescribing, recording, and reporting of stereotactic treatments with small photon beams : Statement from the DEGRO/DGMP working group stereotactic radiotherapy and radiosurgery. *Strahlenther Onkol 195*, 3 (Mar 2019), 193–198. 111

[194] Willoughby T., Kupelian P., Pouliot J., Shinohara K., Aubin M., Roach M., Skrumeda L., Balter J., Litzenberg D., Hadley S., Wei J., and Sandler H. Target localization and real-time tracking using the Calypso 4D localization system in patients with localized prostate cancer. *Int. J. Radiat. Oncol. Biol. Phys. 65* (2006), 528–34. 59, 71

[195] Woods K., Nguyen D., Tran A., Yu V. Y., Cao M., Niu T., Lee P., and Sheng K. Viability of Non-Coplanar VMAT for Liver SBRT as Compared to Coplanar VMAT and Beam Orientation Optimized 4Ï€ IMRT. *Adv Radiat Oncol 1*, 1 (2016), 67–75. 120

[196] Woudstra E., and Storchi P. R. M. Constrained treatment planning using sequential beam selection. *Phys. Med. Biol. 45* (2000), 2133–2149. 19

[197] Wu B., Pang D., Lei S., Gatti J., Tong M., McNutt T., Kole T., Dritschilo A., and Collins S. Improved robotic stereotactic body radiation therapy plan quality and planning efficacy for organ-confined prostate cancer utilizing overlap-volume histogram-driven planning methodology. *Radiother. Oncol. 112* (2014), 221–6. 41, 59

[198] Yeoh E., Botten R., Butters J., Di Matteo A., Holloway R., and Fowler J. Hypofractionated versus conventionally fractionated radiotherapy for prostate carcinoma: Final results of phase iii randomized trial. *Int. J. Radiat. Oncol. Biol. Phys. 81*, 5 (2011), 1271–1278. 19, 41

[199] Zarepisheh M., Long T., Li N., Tian Z., Romeijn H., Jia X., and Jiang S. A DVH-guided IMRT optimization algorithm for automatic treatment planning and adaptive radiotherapy replanning. *Med. Phys. 41* (2014), 061711. 41, 59, 77, 83

[200] Zhang Q., Zheng D., Lei Y., Morgan B., Driewer J., Zhang M., Li S., Zhou S., Zhen W., Thompson R., Wahl A., Lin C., and Enke C. A new variable for SRS plan quality evaluation based on normal tissue sparing: the effect of prescription isodose levels. *Br J Radiol 87*, 1043 (Nov 2014), 20140362. 84

[201] Zhang X., Li X., Quan E. M., Pan X., and Li Y. A methodology for automatic intensity-modulated radiation treatment planning for lung cancer. *Phys. Med. Biol. 56* (2011), 3873–3893. 59

[202] Zhou R., Ng A., Constine L. S., Stovall M., Armstrong G. T., Neglia J. P., Friedman D. L., Kelly K., FitzGerald T. J., and Hodgson D. C. A Comparative Evaluation of Normal Tissue Doses for Patients Receiving Radiation Therapy for Hodgkin Lymphoma on the Childhood Cancer Survivor Study and Recent Children's Oncology Group Trials. *Int. J. Radiat. Oncol. Biol. Phys. 95*, 2 (06 2016), 707–711. 89

List of Publications

Journal Articles

1. C.R. Hansen, W. Crijns, M. Hussein, **L. Rossi**, P. Gallego, W. Verbakel, E. Damen, J. Unkelbach, D. Verellen, D. Thwaites, B.J.M. Heijmen. *RAdiotherapy Treatment planNIng study Guidelines (RATING): A framework for setting up and reporting on scientific planning studies.* **Submitted**

2. C. Fiandra, **L. Rossi**, A. Alparone, S. Zara, C. Vecchi, A. Sardo, S. Bartoncini, G. Loi, C. Pisani, E. Gino, M.G. Ruoredda, G.M. Deotto, P. Tini, S. Comi, D. Zerini, G. Ametrano, V. Borzillo, L. Strigari, S. Strolin, A. Savini, A. Romeo, S. Reccanello, I.A. Rumeileh, N. Ciscognetti, F. Guerrisi, G. Balestra, U. Ricardi, B.J.M. Heijmen. *Automatic genetic planning for Volumetric Modulated Arc Therapy: a large multi-centre validation for prostate cancer.* **Radiother. Oncol. 2020** [51]

3. R. Bijman, **L. Rossi**, A.W. Sharfo, W. Heemsbergen, L. Incrocci, S. Breedveld, B.J.M. Heijmen. *Automated radiotherapy planning for patient-specific exploration of the trade-off between tumor dose coverage and predicted radiation-induced toxicity in prostate cancer.* **Frontiers in Oncology 2020** [16]

4. **L. Rossi** and P. Cambraia Lopes (the authors contributed equally), J. Leitão, C. Janus, M. van de Pol, S. Breedveld, J. Penninkhof and B.J.M. Heijmen. *On the importance of individualized, non-coplanar beam configurations in mediastinal lymphoma radiotherapy.* **Submitted**

5. R. Bijman, **L. Rossi**, T. Janssen, P. de Ruiter, C. Carbaat, B. van Triest, S. Breedveld, J.J. Sonke, B. Heijmen. *First system for fully-automated multi-criterial treatment planning for a high-magnetic field MR-Linac applied to rectal cancer.* **ACTA Oncologica 2020** [15]

6. A.W. Sharfo, **L. Rossi**, M.L.P. Dirkx, S. Breedveld, S. Aluwini and B.J.M. Heijmen. *Com-*

plementing prostate SBRT VMAT with a two-beam non-coplanar IMRT class solution to enhance rectum and bladder sparing with minimum increase in treatment time. **Submitted**

7 B. Schipaanboord, S. Breedveld, **L. Rossi**, M. Keijzer and B.J.M. Heijmen. *Automated prioritised 3D dose-based MLC segment generation for step-and-shoot IMRT*. **Phys Med Biol. 2019** [150]

8 **L. Rossi**, A. Méndez Romero, M. Milder, E. de Klerck, S. Breedveld, B.J.M. Heijmen. *Individualized automated planning for dose bath reduction in robotic radiosurgery for benign tumors.* **PLoS ONE 2019** [144]

9 **L. Rossi**, R. Bijman, W. Schillemans, S. Aluwini, C. Cavedon, M. Witte, L. Incrocci, B.J.M. Heijmen. *Texture analysis of 3D dose distributions for predictive modelling of toxicity rates in radiotherapy*. **Radiother. Oncol. 2018** [141]

10 M. Loi, M. Duijm, S. Baker, **L. Rossi**, D. Grunhagen, C. Verhoef, J. Nuyttens. *Stereotactic body radiotherapy for oligometastatic soft tissue sarcoma.* **Radiol Med. 2018** [104]

11 **L. Rossi**, A.W. Sharfo, S. Aluwini, M.L.P. Dirkx, S. Breedveld, B.J.M. Heijmen. *First fully automated planning solution for robotic radiosurgery - comparison with automatically planned volumetric arc therapy for prostate cancer*. **ACTA Oncologica 2018** [145]

12 D. Cusumano, M.L. Fumagalli, F. Ghielmetti, **L. Rossi**, G. Grossi, R. Lanzarotti, L. Fariselli, E. De Martin. *Sum signal dosimetry: a new approach for high dose quality assurance with Gafchromic EBT3*. **J Appl Clin Med Phys. 2017** [34]

13 C. Cavedon, G. Meliadó, **L. Rossi**, L. Camera, I. Baglio, F. Caumo, S. Montemezzi. *High-field MR spectroscopy in the multiparametric MRI evaluation of breast lesions.* **Phys Med. 2016** [29]

14 **L. Rossi**, S. Breedveld, S. Aluwini, B.J.M. Heijmen . *Non-coplanar beam angle class solutions to replace time-consuming patient-specific beam angle optimization in robotic prostate SBRT*. **Int J Radiat Oncol Biol Phys. 2015** [142]

15 **L. Rossi**, S. Breedveld, B.J.M. Heijmen, P. Voet, N. Lanconelli and S. Aluwini. *On the beam direction search space in computerized non-coplanar beam angle optimization for IMRT-prostate SBRT*. **Phys Med Biol. 2012** [143]

Oral Presentations at International Conferences

2020, ESTRO 39, Vienna, Austria.

- *Automation of treatment planning process.* **L. Rossi (invited speaker)**, S. Breedveld, B.J.M. Heijmen
- *Inter-observer variability in quality scores of Pareto optimal plans* E. Cagni, **L. Rossi**, A. Botti Andrea, M. Iori, R. Sghedoni, C. Iotti, A. Rosca, G. Timon, S. Cozzi, M. Galaverni, M. Orlandi, E. Spezi, B.J.M. Heijmen

2019, ESTRO 38, Milan, Italy.

- *Using automated planning for bias-free plan comparison.* **L. Rossi (invited speaker)**, A. Sharfo, S. Breedveld, B.J.M. Heijmen
- *Automated (non-coplanar) beam selection for IMRT in young female lymphoma patients reduces OAR doses.* P. Cambraia Lopes, **L. Rossi**, J. Leitão, C. Janus, M. van de Pol, J. Penninkhof, B.J.M. Heijmen
- *A two-beam non-coplanar class solution to supplement VMAT in prostate SBRT.* A.W. Sharfo, **L. Rossi**, M.L.P. Dirkx, S. Aluwini, S. Breedveld, B.J.M. Heijmen

2019, International Day of Medical Physics, Matera, Italy. *Automated IMRT and VMAT radiotherapy treatment planning for left breast cancer: bias-free comparison between techniques.* L. Redapi, **L. Rossi**, L. Marrazzo, J.J. Penninkhof, S. Pallotta, B.J.M. Heijmen

2018, NVKF Lustrum, Haarlem, The Netherlands. *Texture Analysis of 3D dose distributions for toxicity predictive modelling to be applied in automated radiotherapy planning*. **L. Rossi**, R. Bijman, W. Schillemans, S. Aluwini, C. Cavedon, M. Witte, L. Incrocci and B.J.M. Heijmen

2018, ESTRO 37, Barcelona, Spain.

- *Multi-criterial MLC segmentation with column generation, applied to robotic SBRT.* B.W.K. Schipaanboord, S. Breedveld, **L. Rossi**, M. Keijzer, B.J.M. Heijmen
- *Automated planning and prediction models for bias-free treatment technique selection*. A.W. Sharfo, M.L.P. Dirkx, R. Bijman, **L. Rossi**, T. Arts, S. Breedveld, M. Hoogeman, B.J.M. Heijmen

2018, 10th National Congress AIFM, Bari, Italy.

- *Automated planning in radiotherapy* **L. Rossi (invited author, teaching lesson)**

- *Texture Analysis of 3D dose distributions for toxicity predictive modelling in radiotherapy*. **L. Rossi**, R. Bijman, W. Schillemans, S. Aluwini, M. Witte, L. Incrocci and B.J.M. Heijmen (Awarded presentation)

2017, ESTRO 36, Vienna, Austria. *Automated planning, knowledge-based planning and other novelties in treatment planning - how do they work and perform?* B.J.M. Heijmen, P. Voet, **L. Rossi**, A. Sharfo, Y. Wang, S. Breedveld

2016, EANM, European Association of Nuclear Medicine, Barcelona, Spain. *Design and Physical Performance of a Plastic Scintillator Detector to control radioactive waste in a Nuclear Medicine Unit*. F. Zito, A. D'Alessio, G. Galetta, **L. Rossi**, R. Benti

2016, EURO, 28th European Conference on Operational Research, Poznań, Poland. *Multi-Criteria Optimisation and Decision-Making in Radiotherapy*. S. Breedveld, R. van Haveren, **L. Rossi**, S. van de Water, T. Arts, A.W. Sharfo, M. Hoogeman, W. Ogryczak, B.J.M. Heijmen

2016, ESTRO 35, Turin, Italy.

- *Fully automated planning for non-coplanar CyberKnife prostate SBRT - comparison with automatic VMAT*. **L. Rossi**, S. Breedveld, S. Aluwini, B.J.M. Heijmen
- *Fully automated treatment plan generation using Erasmus-iCycle - the Rotterdam experience*. M.L.P. Dirkx , A.W. Sharfo, P. Voet, G. della Gala, **L. Rossi**, D. Fransen, J.J. Penninkhof, M.S. Hoogeman, S.F. Petit, A.M. Méndez Romero, J.W. Mens, L. Incrocci, N. Hoekstra, M. van de Pol, S. Aluwini, S. Breedveld, B.J.M. Heijmen

2016, 9th Congresso Nazionale AIFM, Perugia, Italy. *First clinical system for fully automated planning for non-coplanar Cyberknife - comparison with coplanar VMAT for prostate SBRT*. **L. Rossi**, S. Breedveld, S. Aluwini, B.J.M. Heijmen

2015, IPEM Radiotherapy Treatment Planning conference, London, UK. *Automated IMRT and VMAT planning for standardization in radiotherapy with improved treatment quality and reduced workload*. B.J.M. Heijmen, P. Voet, **L. Rossi**, A. Sharfo, S. van de Water, M.L.P. Dirkx, M. Hoogeman, S. Breedveld

2015, 28th Annual EANM Congress, Hamburg, Germany. *18F-FDG whole body PET/CT dose evaluation in pediatric patients*. F. Zito, G. Galetta, **L. Rossi**, C. Canzi, L. Florimonte, R. Benti

2015, ESTRO 3rd Forum, Barcelona, Spain.

- *Coplanar and non-coplanar optimization in prostate SBRT*. **L. Rossi (invited speaker)**, S. Breedveld, S. Aluwini, B.J.M. Heijmen

- *Automatic planning strategies.* B.J.M. Heijmen, P. Voet, M.L.P. Dirkx, A.W. Sharfo, **L. Rossi**, S. Van de Water, D. Fransen, J. Penninkhof, M.S. Hoogeman, S.F. Petit, A.M. Méndez Romero, J.W. Mens, L. Incrocci, S. Breedveld
- *Sum signal dosimetry: a novel approach for high dose patient specific quality assurance with Gafchromic EBT3.* D. Cusumano, M.L. Fumagalli, F. Ghielmetti, **L. Rossi**, G. Grossi, R. Lanzarotti, L. Fariselli, E. De Martin

2014, 8th European Conference on Medical Physic, EFOMP, Athens, Greece. *Fully automated treatment plan generation in daily routine.* B.J.M. Heijmen, P. Voet, M.L.P. Dirkx, A. Sharfo, **L. Rossi**, D. Fransen, J. Penninkhof, M. Hoogeman, S. Petit, J.W. Mens, A. Méndez Romero, A. Al-Mamgani, L. Incrocci, S. Breedveld

2014, ESTRO 33, Vienna, Austria. *Development of a beam angle class solution to replace full beam angle optimization in non-coplanar prostate SBRT*. **L. Rossi**, S. Breedveld, S. Aluwini & B.J.M. Heijmen

2013, 2nd ESTRO Forum, Geneva, Switzerland. *Strongly reduced rectum dose for prostate treatment with non-coplanar beam setup of a CyberKnife equipped with an MLC.* **L. Rossi**, B.J.M. Heijmen, S. Breedveld, P. Voet, S. Aluwini

2013, 1st European Conference on SRS/SBRT & IG-IMRT, Milan, Italy. *Clinical added value of non-coplanar treatments.* B.J.M. Heijmen, **L. Rossi**, S. Breedveld, P. Voet, S. Aluwini

Posters at International Conferences

2020, ESTRO 39, Vienna, Austria.

- *Individualized Beam Angle Selection for MR-Linac Treatment of Rectal Cancer Patients* R. Bijman, **L. Rossi**, T. Janssen, P. de Ruijter, B. van Triest, S. Breedveld, J.J. Sonke, B.J.M. Heijmen (poster discussion)
- *Large treatment plan quality enhancement in robotic radiotherapy* M.K. Giżyńska, **L. Rossi**, W. den Toom, M. Milder, K. de Vries, J. Nuyttens, L. Incrocci, B.J.M. Heijmen

2019, ESTRO 38, Milan, Italy. *First system for fully automated multi-criterial planning for an MR-Linac applied to rectal cancer.* R. Bijman, **L. Rossi**, T. Janssen, P. de Ruijter, C. Carbaat, B. van Triest, S. Breedveld, J.J. Sonke, B.J.M. Heijmen (poster discussion)

2018, ESTRO 37, Barcelona, Spain.

- *Texture Analysis of 3D dose distributions for toxicity predictive modelling in*

radiotherapy. **L. Rossi**, R. Bijman, W. Schillemans, S. Aluwini, M. Witte, L. Incrocci and B.J.M. Heijmen (poster viewing)

- *Enhanced prostate SBRT using VMAT + a single computer-optimized non-coplanar IMRT beam*. A.W. Sharfo, **L. Rossi**, M.L.P. Dirkx, S. Aluwini, S. Breedveld, B.J.M. Heijmen

2017, ESTRO 36, Vienna, Austria. *Automated planning to reduce integral dose in robotic radiosurgery for benign tumors*. **L. Rossi**, A. Méndez Romero, M. Milder, E. de Klerck, S. Breedveld, B.J.M. Heijmen

2014, ASTRO 56th Annual Meeting, San Francisco, USA. *Fully Automatic IMRT and VMAT Treatment Planning in Routine Clinical Practice*. B.J.M. Heijmen, P. Voet, M.L.P. Dirkx, A. Sharfo, **L. Rossi**, D. Fransen, J. Penninkhof, M. Hoogeman, S. Petit, J. Mens, A. Méndez Romero, A. Al-Mamgani, L. Incrocci, S. Breedveld

2013, 8th Annual Meeting AIFM, Turin, Italy. *IRIS and fixed collimators comparison for CyberKnife stereotactic radiosurgery of petroclival meningiomas*. **L. Rossi**, M.L. Fumagalli, F. Ghielmetti, M. Marchetti, L. Fariselli, E. De Martin

2012, AAPM 54th Annual Meeting, Charlotte, NC, USA. *On the beam direction search space in computerized non-coplanar beam angle optimization for IMRT; prostate SBRT*. **L. Rossi**, P. Voet, S. Breedveld, S. Aluwini, B.J.M. Heijmen

2012, ESTRO 31, Barcelona, Spain. *On the extent of the beam direction search space in computerized non-coplanar beam angle optimization for IMRT*. B.J.M. Heijmen, **L. Rossi**, S. Breedveld, P. Voet, N. Lanconelli, S. Aluwini

Erasmus MC
University Medical Center Rotterdam

PhD Portfolio

Summary of PhD training and teaching

Name PhD student: Linda Rossi

PhD period: 2013 - 2019
(0.6 FTE, equivalent to 4 years 1.0 FTE)

Erasmus MC Department: Radiation Oncology
Research School: Molecular Medicine

Promotor: Prof. dr. B.J.M. Heijmen
Copromotor: Dr. ir. S. Breedeveld

1. PhD training

General courses		
▪ Programming techniques in MATLAB	(MathWorksC) Turin, IT	2010
▪ Research Integrity	(Erasmus MC) Rotterdam, NL	2014
▪ Programming with Python	(Erasmus MC) Rotterdam, NL	2016
Specific courses		
▪ Physics for clinical radiotherapy	(ESTRO) Budapest, HU	2010
▪ IGRT, Respiratory movement control and advanced imaging in radiotherapy	(AIFM) Verona, IT	2012
▪ Statistics for radiotherapy data	(ESTRO 32, 2nd Forum) Geneva, CH	2013
▪ Exposition evaluation to incoherent artificial optical radiation	(ANPEQ) Milan, IT	2013
▪ Advanced semiconductor dosimetry in radiation therapy: current research and future perspectives	(IRCCS INT) Milan, IT	2013
▪ Medical Physicist contribution in physical risk evaluations in hospitals: TU 81/08	(AIFM) Milan, IT	2013
▪ Neutron contamination in radiotherapy beams	(AIFM) Como, IT	2013
▪ Current Advances in Treatment Planning Optimisation	(ESTRO 33) Vienna, AT	2014
▪ Voxel based dosimetry in nuclear medicine therapy with tomographic SPECT and PET	(AIFM) Rome, IT	2015
▪ Incorporating Imaging in Radiation Oncology Treatment Delivery	(ESTRO 34, 3rd Forum) Barcelona, ES	2015
▪ QA for advanced MR procedures	(AIFM) Brescia, IT	2015

▪ Multidimensional dosimetry systems		(ESTRO 35) Turin, IT	2016
▪ Statistics applied to biomedical research		(AIFM) Milan, IT	2016
▪ Predictive models for external radiotherapy effects		(AIFM) Milan, IT	2016
▪ Small and modulated photon field dosimetry		(AIFM) Verona, IT	2016
▪ Multimodality imaging in radiation oncology to improve target definition and modified dose prescription		(ESTRO 36) Vienna, AT	2017
▪ Big-Data, Radiomics and Artificial Intelligence		(AIFM) Reggio Emilia, IT	2017
▪ MRI physics for applications in radiation oncology		(ESTRO 37) Barcelona, ES	2018
▪ Machine learning for physicists		(ESTRO 38) Milan, IT	2019
▪ Medical Physics Residency Courses		(Milan University) Milan, IT	2012-2016
Seminars and workshops			
▪ Automate or Perish		(1st ESTRO Physics Worskhsop) Glasgow, UK	2017
International conferences			
▪ ESTRO 32 (2nd Forum)	Oral presentation	Geneva, CH	2013
▪ ESTRO 33	Oral presentation	Vienna, AT	2014
▪ ESTRO 34 (3rd Forum)	Invited speaker: Symposium	Barcelona, ES	2015
▪ 9th National Congress AIFM	Oral presentation	Perugia, IT	2016
▪ ESTRO 35	Oral presentation	Turin, IT	2016
▪ ESTRO 36	Poster	Vienna, AT	2017
▪ ESTRO 37	Poster viewing	Barcelona, ES	2018
▪ 10th National Congress AIFM	Oral presentation	Bari, IT	2018
▪ 10th National Congress AIFM	Invited speaker: Teaching lesson	Bari, IT	2018
▪ ESTRO 38	Invited speaker: Symposium	Milan, IT	2019
▪ ESTRO 39 (2020)	Invited speaker: Symposium	Vienna, AT	2020
National conferences			
▪ RKF-Kringdag	Oral presentation	Amsterdam, NL	2016
▪ NVKF Lustrum	Oral presentation	Haarlem, NL	2018
Other			
▪ CyberKnife physics, Italian user meeting	Invited speaker: 2 oral presentations	Milan, IT	2015
▪ Raystation user meeting	Invited speaker: Oral presentation	Siena, IT	2018
▪ Chair invitation ESTRO 39	Chair	Vienna, AT	2020
▪ Peer-reviewed more than 15 papers in 7 journals	Peer reviewer	Radiotherapy and Oncology, International Journal of Radiation Oncology Biology Physics, Physics in Medicine and Biology, Medical Physics, Physica Medica and International Transactions in Operational Research, Scientific Reports Nature	2013-2020

2. Teaching

Internal Lecturing

▪ Texture analysis: what is it? Application	Journal Club	2016
▪ Tumor Tracking with an MLC, based on Calypso or kV-Imaging	Journal Club	2017
▪ Automated planning for robotic prostate SBRT: non-coplanar Cyberknife comparison with coplanar autoVMAT	Refereeravond Radiotherapie	2018
▪ Texture Analysis of 3D dose distributions for predictive modelling of toxicity rates in radiotherapy	Research Day	2018
▪ Deep learning in radiotherapy treatment planning	Journal Club	2019
▪ Automated planning for Low-Middle Income Country (LMIC)	Research Day	2019

Supervising and Tutoring

▪ Joana Leitão	Bachelor Student, Lisboa University	15 July 2018–15 Sept 2018
▪ Laura Redapi	Medical Physics trainee, Florence	15 Sept 2018–15 Dec 2018
▪ Sven Meijer	Master Student, Delft University	1 Sept 2018–30 Mar 2019
▪ Cecilia Collá Ruvolo	Post Master, Turin University	1 Jan 2019–30 Mar 2019
▪ Rik Bijman	PhD Student, Erasmus MC	1 Aug 2017–Now
▪ Ilja Briggeman	Master Student, Delft University	8 Sept 2019-Now

3. Distinctions and awards

▪ Young medical physics best oral presentation, Adele Rinaldi award, 10th National Congress AIFM	Bari, IT	2018

Curriculum Vitae

Linda Rossi was born in Rimini, Italy on October 16th 1987. After completing mandatory studies in her hometown, she moved in 2006 to Bologna to study physics at the Alma Mater Studiorum Bologna University.

Linda did her bachelor thesis in neutrino research in Bologna, collaborating with Gran Sasso INFN laboratory and CERN, within the OPERA experiment. After obtaining her physics bachelor degree in 2009 (109/110), she felt more attracted towards medical applications and she attended applied physics classes in Bologna, focused on a Master degree in medical physics. In 2011, she performed her master thesis project in the Erasmus Placement project, at the Department of Radiation Oncology, Erasmus Medical Center, in Rotterdam, The Netherlands. She got her physics master degree at the end of 2011 (110/110 cum laude), with a thesis in optimization of radiotherapy planning.

In 2012, she entered the medical physicist training program in Milan, Italy. She followed courses and got trained in radiotherapy, nuclear medicine, radioprotection and diagnostic techniques, in three different institutes in Milan. In 2016, she officially became a Medical Physicist, with a research thesis in high field nuclear magnetic resonance for breast tumors, conducted in Verona Hospital, Italy.

During the training for becoming a medical physicist, Linda kept actively collaborating with the Erasmus Medical Center in Rotterdam on research projects related to plan optimization, intensively travelling between the two countries. After the completion of the training program, she moved to The Netherlands and these researched were continued as PhD project under the supervision of Prof. dr. Ben Heijmen and Dr. ir. Sebastiaan Breedveld.

Currently Linda has a postdoc position in Rotterdam to continue her research on automation and optimization of radiotherapy treatment planning.

Acknowledgements

My first and biggest thanks go to Ben Heijmen, my promoter, for being the best supervisor, colleague and friend I could dream to. You have always treated me as colleague, also when I was just a master student. You believed and invested in me, even further than what I could image myself. You always understood when I needed time and space to investigate, experiment and solve problems by myself, or when I needed your support and actions. You have given credits to my ideas and initiatives, kindly rejecting the not good ones. The trust you put in me, allowed me to freely propose outside-box ideas. I highly enjoy our brainstorms. Thank you for pushing and supporting me. Aside work, you let me enter in your family, and your help and support has been so high that I will never be able to compensate back.

Thank you, Sebastiaan Breedveld, my co-promoter. I should thank you for your great creation, iCycle, and the success that it brought to our department. But I am the lucky one that have much more to thank you for. Thank you for always being on my side, with the right help and/or solicitations. You were the first one that had to handle with my desire of learning and knowing and therefore had to deal with all my questions and (not always smart) emails. You knew the right amount of help that was necessary, and citing you 'you taught me to fish, instead of providing me fish'. You are one of the most intelligent, good, honest and positive person I have ever met. I am proud of being your friend, aside colleague.

Moreover, thanks to both of you, Ben and Sebastiaan, for (conceptually, mentally, logistically, geographically and technically) making the impossible possible. I would not be here, if it would not be for the two of you.

Shafak Aluwini, thank you for your clinical support and help. You have been available for reviewing my plans, answering to all the difficult clinical questions I let you face. You have been always highly professional and kind. It has been a honor and a real pleasure working with you.

Thank you, Alejandra Mendez Romero, for your devotion to patients and your job, and for being the great person that find time to care of you while running as always in the corridor.

Thank you, Patricia Cambraia Lopes Ferreira, I really enjoyed closely collaborating with you, even despite our challenging project; you worked hard to help me finalizing the study in time, and I am really grateful for this.

Thank you, Abdul Wahab (Buddi) Sharfo, collaborate with you, with our different approaches, has been really stimulating and helpful.

Thank you, Rik Bijman, for your loyalty and reliability and for making working together a real pleasure. You are a beautiful person.

Thank you, Maaike Milder, for always being kindly present and available with your clinical view and help. Thank you, Erik de Klerck and Willem de Tom, for your priceless contributions in the projects; thank for being willing and interested in changing and improving the clinical procedures. Thank you, Andras Zolay, for your invaluable support; research and clinic owe you a lot. Thank you, Wilco Schillemans, for your contribution; it has always been a pleasure asking help to you. Thank you, Mischa Hoogeman, for the sharp questions and views; I always enjoyed the challenge and the inspiration of discussing with you. Thank you Joan Penninkhof, I professionally really appreciate you. Thank you Maarten Dirkx, for your clinical and physics support.

Rotterdam and this long/travelling/part-time PhD meant an adventure to me. I had the luck of running into a lot of new and great people and culture on my path.

Thanks to all the colleagues for the warm welcome back, every single time that I was again popping up at the office from Italy. Thank Xander van Doorn since the 1st February 2011. Thank Steven Petit, Vikas Gupta, Steven van de Water, Yibing Wang, Eliana Vasquez Osorio and Wouter Wunderink for all the lunches, dinners and pizzas. Thank Jacqueline van der Valk for being the best, warm and sweet smile a frustrate researcher sometimes really needs. Thank Gijsbert Klop and Ruud Cools for all the interesting discussions we had in your office. Thank you, Martijn Hol and Carly Noordermeer, for the chats about life and cakes. And thank you, Ben Göbel, you know why.

Thank you to my lovely friends and office mates, Emmanuelle Fleury, Iva Vilas Boas Ribeiro and Alba Magallon Baro. You give the boost to come at work every day. And thanks to the whole research group that let me never feel alone, thank Bas, Marta, Domenique, Thyrza, Laura, Rens, Nienke, Jesus, Michelle and the students Joana, Laura, Sven, Cecilia and Ilja. It has been an honor to work with you all.

Special thanks to my core Rotterdammer crew, Marco, Cristiana, Elin, Omar, Eleonora, Jon, Arturo, Luigi, Lisa and Samuele, for being the home atmosphere on Sundays and

Sinterklass, among any other moment together.

Thank you Alessandra Bizzarri, for welcoming me in your family as I couldn't ever image. Thank you for your sweet take-away cakes, that sometimes I found on my desk. You have always been present and willing. You share big part of the beginning acknowledgment. What a good heart you have.

From my Milan period, thanks to my residency companions, Maria Luisa, Francesca, Chiara, Ale, Camilla, Luca, for all good lesson notes I never took but you always provided me. Thank you for taking care of me. And thank you, because I know we will always be there for each other, for any (work related or not) problems. Looking forward for more trips together. Thank you, Sara, Francesca, Margherita and Fabiola, for being the first ones showing me how much a good colleague can impact your day. I really miss you all a lot.

Al mio Pronto Romagna, a Silvia, Valeria, Elsa, Giulia, Esmi, Elena, Biagio, Chiara, Lea, Mattia, Elisa, Katia, Vale, Lele, Xue, Donny, Devis, l'Evina, la Ginny e tutto il resto della banda. Spero non smetteremo mai di prenderci in giro come solo noi sappiamo fare, con il l'affetto costante di una vita dietro. Non potete capire quanto significhi per me condividere insieme ogni momento importante, e il calore che si sente sempre ad ogni rimpatriata.

Grazie Shirley, Gianlu, e bimbe, per amarmi sempre, tanto quanto mi sgridate. Grazie Fabio, per esserci sempre incondizionatamente.

Alla mia famiglia, Mamma, Martina, Davide, Roberto, Matilde, Margherita, Matteo e Sofia. Vi voglio un bene non esprimibile a parole. Siete il mio punto fisso nel mondo. Non importa dove e quanto lontano vada, finchè ci sarete voi, non saró mai persa. Grazie mamma per la tenacia, la forza e la fiducia, e per avermi insegnato quali sono le cose importanti nella vita. Grazie Martina, per essere un esempio da seguire e un riferimento. Grazie Davide e Roby, per esserci sempre, dando il vero significato alla parola famiglia. Grazie Matilde, per avermi fatto scoprire una nuova parte di me, e per avermi fatto sentire sempre speciale nella tua vita, fin da quando eri neonata e nonostante la distanza. Grazie Matteo per essere il padre meraviglioso che sei e il mio cognato preferito (lo saresti comunque anche se non fossi l'unico).

Al mio compagno di viaggio, Gabriele. Grazie per essere davvero al mio fianco ogni giorno, grazie per l'immensa fiducia in me, il supporto, l'amore, la bontá, la comprensione, la pazienza e per l'aiuto a migliorare che ci diamo ogni giorno. Grazie per il viaggio migliore che potessi mai desiderare.

E grazie babbo. Posso solo dirti davvero grazie, per tutto... spero di renderti orgoglioso anche da lassú, quanto io lo sono di te...

Automation of the treatment plan generation in radiotherapy showed to play a key role in patient care. It can highly improve plan quality, reduce planner influence, increase standardization and easily generate a high number of plans.

At the Erasmus MC, an automated treatment planning system has been developed, called Erasmus-iCycle. It automatically generates high-quality Pareto-optimal plans and it can also automatically define patient-specific optimal beam directions, to overcome the not trivial manual beam selections.

In this thesis, Erasmus-iCycle has been used to improve plan quality and to investigate the impact of treatment techniques and beam directions. The latter, especially with focus on the added value of the non-coplanar beam setup, compared to coplanar setup.

ISBN: 978-94-91462-50-4